Department of Energy
Washington, DC 20585

MAR 0 4 2009

Attn: Document Control Desk
Director, Spent Fuel Project Office
Office of Nuclear Material Safety and Safeguards
U.S. Nuclear Regulatory Commission
Washington, D.C. 20555-0001

On September 8, 2008 the U. S. Department of Energy (DOE) submitted an application for revision of the Model No. ATR FFSC package Certificate of Compliance (CoC) USA/9330/AF-96, Docket No. 71-9330, TAC No. L24248 for transportation of four payload types: ATR fuel elements, MIT fuel elements, MURR fuel elements, and unassembled ATR, MIT and MURR fuel elements plates.

In a letter dated December 1, 2008, the NRC requested additional information (RAIs) in support of this revision. This submittal is the response to the RAIs and also includes the updates to the Safety Analysis Report (SAR), Revision 4.

The original of this letter, with attachment is being sent to the Document Control Desk. Seven copies of this letter with attachments are being delivered to Pierre Saverot, Project Manager, Licensing Branch, Division of Spent Fuel Storage and Transportation, Office of Nuclear Material Safety and Safeguards shortly after this letter is sent.

If you have any questions, please contact me at 301-903-5513.

Sincerely,

James M. Shuler

Dr. James M. Shuler
Manager, DOE Packaging Certification Program
Office of Packaging and Transportation
Office of Environmental Management

Enclosure

LIMSS01

Safety Analysis Report

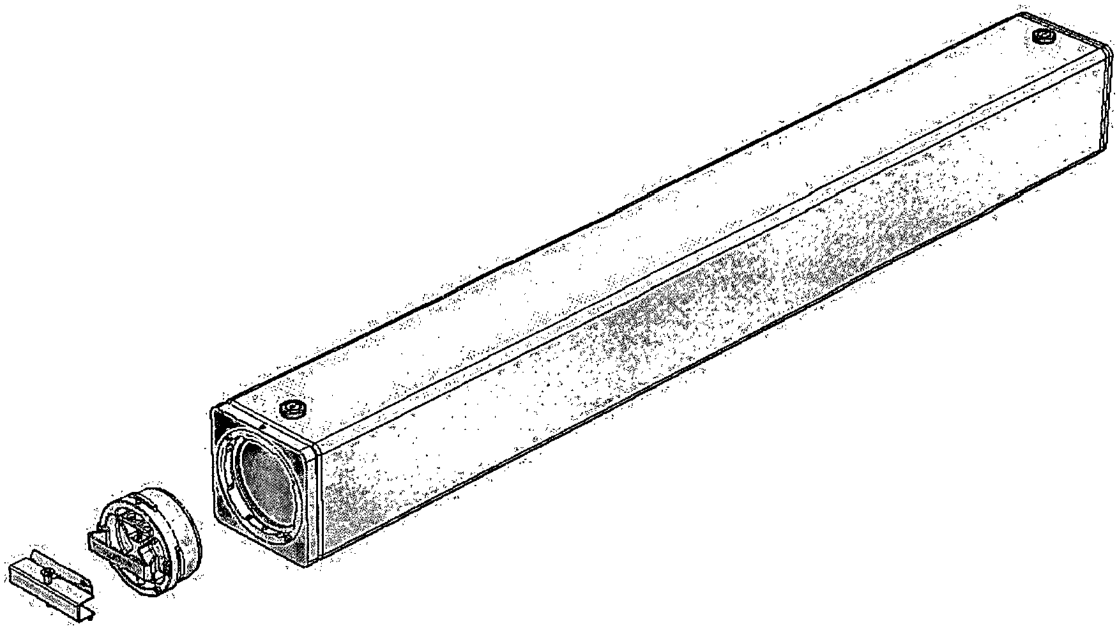

Advanced Test Reactor Fresh Fuel Shipping Container (ATR FFSC)

Revision 4, February 2009

Docket 71-9330

Prepared by:	*Prepared for:*
AREVA **AREVA Federal Services LLC**	INL Idaho National Laboratory **Battelle Energy Alliance, LLC (BEA)**

Safety Analysis Report

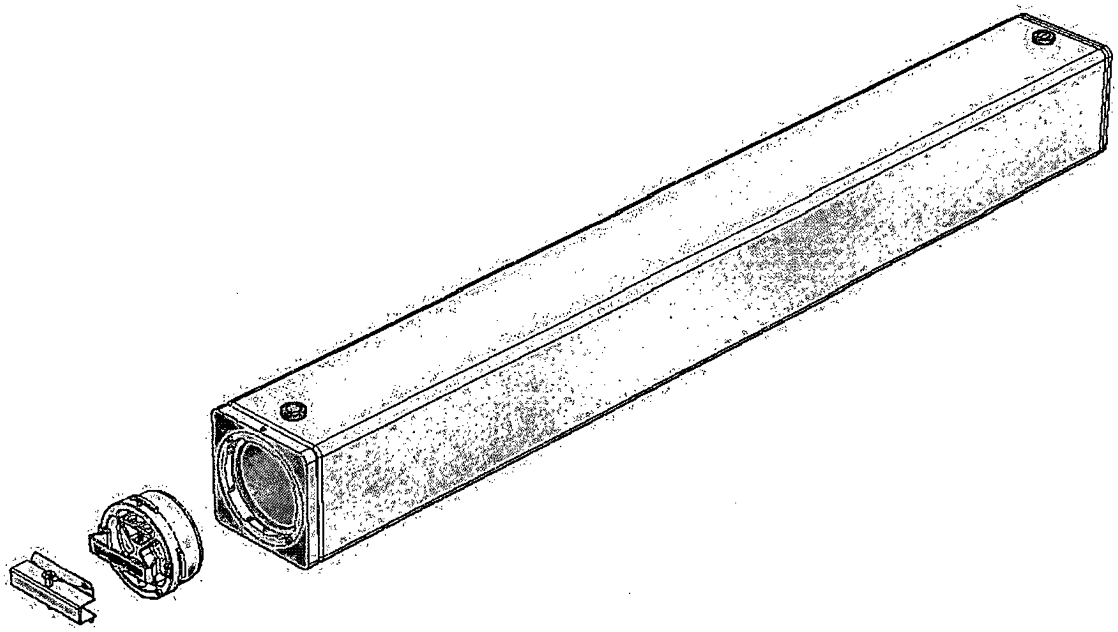

Advanced Test Reactor Fresh Fuel Shipping Container (ATR FFSC)

Revision 4, February 2009

Docket 71-9330

Prepared by:	*Prepared for:*
AREVA **AREVA Federal Services LLC**	INL Idaho National Laboratory **Battelle Energy Alliance, LLC (BEA)**

Page Change Instructions

Page Changes	
Remove Rev. 3	**Insert Rev. 4**
Cover page	Cover page
Cover spine	Cover spine
i to v	i to v
1-1 to 1-7	1-1 to 1-7
1-15	1-15
2-1	2-1
2-4	2-4
2.12.3-1 to 2.12.3-6	2.12.3-1 to 2.12.3-9
3-47 to 3-49	3-47 to 3-49
3-52	3-52
3-55	3-55
6-87 to 6-134	6-87 to 6-144
7-1	7-1
7-3	7-3

TABLE OF CONTENTS

1.0 GENERAL INFORMATION

This chapter of the Safety Analysis Report (SAR) presents a general introduction and description of the Advanced Test Reactor (ATR) Fresh Fuel Shipping Container (FFSC).[1] This application seeks validation of the ATR FFSC as a Type AF fissile materials shipping container in accordance with Title 10, Part 71 of the Code of Federal Regulations (10CFR71).

The major components comprising the package are discussed in Section 1.2.1, *Packaging*, and illustrated in Figure 1.2-1 through Figure 1.2-8. Detailed drawings of the package design are presented in Appendix 1.3.2, *Packaging General Arrangement Drawings*. A glossary of terms is presented in Appendix 1.3.1, *Glossary of Terms*.

1.1 Introduction

The single ATR FFSC has been designed to transport unirradiated fuel. The payload consists of a fresh fuel element for use in either the Advanced Test Reactor located in Idaho Falls, Idaho, the Massachusetts Institute of Technology (MIT) research reactor, or the Missouri University Research Reactor (MURR). Additionally, the package is designed to transport fuel element plates that have either not yet been assembled into a fuel element or have been removed from an unirradiated fuel element. The fuel plates may be either flat or rolled to the geometry required for assembly into a fuel element.

The fuel elements are all fabricated in a similar manner using aluminum-clad uranium aluminide (UAl_x) plates containing high-enriched uranium (HEU) enriched to a maximum of 94% U-235. The fuel plates vary in size and number between the ATR, MIT, and MURR fuel elements with the ATR fuel plates being the longest. Further details of the fuel elements are provided in Section 1.2.2, *Contents*.

Since the A_2 value of the payloads is low and radiation is negligible, the only safety function performed by the package is criticality control. This function is achieved, in the case of a transport accident, by confining the fuel element within the package and by maintaining separation of fuel in multiple packages. The fuel itself is robust and inherently resists unfavorable geometry reconfiguration while contained within the package. For ease of handling and property protection purposes, each fuel assembly is contained within a lightweight aluminum housing referred to as the fuel handling enclosure. The loose ATR fuel plates are contained in a loose plate basket which prevents the fuel from reconfiguring into an unfavorable geometry.

For the fuel elements, the criticality control function is demonstrated via full-scale testing of a prototypic package followed by a criticality analysis using a model which bounds the test results, ensuring that the calculated $k_{eff} + 2\sigma$ is below the upper subcritical limit (USL) in the most limiting case. Two full-scale prototype models are used to perform a number of performance tests including normal conditions of transport (NCT) free drop and hypothetical accident condition (HAC) free drop and puncture tests.

[1] In the remainder of this Safety Analysis Report, *Advanced Test Reactor Fresh Fuel Shipping Container* will be abbreviated as *ATR FFSC*. In addition, the term 'packaging' will refer to the assembly of components necessary to ensure compliance with the regulatory requirements, but does not include the payload. The term 'package' includes both the packaging components and the fresh fuel payload.

Authorization is sought for a Type A(F)-96, fissile material package per the definitions delineated in 10 CFR §71.4[2]. Each ATR fuel element contains up to 1,200 grams of U-235 enriched to a maximum of 94% U-235. The MIT fuel element contains up to 515 grams of U-235 enriched to a maximum of 94% U-235 and the MURR fuel element contains up to 785 grams of U-235 enriched to a maximum of 94% U-235. When shipping loose ATR fuel plates, the package is limited to a maximum fissile payload of 600 grams U-235.

The Criticality Safety Index (CSI) for the package, determined in accordance with the definitions of 10 CFR §71.59, is 4.0. The CSI is based on the number of packages for criticality control purposes (the method and the CSI determination are given in Chapter 6.0, *Criticality Evaluation*).

1.2 Package Description

This section presents a basic description of the ATR FFSC. General arrangement drawings are presented in Appendix 1.3.2, *Packaging General Arrangement Drawings.*

1.2.1 Packaging

1.2.1.1 Packaging Description

The ATR FFSC is designed as Type AF packaging for transportation of four payload types; ATR fuel elements, MIT fuel elements, MURR fuel elements, and unassembled fuel element plates. The packaging is rectangular in shape and is designed to be handled singly with slings, or by fork truck when racked. Package components are shown in Figure 1.2-1. Transport of the package is by highway truck. The maximum gross weight of the package loaded with an ATR fuel element is 280 lbs; with a MIT fuel element, 275 lbs; and with a MURR fuel element, 285 lbs. The maximum gross weight of the package loaded with the ATR unassembled fuel plate payload is 290 lbs.

The ATR FFSC is a two part packaging consisting of the body and the closure. The body is a single weldment that features square tubing as an outer shell and round tubing for the payload cavity. Three 1-inch thick ribs maintain spacing between the inner and outer shells. The components of the packaging are shown in Figures 1.2-2, 1.2-3, and 1.2-4 and are described in more detail in the sections which follow. With the exception of several minor components, all steel used in the ATR FFSC is ASTM Type 304 stainless steel. Components are joined using full-thickness fillet welds (i.e., fillet welds whose leg size is nominally equal to the lesser thickness of the parts joined) and full and partial penetration groove welds.

1.2.1.1.1 ATR FFSC Body

The ATR FFSC body is a stainless steel weldment 73 inches long and 8 inches square weighing (empty) approximately 230 lbs. It consists of two nested shells; the outer shell a square stainless

[2] Title 10, Code of Federal Regulations, Part 71 (10 CFR 71), *Packaging and Transportation of Radioactive Material*, 1-1-06 Edition.

steel tube with a 3/16 inch wall thickness and the inner shell a 6 inch diameter, 0.120 inch wall, stainless steel round tube. There are three 1 inch thick stiffening plates secured to the round tube by fillet welds at equally spaced intervals. The tube is wrapped with thermal insulation and the insulation is overlaid with 28 gauge stainless steel sheet. The stainless steel sheet maintains the insulation around the inner shell. This insulated weldment is then slid into the outer square tube shell and secured at both ends by groove welds. Thermal insulation is built into the bottom end of the package as shown in Figure 1.2-3, and the closure provides thermal insulation at the closure end of the package as shown in Figure 1.2-4.

1.2.1.1.2 ATR FFSC Closure

The closure is a small component designed to be easily handled by one person. It weighs approximately 10 lbs and is equipped with a handle to facilitate use with gloved hands. The closure engages with the body using a bayonet style design. There are four lugs, uniformly spaced on the closure, that engage with four slots in the mating body feature. The closure is secured by retracting two spring loaded pins, rotating the closure through approximately 45°, and releasing the spring loaded pins such that the pins engage with mating holes in the body. When the pins are properly engaged with the mating holes the closure is locked.

A small post on the closure is drilled to receive a tamper indicating device (TID) wire. An identical post is located on the body and is also drilled for the TID wire. For ease in operation, there are two TID posts on the body. There are only two possible angular orientations for the closure installation and the duplicate TID post on the body enables TID installation in both positions.

A cover is placed over the closure handle during transport to render the handle inoperable for inadvertent lifting or tiedown. Figure 1.2-5 illustrates the placement of the handle cover. The profile of the cover depicted in Appendix 1.3.2, *Packaging General Arrangement Drawings*, is optional and may be modified to fit other handle profiles to ensure lifting and tiedown features are disabled as required by 10 CFR §71.45. As an option, the closure handle may be removed for transport rather than installing the handle cover.

1.2.1.1.3 ATR Fuel Handling Enclosure

The ATR Fuel Handling Enclosure (FHE) is a hinged thin gauge aluminum weldment used with the ATR fuel assembly, as illustrated in Figure 1.2-1. The ATR FHE is a cover used to protect the fuel from handling damage during ATR FFSC loading and unloading operations. It is a thin walled aluminum fabrication featuring a hinged lid and neoprene rub strips to minimize fretting of the fuel element side plates where they are in contact with the container.

During transport the ATR FHE is not relied upon to add strength to the package, or satisfy any safety requirement. For purposes of determining worst case reactivity, the ATR FHE is assumed to be not present.

1.2.1.1.4 MIT Fuel Handling Enclosure

The MIT FHE is comprised of two identical machined segments which surround the MIT fuel element secured by two end spacers and locked together using ball lock pins (see Figure 1.2-6). The primary purpose of end spacers is to secure the two sections of the FHE prior to loading the

FHE into the package. The location of the hole in the end plate of the spacer also facilitates easy removal of the FHE from the package. The MIT FHE is a cover used to protect the fuel from handling damage during ATR FFSC loading and unloading operations. It is an aluminum fabrication featuring machined segments and neoprene rub strips to minimize fretting of the fuel element side plates where they are in contact with the container.

During transport the MIT FHE, including the end spacers, is not relied upon to add strength to the package; however the enclosure does maintain the fuel element within a defined dimensional envelope.

1.2.1.1.5 MURR Fuel Handling Enclosure

The MURR FHE is very similar to the MIT FHE and is comprised of two identical machined segments which surround the MURR fuel element secured by two end spacers and locked together using ball lock pins (see Figure 1.2-7). The primary purpose of end spacers is to secure the two sections of the FHE prior to loading the FHE into the package. The location of the hole in the end plate of the spacer also facilitates easy removal of the FHE from the package. The MURR FHE is a cover used to protect the fuel from handling damage during ATR FFSC loading and unloading operations. It is an aluminum fabrication featuring machined segments and neoprene rub strips to minimize fretting of the fuel element side plates where they are in contact with the container.

During transport the MURR FHE, including the end spacers, is not relied upon to add strength to the package; however the enclosure does maintain the fuel element within a defined dimensional envelope.

1.2.1.1.6 ATR FFSC Loose Fuel Plate Basket

The Loose Plate Fuel Basket (LFPB) is comprised of four identical machined segments joined by threaded fasteners (reference Figure 1.2-12). The fasteners joining the segments in the lengthwise direction are permanently installed. The basket is opened/closed using the 8 hand tightened fasteners. For criticality control purposes during transport the loose fuel plate basket maintains the fuel plates within a defined dimensional envelope.

Additional aluminum plates may be used as dunnage to fill gaps between the fuel plates and the basket payload cavity. The dunnage is used for property protection purposes only.

1.2.1.2 Gross Weight

The maximum shipped weight of the ATR FFSC with the specified payload is detailed in Table 1.2-1. Further discussion of the gross weight is presented in Section 2.1.3, *Weights and Centers of Gravity*.

Table 1.2-1 – ATR FFSC Gross Weights

ATR FFSC With Payload	Gross Weight, lb
ATR FFSC with ATR Fuel Assembly	280
ATR FFSC with MIT Fuel Assembly	275
ATR FFSC with MURR Fuel Assembly	285
ATR FFSC with Loose Plate Payload	290

1.2.1.3 Neutron Moderator/Absorption

There are no moderator or neutron absorption materials in this package.

1.2.1.4 Heat Dissipation

The uranium aluminide payload produces a negligible thermal heat load. Therefore, no special devices or features are needed or utilized in the ATR FFSC to dissipate heat. A more detailed discussion of the package thermal characteristics is provided in Chapter 3.0, *Thermal*.

1.2.1.5 Protrusions

The closure handle protrudes 1 3/8-inches from the face of the closure. The handle is secured to the closure by means of four 10-24 UNC screws. The screws will fail prior to presenting any significant loading to either the closure engagement lugs or the locking pins.

On one face of the package body, two index lugs are secured to the package to facilitate stacking of the packages. The opposite face of the package has pockets into which the index lugs nest as illustrated in Figure 1.2-8. Each index lug is secured to the package by means of a 3/8-16 socket flat head cap screw. Under any load condition, the screw will fail prior to degrading the safety function of the package.

1.2.1.6 Lifting and Tiedown Devices

The ATR FFSC may be lifted from beneath utilizing a standard forklift truck when the package is secured to a fork pocket equipped pallet, or in a package rack. Swivel lift eyes may be installed in the package to enable package handling with overhead lifting equipment. The swivel eyes are installed after removing the 3/8-16 socket flat head cap screws and index lugs.

The threaded holes into which the swivel lift eyes are installed for the lifting the package are fitted with a 3/8-16 UNC screw and an index lug (see Figure 1.2-8) during transport. When the packages are stacked and the index lugs are nested in the mating pockets of the stacked packages, the index lugs can serve to carry shear loads between stacked packages.

1.2.1.7 Pressure Relief System

There are no pressure relief systems included in the ATR FFSC design. There are no out-gassing materials in any location of the package that are not directly vented to atmosphere. The package insulation, located in the enclosed volumes of the package, is a ceramic fiber. The insulation does not off-gas under normal or hypothetical accident conditions. The closure is not equipped with either seals or gaskets so that potential out-gassing of the FHE neoprene material and fuel element plastic bag material will readily vent without significant pressure build-up in the payload cavity.

1.2.1.8 Shielding

Due to the nature of the uranium aluminide payload, no biological shielding is necessary or specifically provided by the ATR FFSC.

1.2.2 Contents

The ATR FFSC is loaded with contents consisting of unirradiated fuel of three types (ATR, MIT, and MURR) and ATR loose fuel element plates.

1.2.2.1 ATR Fuel Element

Each ATR fuel element contains up to 1,200 g U-235, enriched up to 94% U-235. The weight percents of the remaining uranium isotopes are 1.2 wt.% U-234 (max), 0.7 wt.% U-236 (max), and 5.0-7.0 wt.% U-238. The fuel element (ATR Mark VII) fissile material is uranium aluminide (UAl_x). The fuel element weighs not more than 25 lbs, is bagged, and is enclosed in the ATR FHE weighing 15 lbs.

There are four different ATR Mark VII fuel element types designated 7F, 7NB, 7NBH, and YA. The construction of these fuel elements are identical, varying only in the content of the fuel matrix. In the 7F fuel element, all 19 fuel plates are loaded with enriched uranium in an aluminum matrix with the eight outer plates (1 through 4 and 16 through 19) containing boron as a burnable poison. The fuel element with the greatest reactivity is the 7NB which contains no burnable poison. The 7NBH fuel element is similar to the 7NB fuel element except that it contains one or two borated plates. The YA fuel element is identical to the 7F fuel element except that plate 19 of the YA fuel element is an aluminum alloy plate containing neither uranium fuel nor boron burnable poison. The total U-235 and B-10 content of the YA fuel element is reduced accordingly. A second YA fuel element design (YA-M) has the side plate width reduced by 15 mils.

The ATR fuel elements contain 19 curved fuel plates. A section view of an ATR fuel element is given in Figure 1.2-9. The fuel plates are rolled to shape and swaged into the two fuel element side plates. Fuel plate 1 has the smallest radius, while fuel plate 19 has the largest radius. The fissile material (uranium aluminide) is nominally 0.02-in thick for all 19 plates. Fuel element side plates are fabricated of ASTM B 209, aluminum alloy 6061-T6 or 6061-T651 and are approximately 0.19-in thick. The fuel plates are typically spaced with a 0.08-in gap between plates.

1.2.2.2 MIT Fuel Element

Each MIT element contains up to 515 g U-235, enriched up to 94 wt.%. The weight percents of the remaining uranium isotopes are 1.2 wt.% U-234, 0.7 wt.% U-236, and 5.0-7.0 wt.% U-238. Like the ATR fuel element, the MIT fuel element fissile material is uranium aluminide (UAl_x). The fuel element weighs not more than 10 lbs, is bagged, and is enclosed in the MIT FHE weighing 25 lbs.

Each MIT fuel element contains 15 flat fuel plates, as shown in Figure 1.2-10. The fuel plates are fabricated and swaged into the two fuel element side plates. The fuel "meat" is a mixture of uranium metal and aluminum, while the cladding and structural materials are an aluminum alloy. The fissile material (uranium aluminide) is nominally 0.03-in thick and the cladding is nominally 0.025-in thick. Fuel element side plates are fabricated of ASTM B 209, aluminum alloy 6061-T6 and are approximately 0.19-in thick. The fuel plates are nominally 0.08 inches apart.

1.2.2.3 MURR Fuel Element

Each MURR element contains up to 785 g U-235, enriched up to 94 wt.%. The weight percents of the remaining uranium isotopes are 1.2 wt.% U-234, 0.7 wt.% U-236, and 5.0-7.0 wt.% U-238. Like the ATR fuel element, the MURR fuel element fissile material is uranium aluminide (UAl_x). The fuel element weighs not more than 15 lbs, is bagged, and is enclosed in the MURR FHE weighing 30 lbs.

Each MURR fuel element contains 24 curved fuel plates. Fuel plate 1 has the smallest radius, while fuel plate 24 has the largest radius, as shown in Figure 1.2-11. The fuel "meat" is a mixture of uranium metal and aluminum, while the cladding and structural materials are an aluminum alloy. The fuel plates are rolled to shape and swaged into the two fuel element side plates. The fissile material (uranium aluminide) is nominally 0.02-in thick for all 24 plates. Fuel element side plates are fabricated of ASTM B 209, aluminum alloy 6061-T6 or 6061-T651 and are approximately 0.15-in thick. The fuel plates are typically spaced with a 0.08-in gap between plates.

1.2.2.4 Loose Fuel Plates

The maximum weight of the loose plate payload (Figure 1.2-12) is 50 lbs. This weight is made up of the maximum basket contents weight of 20 lbs and the loose fuel plate basket weight of 30 lbs.

The loose plate payload is limited to 600 grams U-235. The plates may only be for the ATR fuel elements. The plates may either be flat or rolled to the geometry required for assembly into the fuel element. For handling convenience, the loose plate basket will be loaded with either flat or rolled plates. Additionally, the plates may be banded or wire tied in a bundle.

1.3 Appendix

1.3.1 Glossary of Terms

ANSI –	American National Standards Institute.
ASME B&PV Code –	American Society of Mechanical Engineers Boiler and Pressure Vessel Code.
ASTM –	American Society for Testing and Materials.
AWS –	American Welding Society.
HAC –	Hypothetical Accident Conditions.
NCT –	Normal Conditions of Transport.
Closure –	The ATR FFSC package component used to close the package.
Body –	The ATR FFSC package component which houses the payload.
Fuel element	Fuel element and fuel assembly are used interchangeably throughout this document to be the ATR, MIT, or MURR fuel element as described in Section 1.2.2, *Contents*.
Index lug –	A thick washer like component secured to the package body at the lift point locations. The index lug provides shear transfer capability between stacked packages.
Pocket –	A recessed feature on the package body that accepts the index lug when packages are stacked.
Fuel Handling Enclosure (FHE)–	Aluminum fabrications used to protect the ATR, MIT, and MURR fuel elements from handling damage. The enclosures are faced with neoprene at locations where the fuel element contacts the FHE to minimize fretting of the fuel element at the contact points.
Loose plate basket –	A machined aluminum container in which the unassembled fuel element plates are secured during transport in the ATR FFSC. The loose plate basket is a geometry based criticality control component.

1.3.2 Packaging General Arrangement Drawings

The packaging general arrangement drawings consist of:

- 60501-10, *ATR Fresh Fuel Shipping Container SAR Drawing,* 5 sheets
- 60501-20, *Loose Plate Basket Assembly ATR Fresh Fuel Shipping Container SAR Drawing,* 1 sheet
- 60501-30, *Fuel Handling Enclosure, ATR Fresh Fuel Shipping Container SAR Drawing,* 1 sheet
- 60501-40, *MIT Fuel Handling Enclosure, ATR Fresh Fuel Shipping Container SAR Drawing,* 1 sheet
- 60501-50, *MURR Fuel Handling Enclosure, ATR Fresh Fuel Shipping Container SAR Drawing,* 1 sheet.

2.0 STRUCTURAL EVALUATION

This section presents evaluations demonstrating that the ATR FFSC package meets all applicable structural criteria. The ATR FFSC packaging, consisting of the body and closure, is evaluated and shown to provide adequate protection for each payload; the ATR fuel element, MIT fuel element, MURR fuel element, or ATR loose fuel plates. Each fuel element is contained within a corresponding fuel handling enclosure (FHE). The loose fuel plate basket (LFPB) is evaluated to contain only loose fuel plates associated with the ATR fuel element.

Normal conditions of transport (NCT) and hypothetical accident condition (HAC) evaluations are performed to address 10 CFR §71[1] performance requirements primarily through physical testing. Physical demonstration by testing, including the free drop and puncture events, consists of certification testing utilizing two full-scale certification test units (CTU-1 and CTU-2). CTU-1 included the ATR fuel element payload and CTU-2 included the ATR LFPB and loose plates payload. Certification testing has demonstrated that the key performance objective of criticality control will be met by the ATR FFSC package. Details of the certification test program are provided in Appendix 2.12.1, *Certification Tests on CTU-1*, and Appendix 2.12.2, *Certification Tests on CTU-2*. The evaluation for the MIT and MURR fuel elements is provided in Appendix 2.12.3, *Structural Evaluation for MIT and MURR Fuel.*

2.1 Structural Design

2.1.1 Discussion

The ATR FFSC is a two part packaging consisting of the body and the closure. The body is a single weldment that features square tubing as an outer shell and round tubing for the payload cavity. The closure engages with the body using a bayonet style design. There are four lugs, uniformly spaced on the closure that engages with four slots in the mating body feature. The closure is secured by retracting two spring loaded pins, rotating the closure through approximately 45°, and releasing the spring loaded pins such that the pins engage with mating holes in the body. When the pins are properly engaged with the mating holes the closure is locked.

With the exception of several minor components, all steel used in the ATR FFSC packaging is of a Type 304 stainless steel. Components are joined using full-thickness fillet welds (i.e., fillet welds whose leg size is nominally equal to the lesser thickness of the parts joined) and full and partial penetration groove welds. The fuel containers for the package, the FHEs and the LFPB, are principally of aluminum construction and secured with stainless steel fasteners. The FHEs are a fabrication and the LFPB consists of four machined aluminum components.

A comprehensive discussion of the ATR FFSC packaging design and configuration is provided in Section 1.2, *Package Description.*

[1] Title 10, Code of Federal Regulations, Part 71 (10 CFR §71), *Packaging and Transportation of Radioactive Material*, 01-01-06 Edition.

Table 2.1-1 – ATR FFSC Component Weights

Item	Weight, lb	
	Component	Assembly
ATR FFSC Packaging	- -	240
Body Assembly	230	- -
Closure Assembly	10	- -
Payload – ATR Fuel Assembly	- -	40
ATR Fuel Assembly	25	- -
ATR Fuel Handling Enclosure	15	- -
Payload – MIT Fuel Assembly	- -	35
MIT Fuel Assembly	10	- -
MIT Fuel Handling Enclosure	25	- -
Payload – MURR Fuel Assembly	- -	45
MURR Fuel Assembly	15	- -
MURR Fuel Handling Enclosure	30	- -
Payload – Fuel Plates	- -	50
ATR Loose Fuel Plates (including optional dunnage)	20	- -
Loose Fuel Plate Basket	30	- -
Total LFPB Loaded Package (maximum)	- -	290
Total MURR Loaded Package	- -	285
Total ATR Loaded Package	- -	280
Total MIT Loaded Package	- -	275

2.1.4 Identification of Codes and Standards for Package Design

As a Type AF package, the ATR FFSC is designed to meet the performance requirements of 10 CFR 71, Subpart E. Compliance with these requirements is demonstrated via full scale testing of the package under both NCT and HAC, as documented in Section 2.12, *Appendices*. In addition, structural materials which are important to safety are specified using American Society for Testing and Materials (ASTM) standards as shown on the drawings in Appendix 1.3.2, *Packaging General Arrangement Drawings*. Welding procedures and personnel are qualified in accordance with the ASME Code, Section IX. All welds are visually examined on each pass per the requirements of AWS D1.6:1999[2] for stainless steel and AWS D1.2:2003[3] for aluminum. All welds which are important to safety are examined by liquid penetrant test on the final pass using procedures compliant with ASTM E165-02[4].

[2] ANSI/AWS D1.6:1999, *Structural Welding Code – Stainless Steel*, American Welding Society (AWS).

[3] ANSI/AWS D1.2:2003, *Structural Welding Code – Aluminum*, American Welding Society (AWS)

[4] American Society for Testing and Materials (ASTM International), ASTM E165-02, *Standard Test Method for Liquid Penetrant Examination*, Feb 2002.

2.12.3 Structural Evaluation for MIT and MURR Fuel

The ATR FFSC may be utilized to transport a MIT fuel assembly or a MURR fuel assembly. Both of these fuels are high-enriched aluminum-clad uranium aluminide plate type fuel elements similar to the ATR fuel evaluated in this chapter. Since no MIT or MURR fuel elements were included in the drop tests, the following evaluation conservatively estimates a degree of failure and movement of the MIT and MURR Fuel Handling Enclosures (FHE) to develop a worst case pitch expansion of the corresponding fuel elements for evaluation in Section 6.10, *Criticality Analysis for MIT and MURR Fuel*. By conservatively bounding potential damage and evaluating the exceptional worst case pitch expansion of the MIT and MURR fuel elements the ATR FFSC complies with the performance requirements of 10 CFR §71.

2.12.3.1 Structural Design Discussion

A comparison is provided to highlight the similarities and differences between the MIT and MURR designs and the physically tested ATR design. Through this comparison, it is expected that both NCT and HAC testing would result in similar results for the MIT and MURR fuel elements. Similar to the ATR LFPB, the MIT and MURR FHEs are designed to restrict postulated fuel element pitch expansion under the HAC conditions.

The results of NCT conditions on the MIT and MURR payload are assumed to be equivalent to the ATR payload; i.e. there is no damage to the FHE or fuel element under NCT.

For conservatism in evaluating the HAC conditions, the MIT and MURR FHE damage postulated exceeds the results obtained during testing of the ATR payloads. The MIT and MURR FHEs are assumed to separate (fail) and spread apart to permit a worst case reactivity configuration of the fuel elements. The individual fuel plates of the fuel elements are assumed to spread apart uniformly to fill the resulting space.

2.12.3.1.1 Fuel Elements

The ATR FFSC packaging is not modified for the use of the MIT and MURR fuel elements. The MIT and MURR FHE are used in place of the ATR FHE or the LFPB within the ATR FFSC packaging. Similar to the ATR FHE and LFPB, the MIT and MURR FHEs are principally fabricated of aluminum construction and secured with stainless steel locking pins.

The MIT and MURR fuel elements are very similar to the ATR fuel element in design, materials, and fabrication. The weight of the fuel elements are 10 lb, 15 lb, and 25 lb, for the MIT, MURR, and ATR fuel elements respectively. All three fuel elements are fabricated of the same fuel type, aluminum-clad uranium aluminide fuel plates, with all fuel plates swaged into the side plates, and include cast or wrought aluminum end boxes. As such, the structural performance of the MIT and MURR fuel types are anticipated to behave very similarly to the ATR fuel element. Table 2.12.3-1 compares the three fuel element design dimensions. Figure 2.12.3-1 compares the three fuel elements in their overall length and fuel plate length in inches. In this figure, the inside dimension identifies the fuel plate length.

For comparative purposes, an approximate moment of inertia is calculated for all three fuel elements using AutoCAD®. The results are presented in Figure 2.12.3-2. The values were determined by taking a cross section of the fuel plate region and selecting the solid boundaries to compute the moments of inertia about the identified axes.

The comparison of the moments of inertia demonstrates that the three fuel elements are similar in stiffness and expected to perform in a similar fashion during NCT and HAC drop events. The length and weight of the fuel elements is clearly bounded by the ATR fuel element. The materials of construction and fabrication techniques are the same for each fuel type. The relatively minor dimensional changes of the ATR fuel element plates as a consequence of the testing identified in Section 2.6, *Normal Conditions of Transport*, and Section 2.7, *Hypothetical Accident Conditions*, further justifies the similar performance of the MIT and MURR fuel elements.

Table 2.12.3-1 –Fuel Element Design

Component	MIT	MURR	ATR
Approximate Weight, lbs	10	15	25
Number of Fuel Plates	15	24	19
Nominal Plate Spacing, in.	.08	.08	.08
Fuel Plate Length, in.	23.00	25.50	49.50
Fuel Plate Thickness, in.	.08	.05	.05, .08, .10
Approximate Fuel Plate Width, in.	2.5	2.0 - 4.3	2.0 – 3.9

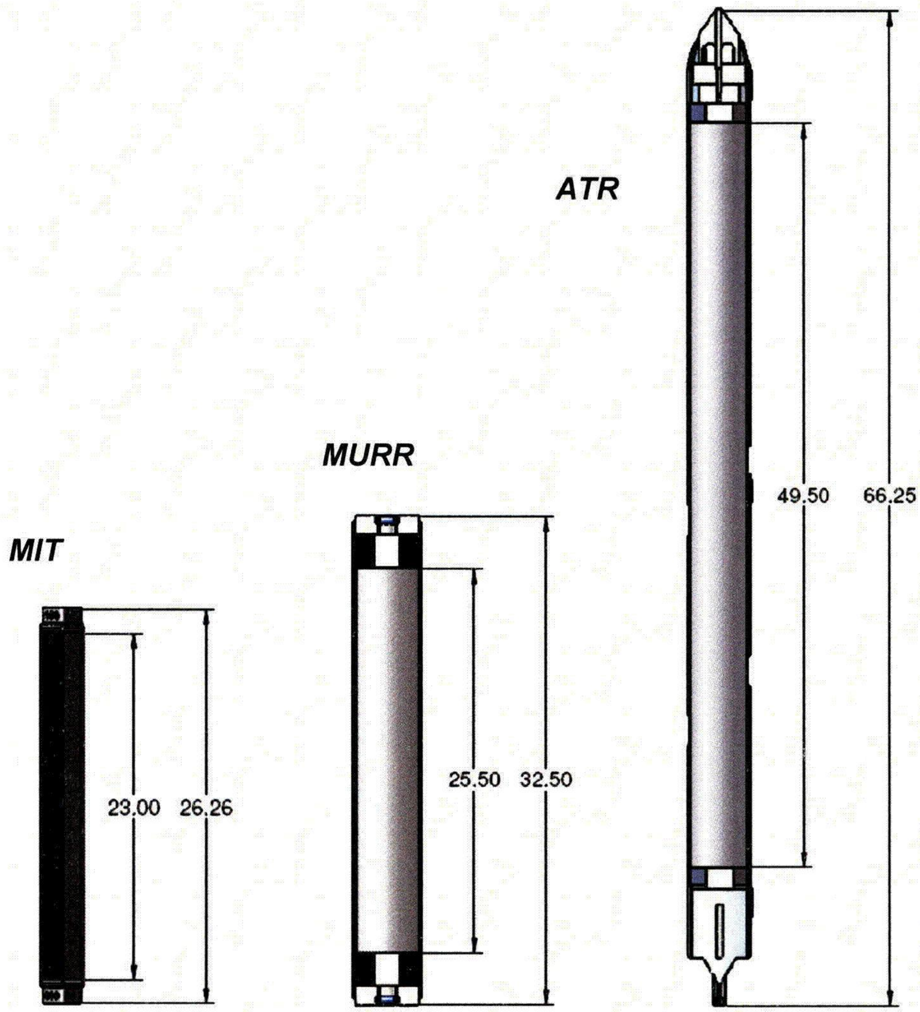

Figure 2.12.3-1 – MIT, MURR, and ATR Fuel Elements

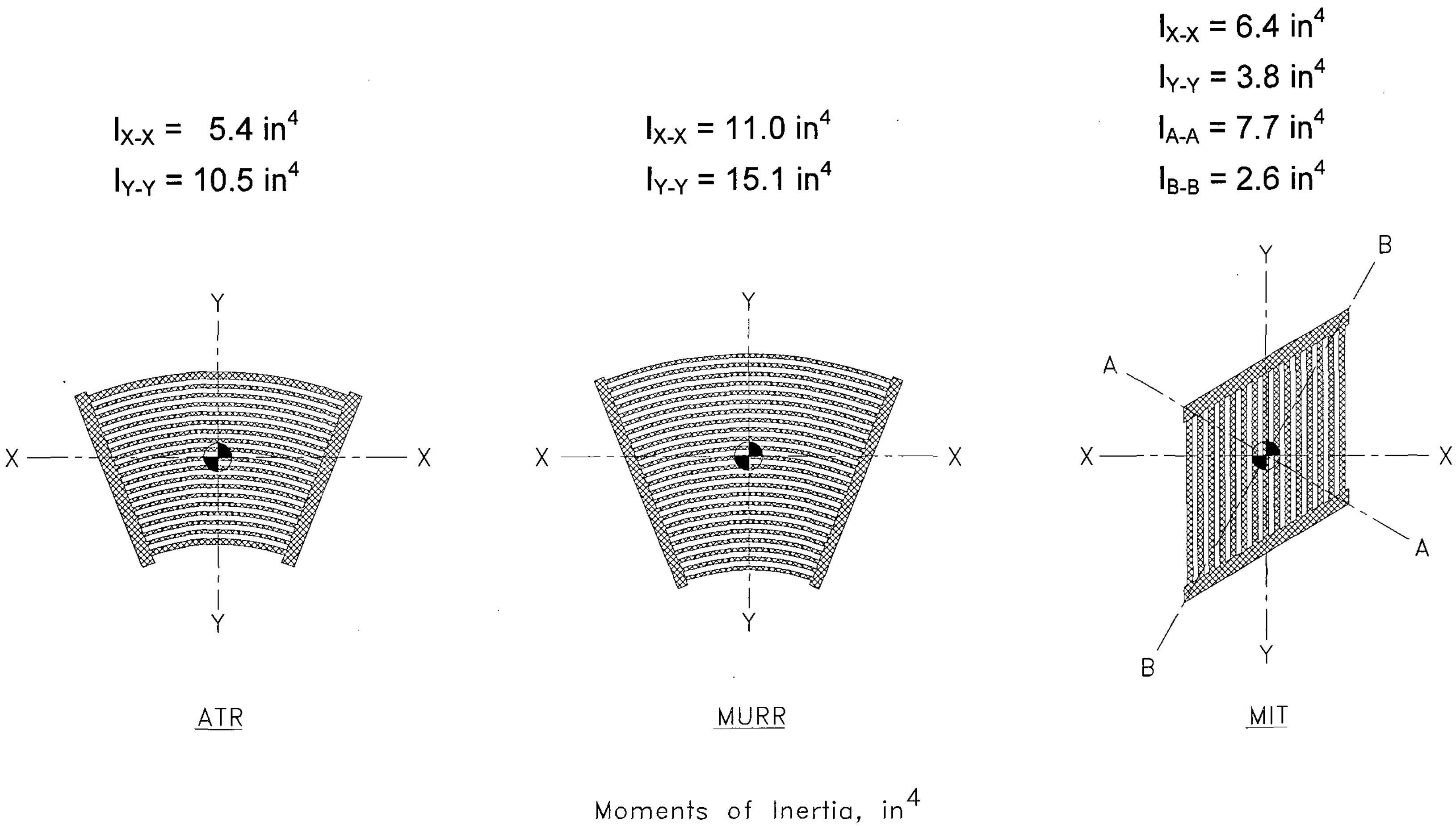

Figure 2.12.3-2 – Fuel Element Moments of Inertia

2.12.3.1.2 Fuel Handling Enclosures

The MIT FHE incorporates two end spacers and a two-piece machined aluminum enclosure to protect the MIT fuel element from damage during loading and unloading operations. The enclosure halves are identical segments machined from 6061 aluminum plate. Neoprene rub strips are used to cushion the contact points between the fuel element and enclosure. The end spacers are also fabricated of 6061 aluminum. The end spacers lock the enclosure halves together and are secured using stainless steel ball lock pins. The end spacers also prevent axial movement since the MIT fuel element is much shorter than the package cavity. The weight of the MIT FHE is 25 lb. Figure 2.1-3 illustrates the assembly view of the MIT FHE.

The MURR FHE is designed in the same manner as the MIT FHE. The weight of the MURR FHE is 30 lb. Figure 2.1-4 illustrates the assembly view of the MIT FHE.

The MIT and MURR FHE design is similar to the 30-lb LFPB in that it utilizes machined enclosure halve segments to encase the payload. The use of the enclosure halves makes the MIT and MURR FHEs more robust than the ATR FHE, which weighs 15 lb. The wall thickness of the enclosure halves is 0.19 in compared to the 0.09 in thick sheet used in the ATR FHE. For comparison, the typical machined wall thickness of the LFPB is also 0.19 in thick. The weight of the enclosures and fuel elements are 35 lb, 45 lb, 40 lb, and 50 lb for the MIT payload, MURR payload, ATR payload, and LFPB payload respectively.

Based on the similarity in design and function, the structural and thermal performance of the MIT and MURR FHEs is anticipated to be similar to the physical testing performed using the ATR FHE and LFPB.

2.12.3.1.3 Loose Fuel Plates

MIT and MURR loose fuel plates are not evaluated for use within the LFPB.

2.12.3.2 Allowable Damage

For HAC tests the MIT and MURR fuel elements are anticipated to perform in a similar manner to the ATR fuel element based on the comparable designs and assembly techniques. To conservatively encompass potential damage, the FHE halves are considered to separate while each half is sized at the extreme tolerances to encourage the maximum space around each fuel element. Based on the maximum space developed by the separated FHE, the fuel element plates separate to create a more reactive configuration for the fuel. The proposed pitch expansion greatly exceeds the results of the physical testing performed on the ATR fuel element.

Axial movement of the fuel element within the package inner tube, which occurs by hypothetical neglect of the FHE end spacers, has no adverse effect on the performance of the ATR FFSC. Energy dissipated by failure of the spacers would result in lowering the HAC loads to the MIT and MURR elements. However, the structural tests identified that the ATR fuel element survives the impact loads with damage that has no impact on reactivity. The MURR and MIT fuel elements are of similar materials and of similar construction to the ATR fuel elements. Assuming the spacers to fail with no energy absorption, the impact velocities of the MURR and MIT FHEs on the end fitting of the package would be nearly identical. It is therefore concluded that the damage to MURR and MIT fuel elements is bounded by the damage sustained by the ATR fuel element in the structural tests. However, for conservatism, the fuel plate pitch of the MURR and MIT elements is set to the condition that results in the worst case reactivity under the volumetric constraints presented by the FHEs.

The HAC criticality array model is a 5x5x1 array of packages and all fuel elements are positioned at the same axial location. The FHE end spacers are conservatively neglected and modeled as water. Axial shifting of fuel elements from the modeled configuration would result in a less reactive condition; therefore, failure of the FHE end spacers is not a criticality concern. For the thermal evaluation, the position of the MIT or MURR fuel element is naturally bounded by the ATR fuel element since its length extends to each end of the package.

The modeled separation of the FHE halves inside the inner tube of the package is determined by using the maximum inner diameter of the package's inner tube and the minimum outer radius of each FHE half as illustrated in Figures 2.12.3-3 and 2.12.3-4. The FHE cavity dimensions are expanded using the maximum tolerance of the parts. Note that this is only hypothetically possible, since this causes the corners of the FHE for both the MIT and MURR to exceed the point of interference with the inner tube wall.

The dimensions for the criticality model of the MIT FHE are determined in the following manner:

- Package inner tube maximum inside diameter: Diameter is specified as 6.0 in. OD X 0.12 in. wall thickness ± 0.030 in. OD and ± 10% thickness (per drawing 60501-10 and ASTM A269). Resulting maximum ID is 5.814 in.
- Minimum outside radius of the FHE half: Radius is specified as 2.8 in ± 0.2 (per drawing 60501-40). Resulting minimum radius is 2.6 in.
- Minimum wall thickness of the FHE half: Wall is specified as 0.19 in ± 0.06 (per drawing 60501-40). Resulting minimum thickness is 0.13 in.
- Maximum cavity height of the FHE half: Wall height specified as 2.82 in ± 0.06 (per drawing 60501-40). Resulting maximum height is 2.88 in. (which is greater than the 2.6 maximum radius).
- Maximum cavity width of the FHE half: Wall width specified as 1.62 in ± 0.06 (per drawing 60501-40). Resulting maximum width is 1.68 in.

The dimensions for the criticality model of the MURR FHE are determined in the following manner:

- Package inner tube maximum inside diameter: Diameter is specified as 6.0 in. OD X 0.12 in. wall thickness ± 0.030 in. OD and ± 10% thickness (per drawing 60501-10 and ASTM A269). Resulting maximum ID is 5.814 in.
- Minimum outside radius of the FHE half: Radius is specified as 2.8 in ± 0.2 (per drawing 60501-50). Resulting minimum radius is 2.6 in.
- Minimum wall thickness of the FHE half: Wall is specified as 0.19 in ± 0.06 (per drawing 60501-50). Resulting minimum thickness is 0.13 in.
- Maximum cavity height of the FHE half: Wall height specified as 2.00 in ± 0.06 (per drawing 60501-50). Resulting maximum height is 2.06 in.

- Maximum cavity width of the FHE half: Wall width specified as 1.85 in ± .06 (per drawing 60501-50). Resulting maximum width is 1.91 in.

The thermal evaluation in Section 3.6, *Thermal Evaluation for MIT and MURR Fuel*, makes the following conservative assumptions to bound damage to the fuel elements and FHEs as a result of NCT and HAC events.

- Idealized contact between the FHE and the package inner tube. The majority of the heat input to the fuel element comes from the radial direction rather than the axial direction. By maximizing the contact, the greatest heat is transferred. Deformation of the payload would have the effect of reducing the contact area, and therefore reducing the conductive heat input.
- Axial movement of the fuel element, as a result of deformation of the FHE end spacers has a negligible effect. The majority of the heat input to the fuel element comes from the radial direction rather than the axial direction (ends). As the fuel element moves closer to the ends of the package the heat input rises. However, the heat input from either end of the package is negligible compared to the heat input received axially from the sides. Furthermore, any credible axial distance of the MIT and MURR fuel elements to the end of the package is bounded by the ATR fuel element.

The criticality evaluation in Section 6.10, *Criticality Analysis for MIT and MURR Fuel*, makes the following conservative assumptions to bound damage to the fuel element as a result of HAC events.

- Neglecting the function of the end spacers, the two halves are pushed apart to the maximum extent to maximize the available space for pitch expansion.
- Although it is not feasible in actual practice to push the FHEs to the center of the array if the two FHE halves are already pushed apart, both the MIT and MURR models are shifted by 0.307-in towards the center of the array.
- Fuel element end boxes are not modeled. For criticality purposes, any amount of damage to the end boxes is acceptable.
- Note that the MIT and MURR FHEs are "sliced off" in the corners because such a translation is not possible without interference.

Due to the conservative assumptions utilized for the thermal and criticality evaluations, the allowable damage to the FHEs is considered severe and therefore far exceeding the physical testing results performed using the ATR fuel element and LFPB payloads covered in Section 2.12.1, *Certification Tests on CTU-1*, and Section 2.12.2, *Certification Tests on CTU-2*.

For containment purposes, the MIT and MURR fuel element plates must remain intact to prevent the fuel meat from within the fuel plate from exiting the package. The MIT and MURR fuel elements are fully supported over the length of the fuel plates by the FHE enclosure halves. The enclosure halves are specifically designed to fully support each fuel element and minimize any deformation or change in the fuel plate geometry. By design the MIT and MURR FHEs are more robust (thicker side walls) than the ATR FHE and therefore provide better support compared to the testing performed using the ATR fuel element and ATR FHE.

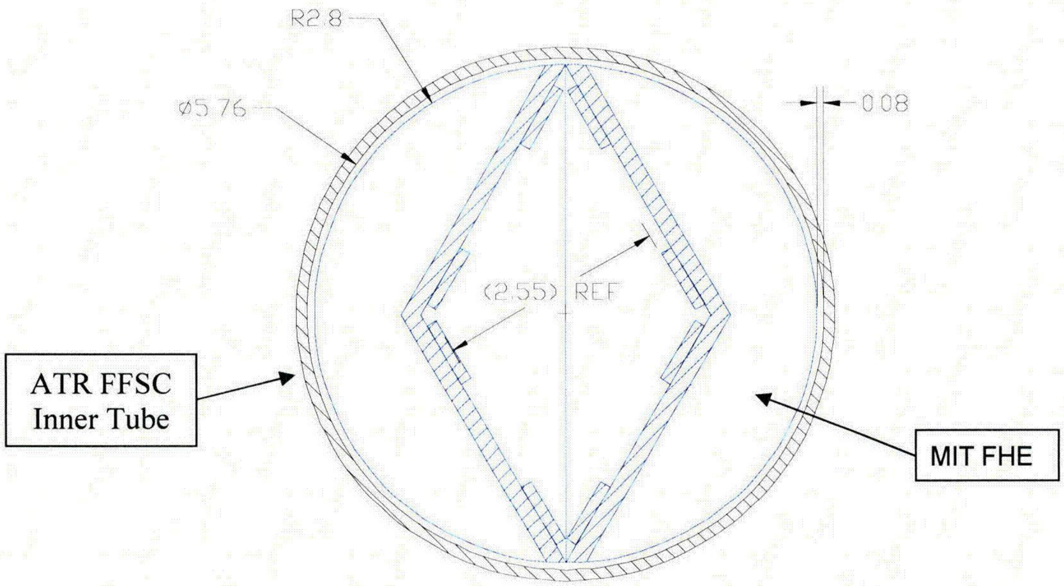

Nominal MIT FHE Dimensions

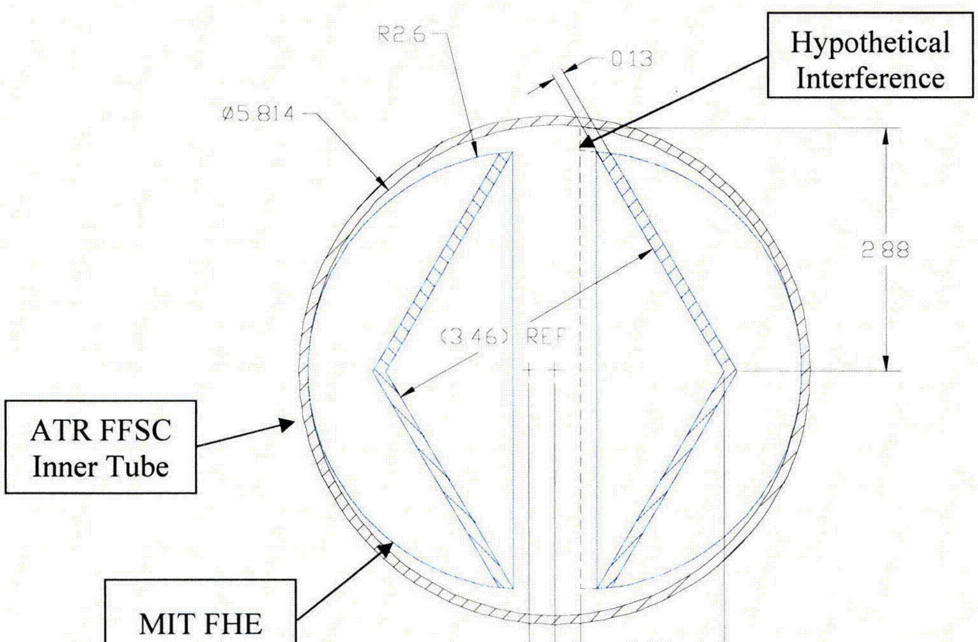

Maximum Tolerances Incorporated to Separate FHE Halves

Figure 2.12.3-3 – MIT FHE Damage

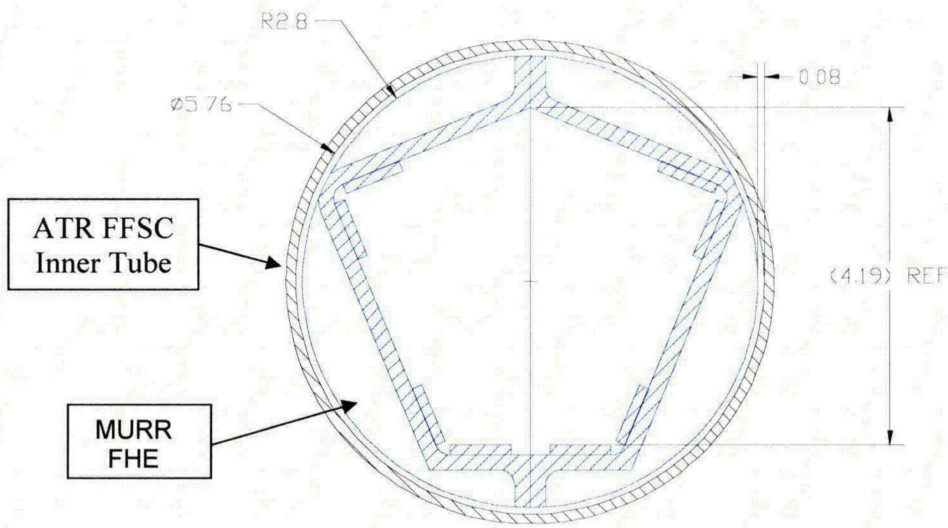

Nominal MURR FHE Dimensions

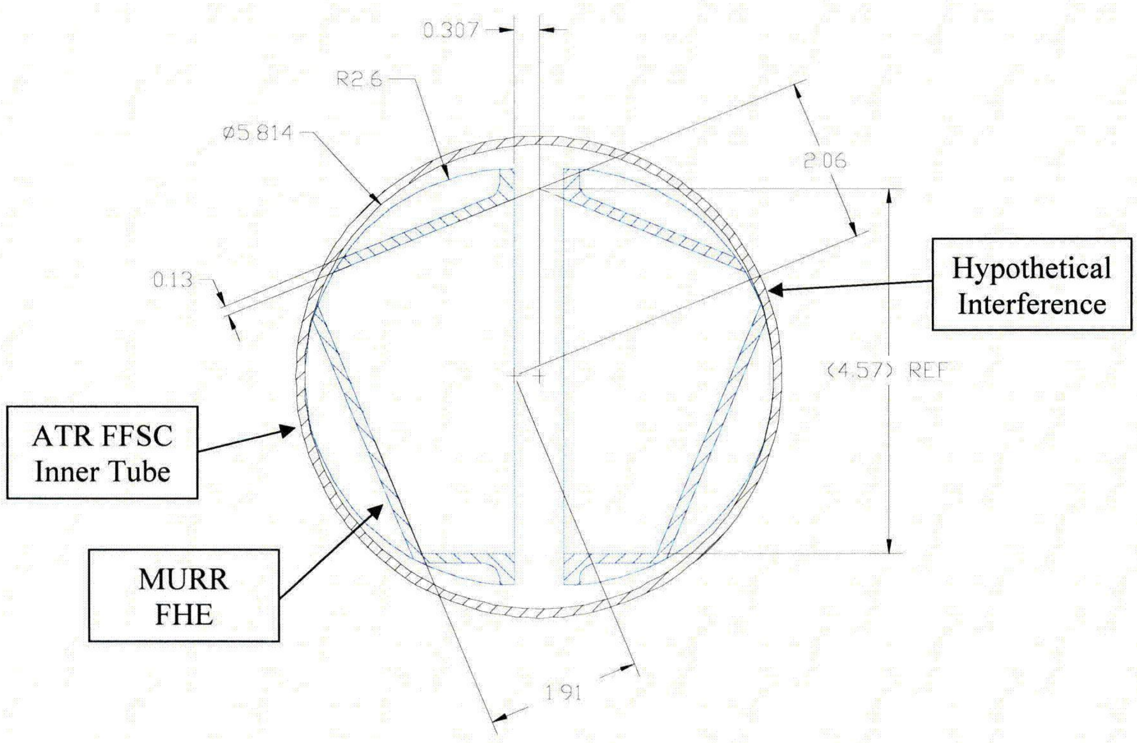

Maximum Tolerances Incorporated to Separate FHE Halves

Figure 2.12.3-4 – MURR FHE Damage

3.6 Thermal Evaluation for MIT and MURR Fuel Elements

This section identifies and describes the principal thermal design aspects of the ATR FFSC for the transport of one assembled MIT fuel element, one assembled MURR fuel element. The evaluation presented herein demonstrates that the thermal performance of the ATR FFSC when transporting these fuel element payloads is bounded by the temperatures reported for the transport of the ATR fuel element payload. Specifically, the evaluations presented herein demonstrate the thermal safety of the ATR FFSC package[30] complies with the thermal requirements of 10 CFR 71[31] when transporting a payload consisting of either an assembled, unirradiated MIT fuel element, or an assembled, unirradiated MURR fuel element.

All package components are shown to remain within their respective temperature limits under the normal conditions of transport (NCT). Further, per 10 CFR §71.43(g), the maximum temperature of the accessible package surfaces is demonstrated to be less than 122 °F for the maximum decay heat loading, an ambient temperature of 100 °F, and no insolation. Finally, the ATR FFSC package is shown to retain sufficient thermal protection following the HAC free and puncture drop scenarios to maintain all package component temperatures within their respective short term limits during the regulatory fire event and subsequent package cool-down.

3.6.1 Description of Thermal Design

The ATR FFSC package, as described and illustrated in Chapter 1.0, *General Information*, consists of three basic components: 1) a Body assembly, 2) a Closure assembly, and 3) either a Fuel Handling Enclosure (FHE) or a Loose Fuel Plate Basket (LFPB). The FHE is configured to house an assembled MIT or MURR fuel element, while the LFPB is configured to house loose ATR fuel element plates. The maximum gross weight of the package loaded with a MIT FHE and MIT fuel element is approximately 275 lbs and 285 lbs when loaded with a MURR FHE and MURR fuel element. The maximum gross weight of the package loaded with a LFPB containing its maximum payload of loose ATR fuel plates is approximately 290 lbs.

The ATR FFSC is designed as a Type AF packaging. The packaging is rectangular in shape and is intended to be transported in racks of multiple packages by highway truck. Since the payload generates essentially no decay heat, the worst case thermal conditions will occur with an individual package fully exposed to ambient conditions. The package performance when configured in a rack of multiple packages will be bounded by that seen for an individual package.

The thermal design aspects of the principal components of the packaging are described in more detail in Section 3.1, *Description of Thermal Design*. The paragraphs below present the thermal design features of the MIT and MURR fuel elements and their associated FHEs.

---

[30] In the remainder of this chapter, the term 'packaging' refers to the assembly of components necessary to ensure compliance with the regulatory requirements, but does not include the payload. The term 'package' includes both the packaging components and the payload of ATR fuel.

[31] Title 10, Code of Federal Regulations, Part 71 (10 CFR 71), *Packaging and Transportation of Radioactive Material*, 01-01-03 Edition.

3.6.2 Design Features

3.6.2.1 MIT FHE

The MIT FHE is a machined, two-piece aluminum enclosure used to protect the MIT fuel element from damage during loading and unloading operations. The FHE consists of two identical machined segments fabricated from 3-inch 6061 aluminum plate stock. The FHE features neoprene rub strips to minimize fretting of the fuel element side plates where they contact the FHE. The FHE is neither anodized nor coated, but is left as unfinished aluminum. Spacer weldments on either end of the enclosure halves are used to position and support the MIT FHE within the ATR FFSC cavity. The spacers are also fabricated of 6061 aluminum. Figure 1.2-6 presents an exploded view of the MIT FHE and its spacers. Figure 1.2-10 presents a section view of a MIT fuel element. A polyethylene bag is used as a protective sleeve over the MIT fuel element.

3.6.2.2 MURR FHE

The MURR FHE is also a machined, two-piece aluminum enclosure used to protect the MURR fuel element from damage during loading and unloading operations. Like the MIT FHE, the two identical machined segments of the MURR FHE are fabricated from 3-inch 6061 aluminum plate stock and features neoprene rub strips to minimize fretting of the fuel element side plates. The FHE is neither anodized nor coated, but is left as unfinished aluminum. Spacer weldments on either end of the enclosure halves are used to position and support the FHE within the ATR FFSC cavity. The spacers are also fabricated of 6061 aluminum. Figure 1.2-7 presents an exploded view of the MURR FHE and its spacers. Figure 1.2-11 presents a section view of a MURR fuel element. A polyethylene bag is used as a protective sleeve over the MURR fuel element.

3.6.3 Content's Decay Heat

The ATR FFSC is designed as a Type AF packaging for transportation of an unirradiated fuel elements or a bundle of loose, unirradiated fuel plates. The decay heat associated with un-irradiated fuel is negligible. Therefore, no special devices or features are needed or utilized in the ATR FFSC packaging to dissipate the decay heat. Section 1.2.2, *Contents*, provides additional details regarding the potential contents of the ATR FFSC.

3.6.4 Summary Tables of Temperatures

Table 3.6-1 provides a summary of the maximum package component temperatures achieved under NCT and HAC conditions for either the MIT or MURR fuel element payloads. These temperatures are bounded by those reported in Table 3.1-1 for the transport of the ATR fuel element payload.

The temperatures for NCT are based on an analytical model of the ATR FFSC package under extended operation with an ambient temperature of 100°F and a diurnal cycle for the insolation loading. The temperatures for HAC are based on an analytical model of the ATR FFSC package with the worst-case, hypothetical pre-fire damage as predicted based on drop tests using full-scale certification test units (CTUs).

The results for NCT demonstrate that significant thermal margin exists for all package components. This is expected since the only significant thermal loads on the package arise from insolation and ambient temperature changes. The payload dissipates essentially zero decay heat. Further, the evaluations for NCT demonstrate that the package skin temperature will be below the maximum temperature of 122°F permitted by 10 CFR §71.43(g) for accessible surface temperature in an nonexclusive use shipment when transported in a 100°F environment with no insolation.

The results for HAC conditions also demonstrate that the design of the ATR FFSC package provides sufficient thermal protection to yield component temperatures that are significantly below the acceptable limits defined for each component. While the neoprene rubber and polyethylene plastic material used to protect the fuel element from damage are expected to reach a sufficient temperature level during the HAC fire event to induce thermal decomposition, the loss of these components is not critical to the safety of the package.

3.6.5 Summary Tables of Maximum Pressures

Table 3.6-2 presents a summary of the maximum pressures achieved under NCT and HAC conditions. Since the ATR FFSC package is a vented package, both the maximum normal operating pressure (MNOP) and the maximum pressure developed within the payload compartment under the HAC condition are 0 psig.

Although the volume between the outer and inner shells is sealed, it does not contain organic or other materials that may outgas or thermally decompose. Therefore, the maximum pressure that may develop within the space will be limited to that achieved due to ideal gas expansion. The maximum pressure rise under NCT will be less than 4 psig, while the pressure rise under HAC conditions will be 38 psig.

surface and the solar absorptivity (α) value for the exterior surface. The 6061-0 aluminum used for the MIT and MURR fuel components are assumed to have a surface coating of boehmite ($Al_2O_3H_2O$). A 25 μm boehmite film will exhibit a surface emissivity of approximately 0.92 [36]. While a fresh fuel element may have a lower surface emissivity, the use of the higher value will provide a conservative estimate of the temperatures achieved during the HAC event.

3.6.6.2 Technical Specifications of Components

The materials used in the ATR FFSC that are considered temperature sensitive include the aluminum used for the FHEs, the LFPB, and the fuel elements, the neoprene rubber, and the polyethylene wrap used as a protective sleeve around the fuel elements. Of these materials, only the aluminum used for the fuel elements is considered critical to the safety of the package. The other materials either have temperature limits above the maximum expected temperatures or are not considered essential to the function of the package.

Section 3.2.2, *Technical Specifications of Components*, presents the basis for the temperature limits of the various components. These temperature limits are applicable to this safety evaluation as well.

Table 3.6-3 – Thermal Properties of Package Metallic Materials

Material	Temperature (°F)	Thermal Conductivity (Btu/hr-ft-°F)	Specific Heat (Btu/lbm-°F)	Density (lbm/in³)
Aluminum Type 6061-T651 / T6511	70	96.1	0.214	0.098
	100	96.9	0.216	
	150	98.0	0.220	
	200	99.0	0.222	
	250	99.8	0.224	
	300	100.6	0.227	
	350	101.3	0.230	
	400	101.9	0.231	
	1100 ①	101.9	0.231	

Notes:
① Values for 1100°F are assumed equal to values at 400°F.

[36] *Heat Transfer in Window Frames with Internal Cavities*, PhD Thesis for Arild Gustavsen, Norwegian University of Science and Technology, Trondheim, Norway, September 2001.

calculations are performed. Instead, it is assumed that all package components achieve the 100°F temperature under steady-state conditions. The resulting 100°F package skin temperature is below the maximum temperature of 122°F permitted by 10 CFR §71.43(g) for accessible surface temperature in a nonexclusive use shipment.

3.6.7.1.2 Minimum Temperatures

The minimum temperature distribution for the ATR FFSC occurs with a zero decay heat load and an ambient air temperature of -40°F per 10 CFR §71.71(c)(2). The thermal analysis of this condition also represents a trivial case and no thermal calculations are performed. Instead, it is assumed that all package components achieve the -40°F temperature under steady-state conditions. As discussed in Section 3.2.2, *Technical Specifications of Components*, the -40°F temperature is within the allowable operating temperature range for all ATR FFSC package components.

3.6.7.2 Maximum Normal Operating Pressure

The payload cavity of the ATR FFSC is vented to the atmosphere. As such, the maximum normal operating pressure (MNOP) for the package is 0 psig.

While the volume between the outer and inner shells is sealed, it does not contain organic or other materials that may outgas or thermally decompose. Therefore, the maximum pressure that may develop within the space will be limited to that achieved due to ideal gas expansion. Assuming a temperature of 70°F at the time of assembly and a maximum operating temperature of 190°F (based on the outer shell temperature, see Table 3.6-5, conservatively rounded up), the maximum pressure rise within the sealed volume will be less than 4 psi.

6.10 Criticality Analysis for MIT and MURR Fuel

The ATR FFSC may be utilized to transport MIT fuel and MURR fuel. Both of these fuels are high-enriched plate-type fuels similar to the ATR fuel analyzed in this chapter, although the fuel geometries are different. The following analyses demonstrate that the ATR FFSC with the MIT and MURR fuel complies with the requirements of 10 CFR §71.55 and §71.59. Based on a 5x5 array of damaged packages, the Criticality Safety Index (CSI), per 10 CFR §71.59, is 4.0.

6.10.1 Description of Criticality Design

6.10.1.1 Design Features Important for Criticality

No special design features are required to maintain criticality safety. No poisons are utilized in the package. The MURR and MIT fuel handling enclosures (FHEs) restrict postulated fuel element pitch expansion under hypothetical accident conditions. In addition, the separation provided by the packaging (outer flat-to-flat dimension of 7.9-in), along with the limit on the number of packages per shipment, is sufficient to maintain criticality safety.

6.10.1.2 Summary Table of Criticality Evaluation

The upper subcritical limit (USL) for ensuring that the ATR FFSC (single package or package array) is acceptably subcritical, is:

$$USL = 0.9209$$

The package is considered to be acceptably subcritical if the computed k_{safe} (k_s), which is defined as $k_{effective}$ (k_{eff}) plus twice the statistical uncertainty (σ), is less than or equal to the USL, or:

$$k_s = k_{eff} + 2\sigma \leq USL$$

The USL is determined on the basis of a benchmark analysis and incorporates the combined effects of code computational bias, the uncertainty in the bias based on both benchmark-model and computational uncertainties, and an administrative margin. The results of the benchmark analysis indicate that the USL is adequate to ensure subcriticality of the package.

The packaging design is shown to meet the requirements of 10 CFR 71.55(b). Moderation by water in the most reactive credible extent is utilized in both the normal conditions of transport (NCT) and hypothetical accident conditions of transport (HAC) analyses. In the single package NCT models, full-density water fills the accessible cavity, while in the single package HAC models, full-density water fills all cavities. In the NCT fuel element models, the fuel element is modeled as undamaged, although the most reactive credible configuration is utilized by maximizing the gap between the fuel plates. Maximizing this gap maximizes the moderation and hence the reactivity because the system is undermoderated. In the HAC fuel element models, a damaged fuel element is assumed, and the fuel element pitch is allowed to expand until constrained by the FHE, which maximizes moderation. In all single package models, 12-in of water reflection is utilized.

In the NCT and HAC array cases, partial moderation is considered to maximize array interaction effects. A 9x9x1 array is utilized for the NCT array, while a 5x5x1 array is utilized in the HAC array. In all array models, 12-in of water reflection are utilized.

The maximum results of the criticality calculations are summarized in Table 6.10-1. The MURR fuel is significantly more reactive than the MIT fuel. The maximum calculated k_s is 0.85881, which occurs for the optimally moderated MURR HAC array case. In this case, the FHE is moderated with full-density water, the inner tube (outside the FHE) is moderated with 0.8 g/cm^3 water, and void is modeled between the insulation and outer tube.

6.10.1.3 Criticality Safety Index

The criticality safety index of 4.0 for MIT and MURR fuel is unchanged from the value provided in Section 6.1.3, *Criticality Safety Index*.

Table 6.10-1 – Summary of Criticality Evaluation

	MURR	**MIT**
Normal Conditions of Transport (NCT)		
Case	k_s	k_s
Single Unit Maximum	0.43482	0.33606
9x9 Array Maximum	0.84596	0.62285
Hypothetical Accident Conditions (HAC)		
Case	k_s	k_s
Single Unit Maximum	0.54584	0.43666
5x5 Array Maximum	0.85881	0.67309
USL = 0.9209		

6.10.2 Fissile Material Contents

The package can accommodate either one MURR or one MIT fuel element. The geometry and composition of these fuel elements are described in the following sections.

6.10.2.1 MURR Fuel Element

Each MURR element contains up to 785 g U-235, enriched up to 94 wt.%. The weight percents of the remaining uranium isotopes are 1.2 wt.% U-234, 0.7 wt.% U-236, and 5.0-7.0 wt.% U-238. Each fuel element contains 24 curved fuel plates. Fuel plate 1 has the smallest radius, while fuel plate 24 has the largest radius, as shown in Figure 6.10-1 and Figure 6.10-3. The fuel "meat" is a mixture of uranium metal and aluminum, while the cladding and structural materials are an aluminum alloy.

The geometry of the fuel element is defined in Figure 6.10-1. Each fuel plate is nominally 0.05-in thick, with a thickness tolerance of ±0.002-in. The fuel meat is nominally 0.02-in thick, and the cladding is nominally 0.015-in thick. The plate cladding material is aluminum. Fuel element side plates are fabricated of ASTM B 209, aluminum alloy 6061-T6 or 6061-T651. These fuel element side plates have a minimum thickness of 0.145-in. The channel width between the plates is 0.080 ± 0.008-in. This tolerance represents average and not localized channel width. For an actual fuel element, the channel width may exceed this tolerance in localized areas.

The arc length of the fuel meat changes from plate to plate. Reference fuel meat arc length and inner radius dimensions for each plate are provided in Table 6.10-2. The active fuel length ranges from 23.25-in to 24.75-in as illustrated in Figure 6.10-1.

It is necessary to determine the number densities of the fuel meat, which are the same for all fuel plates. To determine the number densities of the fuel meat, it is first necessary to compute the volume of the fuel meat. The volume of the fuel meat for each plate is the arc length of the meat (nominal + 0.065-in) multiplied by the active fuel length (24.0-in) and meat thickness (0.02-in). The active fuel length and meat thickness are modeled at nominal values in all final (i.e., non-parametric) fuel element models, and the use of these dimensions is justified in Section 6.10.4.1.2, *HAC Single Package Configuration*. It is demonstrated that reactivity increases with increasing meat arc length. The results of the fuel meat volume computations for all 24 plates are provided in Table 6.10-2 for maximum fuel arc length.

The midpoint radii of the fuel plates are treated as fixed quantities in the NCT models, and are computed based on nominal dimensions. However, the channel width is modeled at the maximum value of 0.088-in between all plates in all NCT fuel element models. To achieve this channel width between all fuel plates, the cladding is artificially reduced to a thickness of 0.011-in, or a total plate thickness of 0.042-in. This plate thickness is impossible to achieve in actual practice because it is below the allowable minimum plate thickness of 0.048-in.

The U-235 gram density for each fuel plate is computed by dividing the U-235 mass by the total volume, or 785 g/556.4 cm^3 = 1.41 g/cm^3. The fuel itself is a mixture of UAl_x and aluminum. The density of this mixture for ATR fuel is proportional to the U-235 gram density, as shown in Table 6.2-2. Because ATR and MURR fuel are of the same type, this equation is also used to develop the MURR fuel matrix density. These data are perfectly linear, and a linear fit of the data is $\rho_2 = 0.8733\rho_1 + 2.5357$, where ρ_2 is the total gram density of the mixture, and ρ_1 is the gram density of the U-235 in the mixture. Therefore, using this equation, the total density of the fuel matrix is computed to be approximately 3.77 g/cm^3.

From the fuel volumes, U-235 gram densities, and total mixture densities provided, the number densities for the fuel region may be computed. These number densities are provided in Table 6.10-3. The U-235 weight percent is modeled at the maximum value of 94%. Representative weight percents of 0.6% and 0.35% are utilized for U-234 and U-236, respectively, and the balance (5.05%) is modeled as U-238.

6.10.2.2 MIT Fuel Element

Each MIT element contains up to 515 g U-235, enriched up to 94 wt.%. The weight percents of the remaining uranium isotopes are 1.2 wt.% U-234, 0.7 wt.% U-236, and 5.0-7.0 wt.% U-238.

Each fuel element contains 15 flat fuel plates, as shown in Figure 6.10-2 and Figure 6.10-4. The fuel "meat" is a mixture of uranium metal and aluminum, while the cladding and structural materials are an aluminum alloy.

The geometry of the fuel element is defined in Figure 6.10-2. Each fuel plate is nominally 0.08-in thick, with a thickness tolerance of ±0.003-in. The fuel meat is nominally 0.03-in thick, and the cladding is nominally 0.025-in thick. The plate cladding material is aluminum. Fuel element side plates are fabricated of ASTM B 209, aluminum alloy 6061-T6. These fuel element side plates have a nominal thickness of 0.188-in. The channel width between the plates is 0.078 ± 0.004-in. This tolerance represents average and not localized channel width. For an actual fuel element, the channel width may exceed this tolerance in localized areas.

The maximum and minimum active fuel lengths and maximum and minimum active fuel widths may be computed based on Figure 6.10-2:

- Maximum active fuel length = (23.0+0.01)-2(0.125) = 22.76-in
- Minimum active fuel length = (23.0-0.01)-2(0.5) = 21.99-in
- Maximum active fuel width = 2.531 – 2(0.18) = 2.171-in
- Minimum active fuel width = 2.521 – 2(0.27) = 1.981-in.

The nominal active fuel length may be estimated as the average of the maximum and minimum values, or 22.375-in.

It is necessary to determine the number densities of the fuel meat, which are the same for all fuel plates. To determine the number densities of the fuel meat, it is first necessary to compute the volume of the fuel meat. The volume of the fuel meat for each plate is the maximum width of the meat (2.171-in) multiplied by the active fuel length (22.375-in) and meat thickness (0.03-in). The active fuel length and meat thickness are modeled at nominal values in all final (i.e., non-parametric) fuel element models, and the use of these dimensions is justified in Section 6.10.4.1.2, *HAC Single Package Configuration*. It is demonstrated that reactivity increases with increasing meat width. The total meat volume is therefore $(15)(0.03)(22.375)(2.171)(2.54^3)$ = 358.2 cm^3.

The centerlines of the fuel plates are treated as fixed quantities in the NCT models, and are computed based on nominal dimensions. However, the channel width is modeled at the maximum value between all plates in all NCT fuel element models. The maximum channel width is 0.082-in. The fuel plates also have grooves a maximum of 0.012-in deep cut into the surface of the fuel plates to increase heat transfer. Because the grooves cover approximately half the surface area of the cladding, half of the groove depth (i.e., 0.006-in) is removed from each cladding plate, increasing the effective channel width to 0.094-in. To achieve this channel width between all fuel plates, the cladding is artificially reduced to a thickness of 0.017-in, or a total plate thickness of 0.064-in.

The U-235 gram density for each fuel plate is computed by dividing the U-235 mass by the total volume, or 515 g/358.2 cm^3 = 1.44 g/cm^3. The fuel itself is a mixture of UAl_x and aluminum. The density of this mixture for ATR fuel is proportional to the U-235 gram density, as shown in Table 6.2-2. Because ATR and MIT fuel are of the same type, this equation is also used to develop the MIT fuel matrix density. These data are perfectly linear, and a linear fit of the data is $\rho_2 = 0.8733\rho_1 + 2.5357$, where ρ_2 is the total gram density of the mixture, and ρ_1 is the gram density of the U-235 in the mixture. Therefore, using this equation, the total density of the fuel matrix is computed to be approximately 3.79 g/cm^3.

From the fuel volumes, U-235 gram densities, and total mixture densities provided, the number densities for the fuel region may be computed. These number densities are provided in Table 6.10-4. The U-235 weight percent is modeled at the maximum value of 94%. Representative weight percents of 0.6% and 0.35% are utilized for U-234 and U-236, respectively, and the balance (5.05%) is modeled as U-238.

Table 6.10-2 – MURR Fuel Volume Computation (maximum arc length)

Plate	Midpoint Radius (cm)	Fuel Arc (cm)	Volume (cm^3)
1	7.0993	4.5034	13.9460
2	7.4295	4.7625	14.7484
3	7.7597	5.0216	15.5507
4	8.0899	5.2832	16.3608
5	8.4201	5.5423	17.1632
6	8.7503	5.8014	17.9655
7	9.0805	6.0604	18.7678
8	9.4107	6.3195	19.5701
9	9.7409	6.5786	20.3724
10	10.0711	6.8377	21.1747
11	10.4013	7.0968	21.9770
12	10.7315	7.3558	22.7793
13	11.0617	7.6149	23.5816
14	11.3919	7.8765	24.3918
15	11.7221	8.1356	25.1941
16	12.0523	8.3947	25.9964
17	12.3825	8.6538	26.7987
18	12.7127	8.9129	27.6011
19	13.0429	9.1719	28.4034
20	13.3731	9.4310	29.2057
21	13.7033	9.6901	30.0080
22	14.0335	9.9492	30.8103
23	14.3637	10.2083	31.6126
24	14.6939	10.4699	32.4228
Total			556.4024

Table 6.10-3 – MURR Fuel Number Densities (maximum arc length)

Isotope	Number Density (atom/b-cm)
U-234	2.3171E-05
U-235	3.6147E-03
U-236	1.3402E-05
U-238	1.9174E-04
Al	5.0596E-02
Total	5.4439E-02

Table 6.10-4 – MIT Fuel Number Densities (maximum fuel width)

Isotope	Number Density (atom/b-cm)
U-234	2.3613E-05
U-235	3.6835E-03
U-236	1.3657E-05
U-238	1.9539E-04
Al	5.0481E-02
Total	5.4398E-02

Figure Withheld Under 10 CFR 2.390

Figure 6.10-1 – MURR Fuel Element Dimensions

Figure Withheld Under 10 CFR 2.390

Figure 6.10-2 – MIT Fuel Element Dimensions

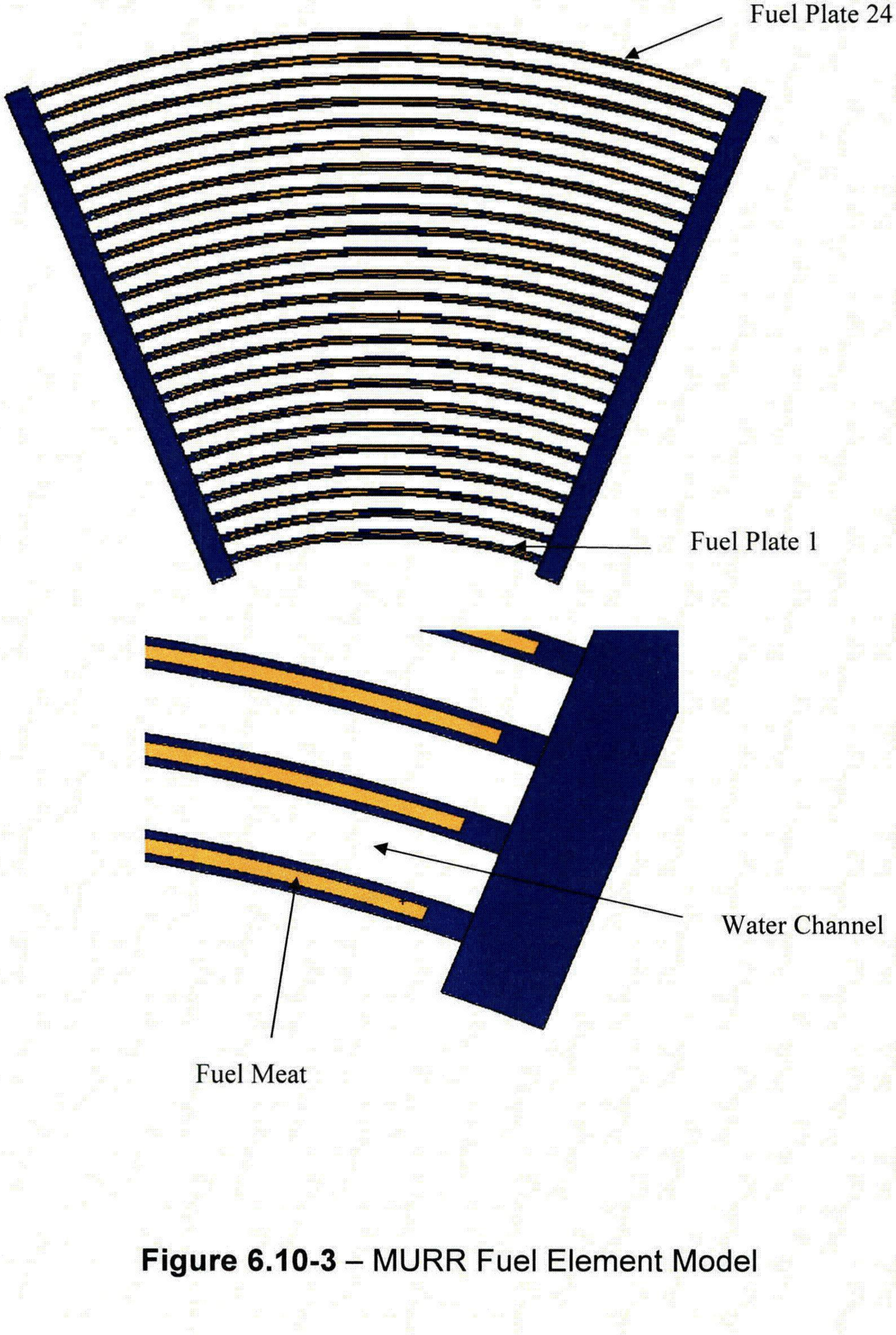

Figure 6.10-3 – MURR Fuel Element Model

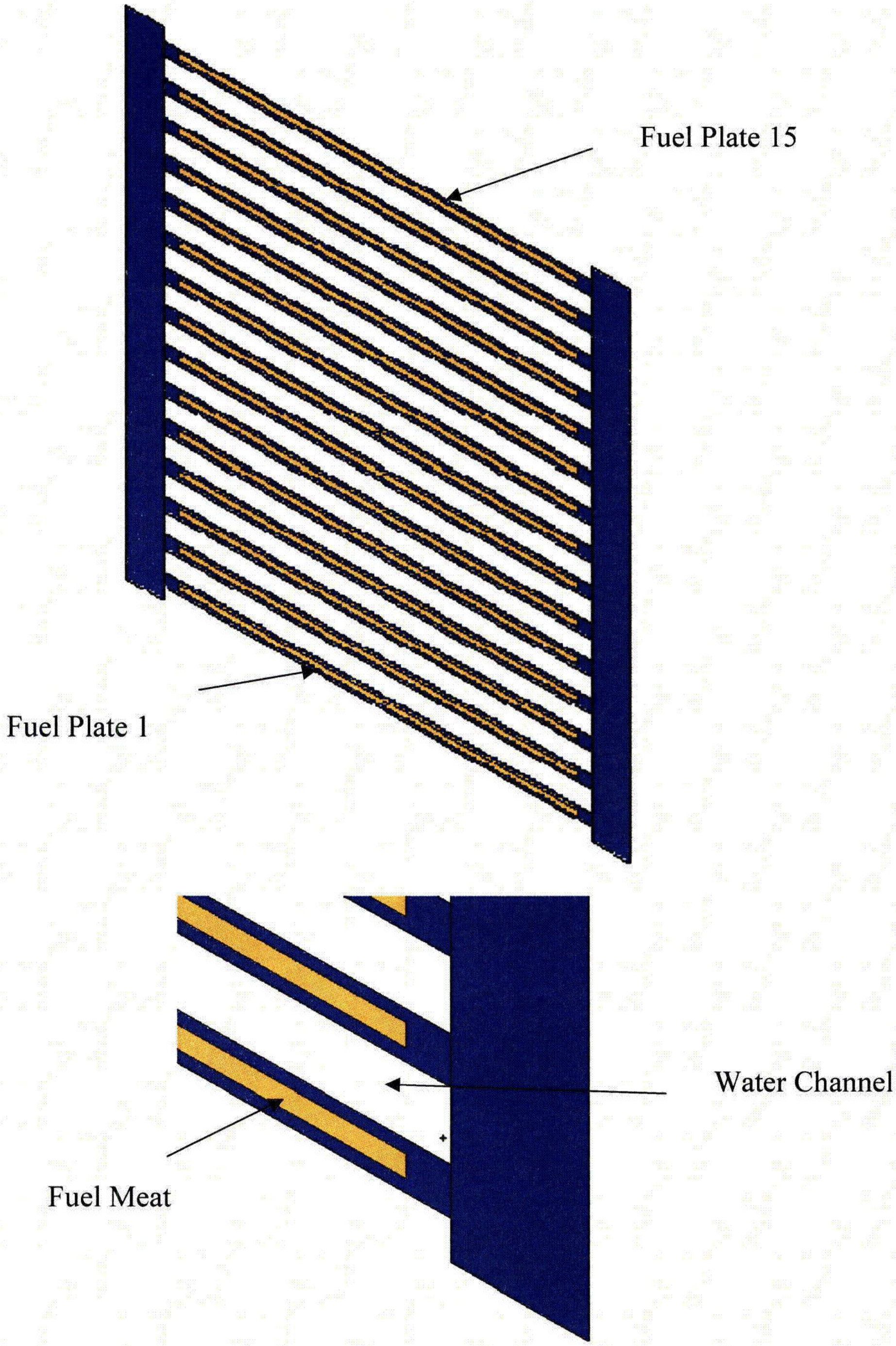

Figure 6.10-4 – MIT Fuel Element Model

6.10.3 General Considerations

6.10.3.1 Model Configuration

The packaging is modeled essentially the same as described in Section 6.3.1, *Model Configuration*, including the number of packages utilized in the NCT and HAC array cases. The only difference is the FHE is modeled explicitly, and the contents are different.

The MURR and MIT FHEs are modeled explicitly over the active fuel length. The FHEs are constructed of aluminum. Maximum dimensional tolerances are selected so that the FHEs are as large as possible, which results in the largest possible pitch expansion in the HAC models. For the MURR FHE, these dimensions are 2.00+0.06-in, 3.56+0.06-in, 1.85+0.06-in, and 22.5°+2° (see the packaging general arrangement drawings for dimension placement). For the MIT FHE, these dimensions are 1.62+0.06-in and 2.82+0.06-in (see the packaging general arrangement drawings for dimension placement). The wall thickness is 0.19 ± 0.06-in for each FHE. The array cases are run with both minimum and maximum wall thickness to determine the most reactive condition. All of the figures in this chapter show minimum wall thickness models. Each FHE is comprised of two pieces held together by ball lock pins. Under NCT, the two FHE halves do not separate.

In the NCT single package models, the inner tube, FHE, insulation, and outer tube are modeled explicitly, as shown in Figure 6.10-5 and Figure 6.10-6 for MURR and MIT, respectively. An axial view is shown in Figure 6.10-7. Note that the thin steel sheet that encases the insulation has been conservatively neglected (the steel sheet would absorb neutrons and lower the reactivity). Although negligible water ingress is expected during NCT, the inner cavity of the package is assumed to be flooded with water because the package lid does not contain a seal. However, the region between the insulation and the outer tube will remain dry because water cannot enter this region. In the models, the fuel element is conservatively positioned at the radial center of the FHE to maximize neutron reflection. The package is reflected with 12-in of full-density water.

The neoprene along the sides of the FHEs is modeled in an approximate manner using a thickness of 1/8-in. In both cases, the neoprene is modeled continuously along two sides for simplicity, rather than modeling the neoprene in detail as narrow strips. Because it was determined in the ATR fuel criticality analysis that neoprene will reduce the reactivity due to parasitic absorption in chlorine, the neoprene is modeled without chlorine, and the density is reduced accordingly.

The HAC single package model is similar to the NCT single package model. Damage in the drop tests was shown to be negligible and concentrated at the ends of the package (See Section 2.12.1, *Certification Tests on CTU-1*). As the ends of the package are not modeled, this end damage does not affect the modeling. The various side drops resulted in only minor localized damage to the outer tube, and no observable bulk deformation of the package. Therefore, the minor damage observed will not impact the reactivity. The insulation is replaced with full-density water, and the region between the insulation and outer tube is also filled with full-density water (see Figure 6.10-8 and Figure 6.10-9 for the MURR and MIT model geometry, respectively). The treatment of the fuel enclosure is the same as the NCT single package models. Cases are developed both with and without the neoprene.

No MURR or MIT fuels were included in the drop tests. Therefore, the damage to the MURR or MIT fuel under HAC is not known precisely. To conservatively bound the potential fuel damage in the HAC models, the fuel plate pitch is allowed to expand uniformly until constrained by the FHE. In addition, the FHEs, which are composed of two halves pinned together, are assumed to separate in a manner that maximizes the space available for pitch expansion. For simplicity, the gap between the two halves is not modeled explicitly in the HAC models. This pitch expansion increases the moderation and the reactivity. In actuality, such a large uniform expansion of the fuel element pitch is not credible, and in the worst case scenario would be localized at one end of the fuel element. Drop tests performed with ATR fuel, which is similar to MURR and MIT fuel, showed no damage that would affect the criticality analysis [See Section 2.12.1, *Certification Tests on CTU-1*]. The modeled damage is intended to bound a damaged fuel element that is otherwise intact.

In the NCT array models, a 9x9x1 array is utilized. To increase the reactivity, fuel elements are pushed toward the center of the array. Because the fuel elements are transported in a thin (~0.01-in) plastic bag, this plastic bag is allowed to act as a boundary for partial moderation effects. The plastic bag is not modeled explicitly, because it is too thin to have an appreciable effect on the reactivity. Therefore, it is postulated that the fuel element channels may fill with full-density water, while the region between the fuel element and FHE fills with variable density water. Different water densities inside and outside the FHE are also addressed. Axial movement of the fuel elements is not considered because axial movement would increase the effective active height of the system (i.e., if some fuel elements shift and others remain in place) and reduce the reactivity due to increased leakage. The presence of chlorine-free neoprene is also considered in the array cases.

In the HAC array models, a 5x5x1 array is utilized, although the moderation conditions considered are similar to the NCT array analysis. Cases in which the insulation is replaced with water are also investigated. The fuel elements are modeled at the maximum pitch, consistent with the most reactive single package models.

The detailed moderation assumptions for these cases are discussed more fully in Section 6.10.5, *Evaluation of Package Arrays under Normal Conditions of Transport*, and Section 6.10.6, *Package Arrays under Hypothetical Accident Conditions*.

6.10.3.2 Material Properties

The fuel meat compositions are provided in Table 6.10-3 and Table 6.10-4 for MURR and MIT fuel, respectively. The material properties of the packaging materials are provided in Section 6.3.2, *Material Properties*. The aluminum of the FHE is modeled as pure with a density of 2.7 g/cm^3.

6.10.3.3 Computer Codes and Cross-Section Libraries

The computer code and cross section libraries utilized are provided in Section 6.3.3, *Computer Codes and Cross-Section Libraries*.

6.10.3.4 Demonstration of Maximum Reactivity

The reactivities of the NCT and HAC single package cases are small, with $k_s < 0.6$.

For the NCT array, a 9x9x1 array is utilized, while for the HAC array, a smaller 5x5x1 array is utilized. Because negligible packaging damage was observed in the drop tests, the package dimensions are the same between the NCT and HAC models. However, the fuel elements are modeled differently between the NCT and HAC models. In the NCT models, the fuel elements are modeled as intact, although with dimensions optimized to maximize the reactivity. In the HAC models, the fuel is assumed to be damaged, and the pitch is allowed to expand until constrained by the FHE. In the HAC cases, the pins connecting the two halves of the FHE are assumed to break, and the two halves are pushed apart to the maximum extent to maximize the available space for pitch expansion. The FHEs and fuel elements are pushed toward the center of the array.

In both NCT and HAC array cases, flooding with partial moderation is allowed in the fuel element itself, between the fuel element and the FHE, and between the FHE and the inner tube. A number of different partial moderation scenarios are considered.

In the NCT array models, insulation is modeled between the inner and outer tubes. In the HAC array models, it is demonstrated that modeling the insulation is more reactive than replacing the insulation with variable density water. In both sets of models, chlorine-free neoprene that is attached to the FHE is modeled, although the effect on the reactivity is small. No models in which the neoprene is allowed to decompose and homogeneously mix with the water are developed, as this scenario is already implicitly included in the search for optimum reactivity using various water densities.

Tolerances of the packaging materials are selected to maximize the reactivity. Both maximum and minimum wall thicknesses for the FHE are modeled to determine the most reactive condition, although the effect on the reactivity of this parameter is not significant.

The MURR fuel is significantly more reactive than the MIT fuel in all scenarios, a difference in k_s of 0.186 comparing the most reactive models. The most reactive case occurs for the HAC array (Case XN9), and results in a $k_s = 0.85881$, which is below the USL of 0.9209. For this case, full-density water is modeled between the fuel plates and inside the FHE, 0.8 g/cm^3 water is modeled between the FHE and inner tube, the FHE is modeled with a thick wall, and insulation is modeled.

When comparing the reactivities of the three fuel types (ATR, MURR, MIT), MURR is the most reactive, MIT is the least reactive.

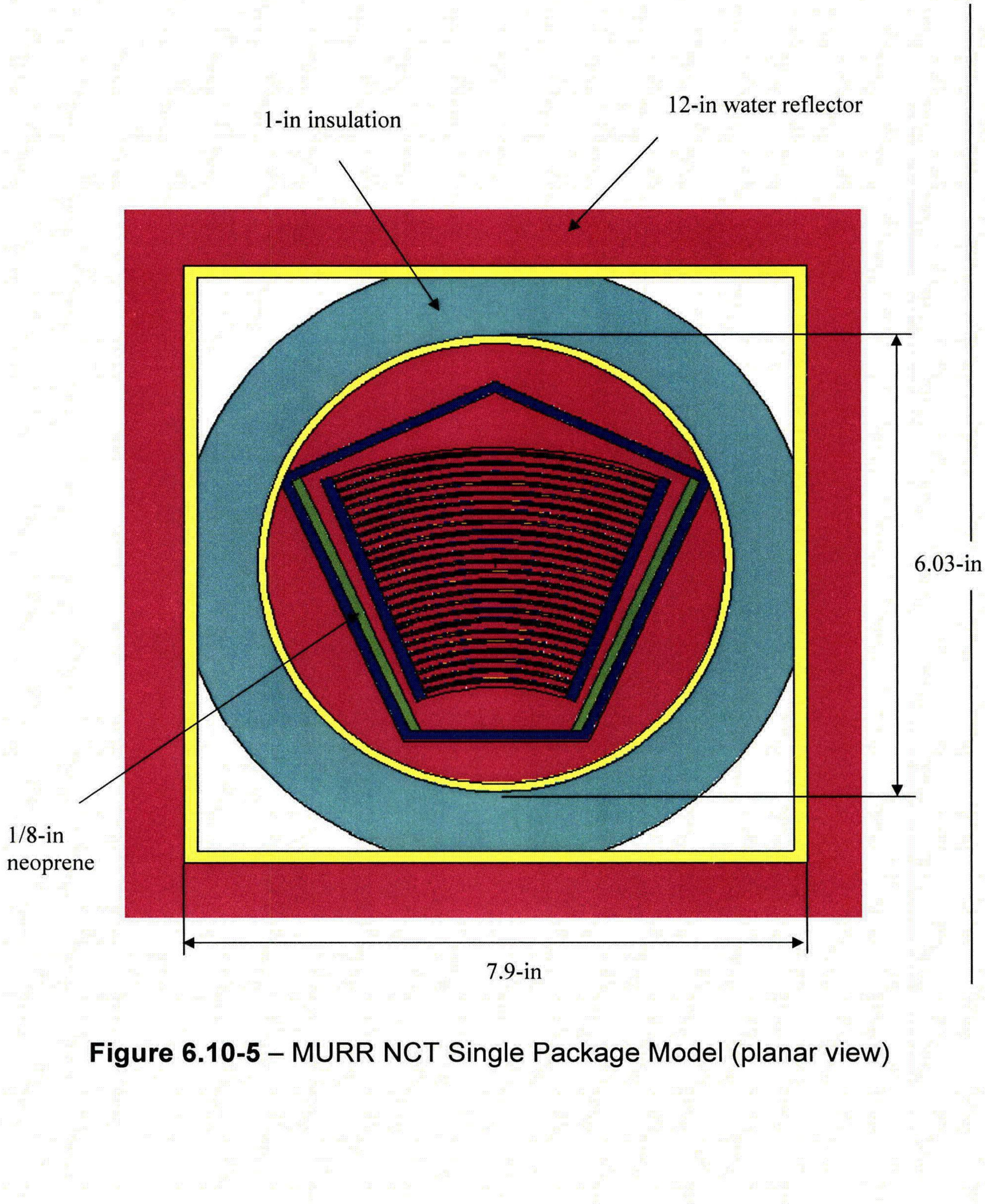

Figure 6.10-5 – MURR NCT Single Package Model (planar view)

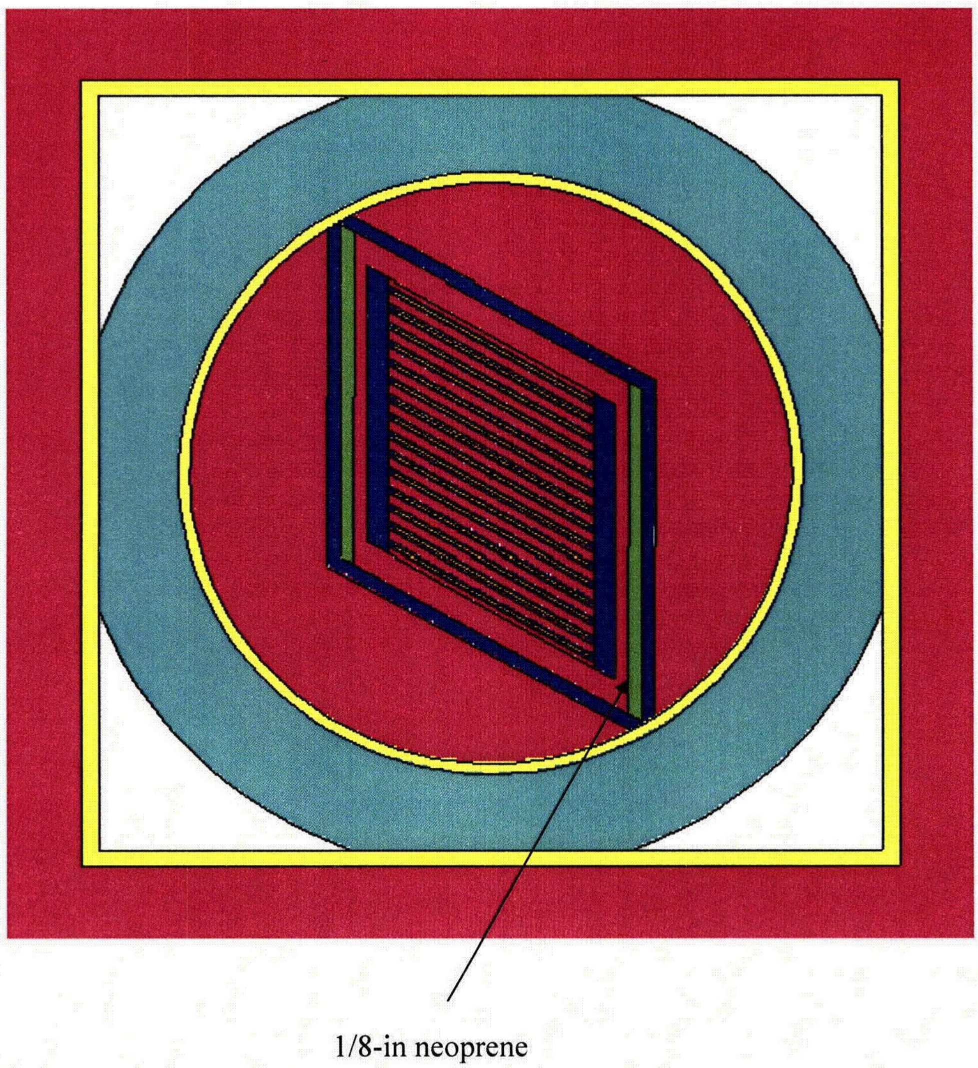

Figure 6.10-6 – MIT NCT Single Package Model (planar view)

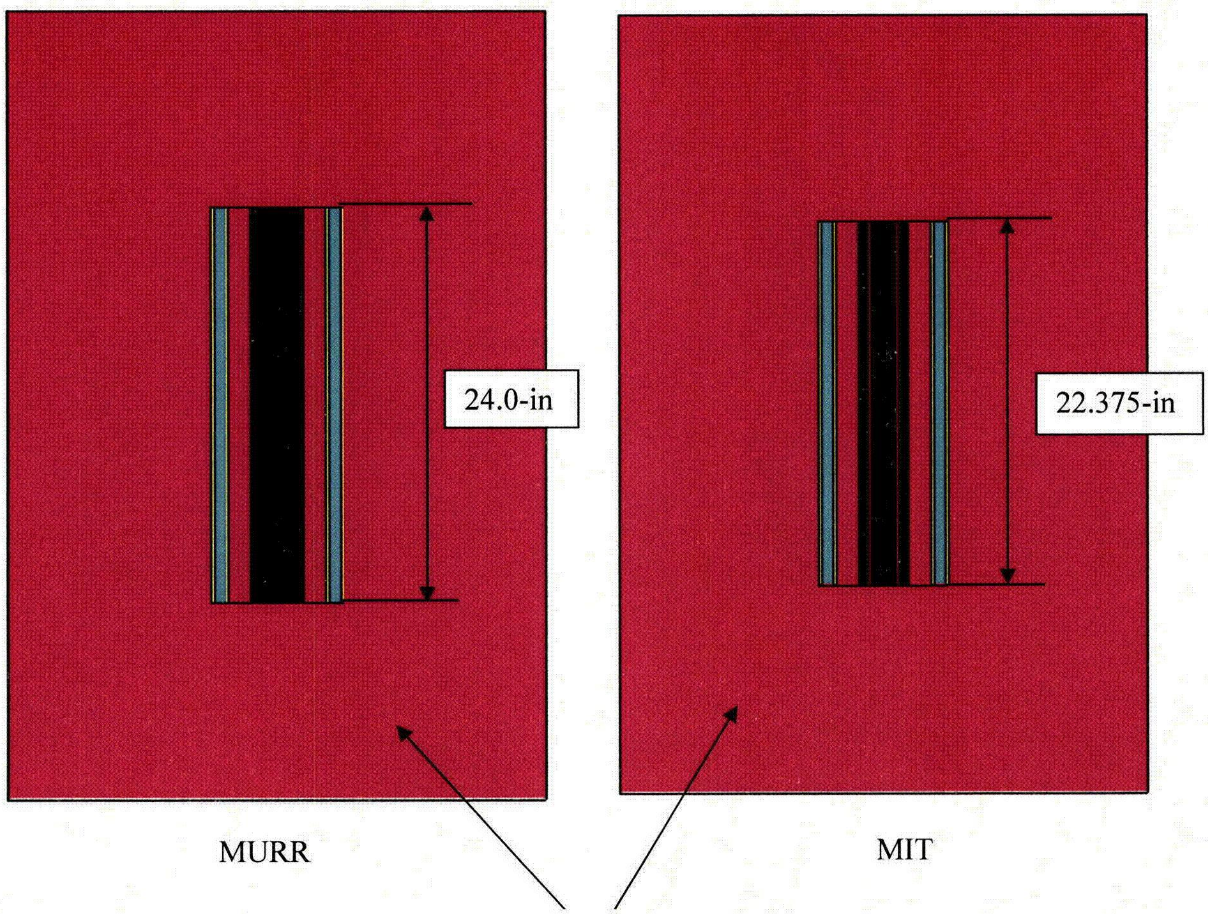

Note that the ends of both the fuel element and package are conservatively treated simply as a water reflector.

Figure 6.10-7 – MURR/MIT NCT Single Package Models (axial view)

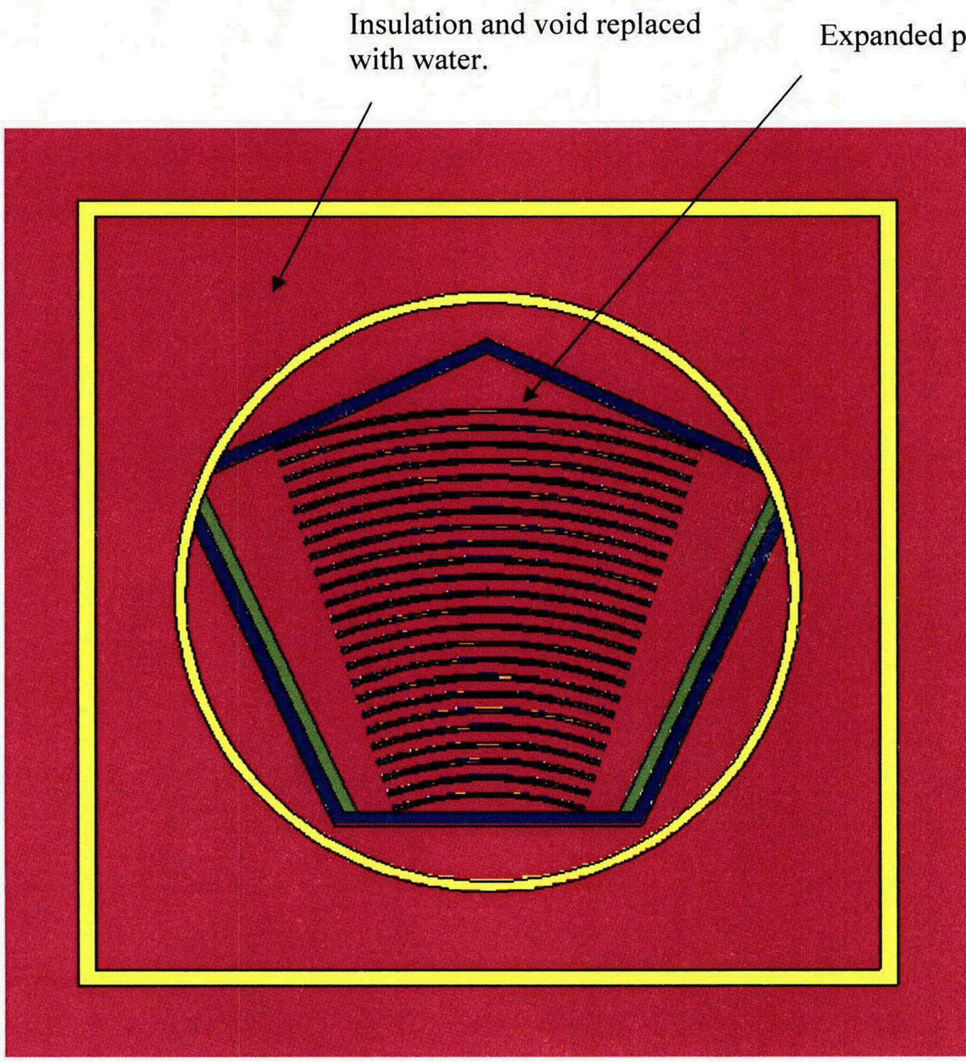

Figure 6.10-8 – MURR HAC Single Package Model (planar view)

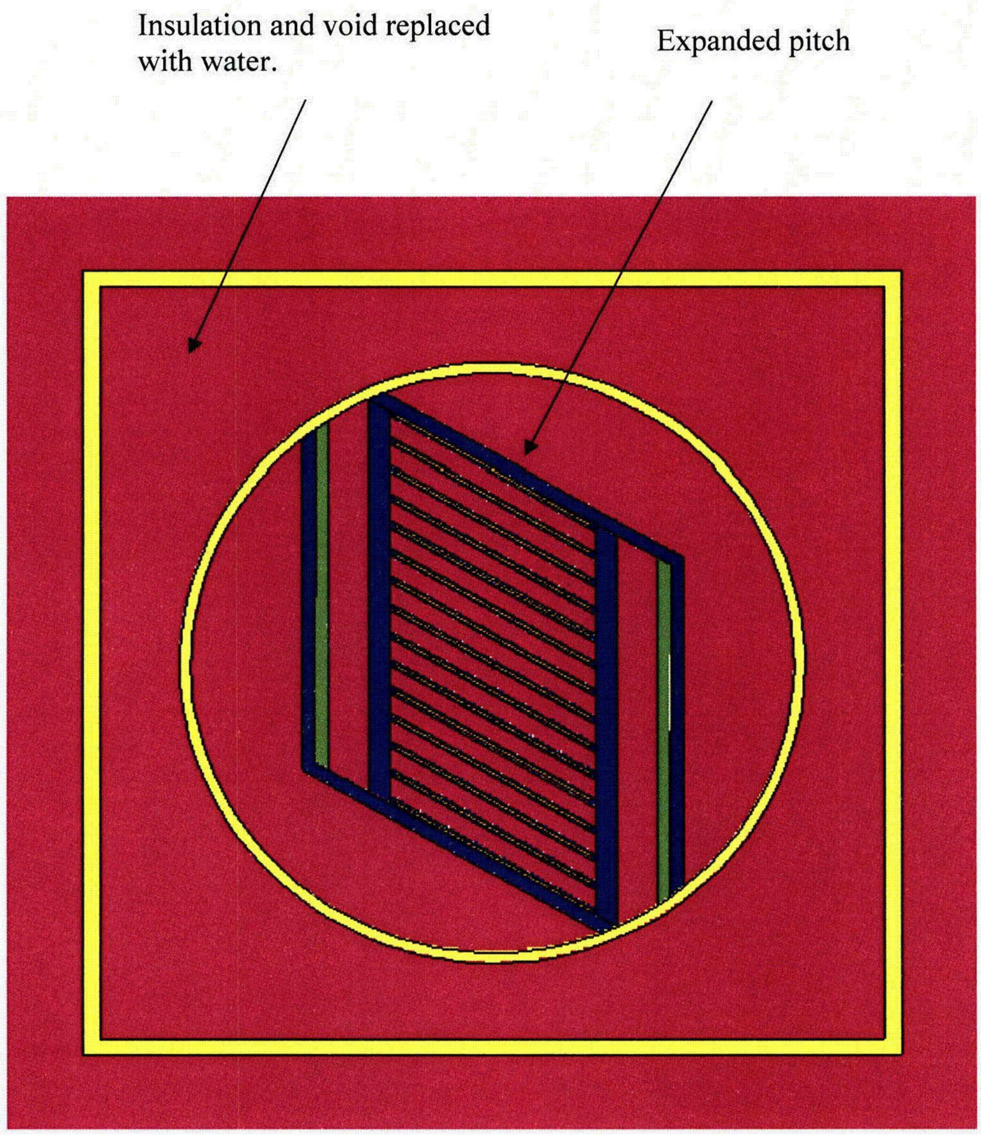

Figure 6.10-9 – MIT HAC Single Package Model (planar view)

6.10.4 Single Package Evaluation

6.10.4.1 Single Package Configuration

Prior to development of a single package model, a parametric analysis is performed to determine the impacts of various fuel element tolerances on the reactivity. In the criticality analysis for ATR fuel (see Section 6.4.1.2.1, *Fuel Element Payload Parametric Evaluation*), it was determined that reactivity was maximized by maximizing the arc length of the fuel meat and the channel thickness. Because ATR, MURR, and MIT fuel are all plate-type and utilize similar enrichments, it is expected that MURR and MIT fuel will also experience maximum reactivity with these parameters maximized. Therefore, the parametric analysis considers the effects of only the following parameters: fuel meat arc length/width, channel width, and active fuel length.

The base configuration for both MURR and MIT consists of plates with a nominal meat arc length/width, nominal active fuel length, and nominal channel width. The minimum, nominal, and maximum meat arc lengths for MURR fuel are provided in Table 6.10-5. The minimum meat arc lengths are obtained directly from Figure 6.10-1 (see dimension B). The maximum meat arc lengths are computed by subtracting twice the fuel-free width (2*0.115-in) from the maximum plate width (dimension C of Figure 6.10-1 + 0.010-in). The nominal value is computed as the average of the minimum and maximum values.

A total of 14 parametric models are developed (7 for each fuel type), as listed in the following table. The detailed model descriptions of the parametric cases are summarized in Table 6.10-6. In each parametric case, the indicated parameter is modified in comparison with the base case. In all parametric models, the fuel element is modeled in the center of an ATR FFSC with the inner tube flooded, and the insulation replaced with full density water. The FHEs are neglected for simplicity.

Case ID	Case Description
XB1	Base MURR case
XB2	Decrease active fuel length to minimum value
XB3	Increase active fuel length to maximum value
XB4	Increase channel width to maximum value
XB5	Decrease width of fuel meat to minimum value
XB6	Increase width of fuel meat to maximum value
XB7	Combine cases XB4 and XB6
Case ID	**Case Description**
YB1	Base MIT case
YB2	Decrease active fuel length to minimum value
YB3	Increase active fuel length to maximum value
YB4	Increase channel width to maximum value
YB5	Decrease width of fuel meat to minimum value
YB6	Increase width of fuel meat to maximum value
YB7	Combine cases YB4 and YB6

The results of the parametric analysis are summarized in Table 6.10-7. Because the uncertainty in the calculation is ~0.001, a difference of at least 0.002 (2 milli-k, abbreviated mk) between the various cases is required in order to distinguish a real effect from statistical fluctuation. For both MURR and MIT fuel, the variation of the active fuel length has a negligible effect on the results. Also, both MURR and MIT fuel show a positive reactivity increase when the fuel meat is widened and the channel width is increased. For MURR fuel, the increase is 23.5 mk (compare Case XB7 with Case XB1), and for MIT fuel, the increase is 8.8 mk (compare Case YB7 with Case YB1). This result is consistent with the results obtained in the ATR fuel analysis. Therefore, in all subsequent NCT MURR and MIT fuel models, the fuel is modeled with nominal active fuel length, maximum fuel width, and maximum channel width. The maximum channel width is achieved by artificially reducing the cladding thickness. In the HAC models, the channel width (or pitch) is allowed to increase.

6.10.4.1.1 NCT Single Package Configuration

The geometry of the NCT single package configuration is discussed in Section 6.10.3.1, *Model Configuration*. In the NCT single package models, the FHEs are modeled explicitly, and the neoprene is modeled in an approximate manner (see Figure 6.10-5 and Figure 6.10-6 for the NCT single package MURR and MIT models, respectively). The inner tube is flooded with full-density water. The fuel element geometry for both MURR and MIT is consistent with the most reactive fuel element model, including tolerances, as determined in the previous section. Neoprene from the FHEs is modeled at the sides of the fuel element. Chlorine is conservatively removed from the neoprene because chlorine acts as a poison. The package is reflected with 12-in of water. Results are provided in Table 6.10-8 for both MURR and MIT fuel. The reactivity is low, with k_s = 0.43482 for MURR and k_s = 0.33606 for MIT. These results are below the USL of 0.9209.

6.10.4.1.2 HAC Single Package Configuration

The geometry of the HAC single package configuration is discussed in Section 6.10.3.1, *Model Configuration*. In the HAC single package models, the FHEs are modeled explicitly, and the neoprene is modeled in an approximate manner (see Figure 6.10-8 and Figure 6.10-9 for the HAC single package MURR and MIT models, respectively). Chlorine is conservatively removed from the neoprene because chlorine acts as a poison. Eliminating the chlorine from the neoprene may be postulated to be a result of decomposition during a fire, although such a scenario is not credible.

The results are summarized in Table 6.10-9. In both the MURR and MIT models, the pitch is varied from the nominal value to the maximum value allowed by the FHE (Cases XC1 through XC6 for MURR and YC1 through YC10 for MIT). For both fuel types, the reactivity increases as the plate pitch increases, reaching the maximum reactivity at the maximum pitch. Neoprene is included in the variable pitch models. Note that the aluminum fuel element side plates are omitted from the MURR model for simplicity. In the MIT models, the aluminum fuel element side plates are allowed to "stretch" with the model for simplicity.

In Cases XC7 and YC11, the maximum-pitch MURR and MIT cases are repeated without neoprene. In both instances, the reactivity increases slightly when neoprene is modeled as water.

Because the fuel may be transported inside of a plastic bag, it is conservatively assumed that the water density inside of the FHE may vary independently of the water density inside of the fuel element. Note that additional surfaces are added to the MURR model to isolate the water between the fuel plates from the water inside the FHE (in Figure 6.10-8 these regions are combined). To maximize neutron reflection, full-density water is always modeled inside and outside the FHE, and the fuel element is centered laterally within the FHE.

In MURR Cases XC8 and XC9, Case XC7 is run with reduced water densities of 0.8 and 0.9 g/cm^3 between the fuel plates, but maximum water density in all other regions of the model. MIT Cases YC12 and YC13 are similar, except the Case YC11 is used as the base case. In both cases, reactivity drops as the water density is reduced between the fuel plates, indicating that the system is undermoderated.

The results are summarized in Table 6.10-9. Case XC7 is the most reactive MURR model, with k_s = 0.54584, while Case YC11 is the most reactive MIT model, with k_s = 0.43666. Both results are below the USL of 0.9209.

6.10.4.2 Single Package Results

Following are the tabulated results for the single package cases. The most reactive configurations are listed in boldface.

Table 6.10-5 – MURR Meat Arc Lengths

Plate	Minimum (in)	Nominal (in)	Maximum (in)
1	1.643	1.708	1.773
2	1.745	1.810	1.875
3	1.847	1.912	1.977
4	1.950	2.015	2.080
5	2.052	2.117	2.182
6	2.154	2.219	2.284
7	2.256	2.321	2.386
8	2.358	2.423	2.488
9	2.460	2.525	2.590
10	2.562	2.627	2.692
11	2.664	2.729	2.794
12	2.766	2.831	2.896
13	2.868	2.933	2.998
14	2.971	3.036	3.101
15	3.073	3.138	3.203
16	3.175	3.240	3.305
17	3.277	3.342	3.407
18	3.379	3.444	3.509
19	3.481	3.546	3.611
20	3.583	3.648	3.713
21	3.685	3.750	3.815
22	3.787	3.852	3.917
23	3.889	3.954	4.019
24	3.992	4.057	4.122

Table 6.10-6 – Parametric Analysis Input Data

MURR					
Parameter	**XB1/XB4**	**XB2**	**XB3**	**XB5**	**XB6/XB7**
Fuel width (in)	nominal	nominal	nominal	nominal-0.065	nominal+0.065
Meat thickness (in)	0.02	0.02	0.02	0.02	0.02
Active fuel height (in)	24	23.25	24.75	24	24
Channel (in)	0.08/0.088	0.08	0.08	0.08	0.08/0.088
Cladding (in)	0.015/0.011	0.015	0.015	0.015	0.015/0.011
Total plate (in)	0.050/0.042	0.050	0.050	0.050	0.050/0.042
Pitch (in)	0.13	0.13	0.13	0.13	0.13
Meat volume (cm3)	544.13	527.13	561.14	531.86	556.40
U-235 mass (g)	785	785	785	785	785
U-235 den (g/cm3)	1.44	1.49	1.40	1.48	1.41
UAlx+Al den (g/cm3)	3.80	3.84	3.76	3.82	3.77
N-234 (atom/b-cm)	2.3694E-05	2.4458E-05	2.2976E-05	2.4241E-05	2.3171E-05
N-235 (atom/b-cm)	3.6962E-03	3.8154E-03	3.5842E-03	3.7815E-03	3.6147E-03
N-236 (atom/b-cm)	1.3704E-05	1.4146E-05	1.3289E-05	1.4020E-05	1.3402E-05
N-238 (atom/b-cm)	1.9607E-04	2.0239E-04	1.9012E-04	2.0059E-04	1.9174E-04
N-Al (atom/b-cm)	5.0460E-02	5.0262E-02	5.0646E-02	5.0319E-02	5.0596E-02
Total (atom/b-cm)	5.4390E-02	5.4319E-02	5.4457E-02	5.4339E-02	5.4439E-02
MIT					
Parameter	**YB1/YB4**	**YB2**	**YB3**	**YB5**	**YB6/YB7**
Fuel width (in)	2.076	2.076	2.076	1.981	2.171
Meat thickness (in)	0.03	0.03	0.03	0.03	0.03
Active fuel height (in)	22.375	21.99	22.76	22.375	22.375
Channel (in)	0.090/0.094	0.090	0.090	0.090	0.090/0.094
Cladding (in)	0.019/0.017	0.019	0.019	0.019	0.019/0.017
Total plate (in)	0.068/0.064	0.068	0.068	0.068	0.068/0.064
Pitch (in)	0.158	0.158	0.158	0.158	0.158
Meat volume (cm^3)	342.53	336.64	348.43	326.86	358.21
U-235 mass (g)	515	515	515	515	515
U-235 den (g/cm3)	1.503	1.530	1.478	1.576	1.438
UAlx+Al den (g/cm3)	3.85	3.87	3.83	3.91	3.79
N-234 (atom/b-cm)	2.4693E-05	2.5125E-05	2.4275E-05	2.5877E-05	2.3613E-05
N-235 (atom/b-cm)	3.8521E-03	3.9195E-03	3.7869E-03	4.0368E-03	3.6835E-03
N-236 (atom/b-cm)	1.4282E-05	1.4532E-05	1.4040E-05	1.4967E-05	1.3657E-05
N-238 (atom/b-cm)	2.0433E-04	2.0791E-04	2.0088E-04	2.1413E-04	1.9539E-04
N-Al (atom/b-cm)	5.0202E-02	5.0090E-02	5.0310E-02	4.9895E-02	5.0481E-02
Total (atom/b-cm)	5.4297E-02	5.4257E-02	5.4336E-02	5.4187E-02	5.4398E-02

Table 6.10-7 – Parametric Analysis Results

Case ID	Filename	k_{eff}	σ	k_s (k+2σ)	Δ from XB1 (mk)
MURR					
XB1	HS_MURR2_P1	0.47068	0.00109	0.47286	--
XB2	HS_MURR2_P2	0.47199	0.00114	0.47427	1.4
XB3	HS_MURR2_P3	0.47075	0.00114	0.47303	0.2
XB4	HS_MURR2_P4	0.49257	0.00101	0.49459	21.7
XB5	HS_MURR2_P5	0.46808	0.00116	0.47040	-2.5
XB6	HS_MURR2_P6	0.47465	0.00097	0.47659	3.7
XB7	**HS_MURR2_P7**	**0.49432**	**0.00102**	**0.49636**	**23.5**
MIT					
Case ID	**Filename**	**k_{eff}**	**σ**	**k_s (k+2σ)**	**Δ from YB1 (mk)**
YB1	HS_MIT_P1	0.37801	0.00089	0.37979	--
YB2	HS_MIT_P2	0.37683	0.00093	0.37869	-1.1
YB3	HS_MIT_P3	0.37722	0.00091	0.37904	-0.8
YB4	HS_MIT_P4	0.38179	0.00095	0.38369	3.9
YB5	HS_MIT_P5	0.37018	0.00087	0.37192	-7.9
YB6	HS_MIT_P6	0.38064	0.00088	0.38240	2.6
YB7	**HS_MIT_P7**	**0.38664**	**0.00097**	**0.38858**	**8.8**

Table 6.10-8 – NCT Single Package Results

Case ID	Filename	Moderator Density (g/cm^3)	k_{eff}	σ	k_s (k+2σ)
MURR					
XA1	NS_MURR	1.0	0.43268	0.00107	0.43482
MIT					
YA1	NS_MIT	1.0	0.33434	0.00086	0.33606

Table 6.10-9 – HAC Single Package Results

Case ID	Filename	Pitch (in)	Water Density Between Plates (g/cm^3)	k	σ	k_s (k+2σ)
			MURR			
XC1	HS_MURR2_NP00	0.130	1.0	0.48916	0.00107	0.49130
XC2	HS_MURR2_NP02	0.138	1.0	0.50506	0.00111	0.50728
XC3	HS_MURR2_NP04	0.146	1.0	0.51620	0.00116	0.51852
XC4	HS_MURR2_NP06	0.154	1.0	0.52285	0.00113	0.52511
XC5	HS_MURR2_NP08	0.161	1.0	0.53481	0.00104	0.53689
XC6	HS_MURR2_NP09	0.167	1.0	0.53887	0.00103	0.54093
XC7	**HS_MURR2_P09**	**0.167**	**1.0**	**0.54374**	**0.00105**	**0.54584**
XC8	HS_MURR2_P09_M080	0.167	0.8	0.47997	0.00111	0.48219
XC9	HS_MURR2_P09_M090	0.167	0.9	0.51244	0.00106	0.51456
			MIT			
YC1	HS_MIT_NP158	0.158	1.0	0.37316	0.00090	0.37496
YC2	HS_MIT_NP16	0.160	1.0	0.37349	0.00095	0.37539
YC3	HS_MIT_NP17	0.170	1.0	0.38238	0.00088	0.38414
YC4	HS_MIT_NP18	0.180	1.0	0.38957	0.00098	0.39153
YC5	HS_MIT_NP19	0.190	1.0	0.39967	0.00105	0.40177
YC6	HS_MIT_NP20	0.200	1.0	0.40825	0.00095	0.41015
YC7	HS_MIT_NP21	0.210	1.0	0.41309	0.00104	0.41517
YC8	HS_MIT_NP22	0.220	1.0	0.41701	0.00100	0.41901
YC9	HS_MIT_NP23	0.230	1.0	0.42605	0.00093	0.42791
YC10	HS_MIT_NP24	0.240	1.0	0.43051	0.00105	0.43261
YC11	**HS_MIT_P24**	**0.240**	**1.0**	**0.43474**	**0.00096**	**0.43666**
YC12	HS_MIT_P24_M080	0.240	0.8	0.39439	0.00098	0.39635
YC13	HS_MIT_P24_M090	0.240	0.9	0.41226	0.00095	0.41416

6.10.5 Evaluation of Package Arrays under Normal Conditions of Transport

6.10.5.1 NCT Array Configuration

6.10.5.1.1 MURR Fuel Element Models

The NCT array model is a 9x9x1 array of the NCT single package model. Although an 8x8x1 array is of sufficient size to justify a CSI = 4.0, the larger 9x9x1 array is utilized simply for modeling convenience. Void is always present between the insulation and the outer tube, as this region is water-tight. The entire array is reflected with 12-in of full-density water.

The FHEs are pushed to the center of the array and rotated to minimize the distance between the fuel elements, see Figure 6.10-10. The modeled lateral shifting of the FHE inside of the tube is computed assuming the maximum inner diameter of the inner tube (5.814-in, see Section 6.3.1, *Model Configuration*) and minimum outer radius of the FHE (2.8-0.2 = 2.6-in, from the packaging general arrangement drawings), or 0.307-in. The fuel element is also modeled at the lateral "top" of the FHE to minimize the distance between the fuel elements.

Five calculational series are developed, as described below. Results are summarized in Table 6.10-10.

Series 1 (Cases XD1 through XD12): In Series 1, the water density is fixed at 1.0 g/cm^3 between the fuel plates, and the water density inside and outside the FHE is modeled at the same density, which is allowed to vary between 0 and 1.0 g/cm^3. This moderation condition simulates the partial moderation effect of assuming the plastic bag that surrounds the fuel element retains water. The neoprene (without chlorine) from the FHEs is modeled in an approximate manner. Also, the FHE is modeled with the minimum wall thickness.

As a point of interest, an additional case (Case XD12) is developed in which the fuel elements are centered in the cavity and not rotated, using the moderation assumptions of the most reactive case (Case XD7). The reactivity drops by 18.5 mk, which essentially represents the additional conservatism of pushing the fuel elements to the center of the array.

Series 2 (Cases XE1 through XE11): Series 2 is the same as Series 1, although the FHE neoprene is not modeled. The results in Table 6.10-10 indicate that the maximum reactivity occurs when chlorine-free neoprene is modeled (compare Cases XD7 and XE7), although the difference is within statistical fluctuation.

Series 3 (Cases XF1 through XF10): In Series 3, the water density inside the FHE is fixed at 1.0 g/cm^3, while the water density outside the FHE is allowed to vary between 0 and 1.0 g/cm^3. This moderation condition simulates the partial moderation effect of assuming the FHE retains water. The maximum reactivity increases slightly compared to Series 1.

Series 4 (Cases XG1 through XG11): Series 4 is the same as Series 3, although the FHE is modeled with the maximum wall thickness. The reactivity increases slightly, although the difference is within statistical fluctuation.

Series 5 (Cases XH1 through XH11): Series 5 is the same as Series 3, although the density within the fuel plates is modeled at a reduced density of 0.9 g/cm^3. The reactivity drops sharply as the water density between the plates is reduced.

Series 1 through 4 result in similar reactivities within the statistical uncertainty of the method. Reactivity is at a maximum for Case XG5, with k_s = 0.84596. In this case, the fuel elements are pushed to the center of the array, full-density water is modeled between the plates and inside the FHE, 0.4 g/cm^3 water is modeled outside the FHE, chlorine-free neoprene is included, and the FHE is modeled with maximum wall thickness. The maximum result is below the USL of 0.9209.

6.10.5.1.2 MIT Fuel Element Models

The NCT array model is a 9x9x1 array of the NCT single package model. Although an 8x8x1 array is of sufficient size to justify a CSI = 4.0, the larger 9x9x1 array is utilized simply for modeling convenience. Void is always present between the insulation and the outer tube, as this region is water-tight. The entire array is reflected with 12-in of full-density water.

The FHEs are pushed to the center of the array and rotated to minimize the distance between the fuel elements, see Figure 6.10-10. The modeled lateral shifting of the FHE inside of the tube is computed assuming the maximum inner diameter of the inner tube (5.814-in, see Section 6.3.1, *Model Configuration*) and minimum outer radius of the FHE (2.8-0.2 = 2.6-in, from the packaging general arrangement drawings), or 0.307-in.

In addition to the lateral shifting of the FHE within the tube, the MIT fuel element is free to move laterally within the FHE. To simplify the model geometry, rather than modeling each fuel element shifted within each FHE, the fuel elements are modeled in the center of the FHE, and the FHE is shifted toward the center of the array an additional 0.13-in (the approximate as-modeled distance between the fuel element and neoprene).

Five calculational series are developed, as described below. Results are summarized in Table 6.10-11.

Series 1 (Cases YD1 through YD12): In Series 1, the water density is fixed at 1.0 g/cm^3 between the fuel plates, and the water density inside and outside the FHE is modeled at the same density, which is allowed to vary between 0 and 1.0 g/cm^3. This moderation condition simulates the partial moderation effect of assuming the plastic bag that surrounds the fuel element retains water. The neoprene (without chlorine) from the FHE is modeled in an approximate manner. Also, the FHE is modeled with the minimum wall thickness.

As a point of interest, an additional case (Case YD12) is developed in which the fuel elements are centered in the cavity and not rotated, using the moderation assumptions of the most reactive case (Case YD7). The reactivity drops by 12.5 mk, which essentially represents the additional conservatism of pushing the fuel elements to the center of the array.

Series 2 (Cases YE1 through YE11): Series 2 is the same as Series 1, although the FHE neoprene is not modeled. Comparing Series 1 to Series 2, the reactivity is slightly higher when chlorine-free neoprene is modeled (compare Cases YD7 and YE7), although the difference is within statistical fluctuation.

Series 3 (Cases YF1 through YF10): In Series 3, the water density inside the FHE is fixed at 1.0 g/cm^3, while the water density outside the FHE is allowed to vary between 0 and 1.0 g/cm^3. This moderation condition simulates the partial moderation effect of assuming the FHE retains water. The maximum reactivity increases slightly compared to Series 1, although the effect is well within statistical fluctuation.

Series 4 (Cases YG1 through YG11): Series 4 is the same as Series 3, although the FHE is modeled with the maximum wall thickness. The reactivity decreases slightly, although the difference may be statistical fluctuation. Note that reactivity increased slightly with the thicker walled FHE in the MURR models.

Series 5 (Cases YH1 through YH11): Series 5 is the same as Series 3, although the density within the fuel plates is modeled at a reduced density of 0.9 g/cm^3. The reactivity drops sharply as the water density between the plates is reduced.

Series 1 through 4 result in similar reactivities within the statistical uncertainty of the method. Reactivity is at a maximum for Case YF7, with $k_s = 0.62285$. In this case, the fuel elements are pushed to the center of the array, full-density water is modeled between the plates and inside the FHE, 0.6 g/cm^3 water is modeled outside the FHE, chlorine-free neoprene is included, and the FHE is modeled with minimum wall thickness. The maximum result is far below the USL of 0.9209.

6.10.5.2 NCT Array Results

The results for the NCT array cases are provided in the following tables. The most reactive configuration in each series is listed in boldface.

Table 6.10-10 – MURR NCT Array Results

Case ID	Filename	Water Density Inside FHE (g/cm^3)	Water Density Outside FHE (g/cm^3)	Water Density Between Plates (g/cm^3)	k_{eff}	σ	k_s (k+2σ)
Series 1: Variable water density inside and outside FHE, with neoprene.							
XD1	NA_MURR2_NW000	0	0	1.0	0.76937	0.00121	0.77179
XD2	NA_MURR2_NW010	0.1	0.1	1.0	0.79729	0.00123	0.79975
XD3	NA_MURR2_NW020	0.2	0.2	1.0	0.81129	0.00129	0.81387
XD4	NA_MURR2_NW030	0.3	0.3	1.0	0.82519	0.00129	0.82777
XD5	NA_MURR2_NW040	0.4	0.4	1.0	0.83449	0.00130	0.83709
XD6	NA_MURR2_NW050	0.5	0.5	1.0	0.83502	0.00123	0.83748
XD7	**NA_MURR2_NW060**	**0.6**	**0.6**	**1.0**	**0.83801**	**0.00124**	**0.84049**
XD8	NA_MURR2_NW070	0.7	0.7	1.0	0.83447	0.00111	0.83669
XD9	NA_MURR2_NW080	0.8	0.8	1.0	0.83185	0.00119	0.83423
XD10	NA_MURR2_NW090	0.9	0.9	1.0	0.82537	0.00123	0.82783
XD11	NA_MURR2_NW100	1.0	1.0	1.0	0.81935	0.00120	0.82175
XD12	NA_MURR2_NW060C	0.6	0.6	1.0	0.81957	0.00123	0.82203
Series 2: Repeat of Series 1 without neoprene							
XE1	NA_MURR2_W000	0	0	1.0	0.75717	0.00117	0.75951
XE2	NA_MURR2_W010	0.1	0.1	1.0	0.78680	0.00103	0.78886
XE3	NA_MURR2_W020	0.2	0.2	1.0	0.80910	0.00116	0.81142
XE4	NA_MURR2_W030	0.3	0.3	1.0	0.82154	0.00114	0.82382
XE5	NA_MURR2_W040	0.4	0.4	1.0	0.83148	0.00129	0.83406
XE6	NA_MURR2_W050	0.5	0.5	1.0	0.83479	0.00111	0.83701
XE7	**NA_MURR2_W060**	**0.6**	**0.6**	**1.0**	**0.83681**	**0.00115**	**0.83911**
XE8	NA_MURR2_W070	0.7	0.7	1.0	0.83504	0.00126	0.83756
XE9	NA_MURR2_W080	0.8	0.8	1.0	0.83138	0.00116	0.83370
XE10	NA_MURR2_W090	0.9	0.9	1.0	0.82487	0.00122	0.82731
XE11	NA_MURR2_W100	1.0	1.0	1.0	0.81734	0.00128	0.81990
Series 3: Variable water density outside FHE, with neoprene.							
XF1	NA_MURR2_FNW000	1.0	0	1.0	0.83204	0.00135	0.83474
XF2	NA_MURR2_FNW010	1.0	0.1	1.0	0.83421	0.00118	0.83657
XF3	NA_MURR2_FNW020	1.0	0.2	1.0	0.84008	0.00131	0.84270
XF4	**NA_MURR2_FNW030**	**1.0**	**0.3**	**1.0**	**0.84082**	**0.00132**	**0.84346**
XF5	NA_MURR2_FNW040	1.0	0.4	1.0	0.84055	0.00120	0.84295
XF6	NA_MURR2_FNW050	1.0	0.5	1.0	0.83832	0.00116	0.84064
XF7	NA_MURR2_FNW060	1.0	0.6	1.0	0.83730	0.00118	0.83966
XF8	NA_MURR2_FNW070	1.0	0.7	1.0	0.83373	0.00130	0.83633
XF9	NA_MURR2_FNW080	1.0	0.8	1.0	0.83100	0.00124	0.83348
XF10	NA_MURR2_FNW090	1.0	0.9	1.0	0.82544	0.00129	0.82802
XD11	NA_MURR2_NW100	1.0	1.0	1.0	0.81935	0.00120	0.82175

(continued)

Table 6.10-10 – MURR NCT Array Results (concluded)

Case ID	Filename	Water Density Inside FHE (g/cm³)	Water Density Outside FHE (g/cm³)	Water Density Between Plates (g/cm³)	k_{eff}	σ	k_s (k+2σ)
Series 4: Same as Series 3 but with maximum thickness FHE.							
XG1	NA_MURR2_TFNW000	1.0	0	1.0	0.83659	0.00121	0.83901
XG2	NA_MURR2_TFNW010	1.0	0.1	1.0	0.83959	0.00114	0.84187
XG3	NA_MURR2_TFNW020	1.0	0.2	1.0	0.84116	0.00126	0.84368
XG4	NA_MURR2_TFNW030	1.0	0.3	1.0	0.84029	0.00128	0.84285
XG5	**NA_MURR2_TFNW040**	**1.0**	**0.4**	**1.0**	**0.84340**	**0.00128**	**0.84596**
XG6	NA_MURR2_TFNW050	1.0	0.5	1.0	0.83927	0.00116	0.84159
XG7	NA_MURR2_TFNW060	1.0	0.6	1.0	0.83816	0.00117	0.84050
XG8	NA_MURR2_TFNW070	1.0	0.7	1.0	0.83704	0.00131	0.83966
XG9	NA_MURR2_TFNW080	1.0	0.8	1.0	0.83199	0.00118	0.83435
XG10	NA_MURR2_TFNW090	1.0	0.9	1.0	0.82930	0.00116	0.83162
XG11	NA_MURR2_TFNW100	1.0	1.0	1.0	0.82461	0.00129	0.82719
Series 5: Same as Series 3 with 0.9 g/cm³ water between fuel plates.							
XH1	NA_MURR2_M90FNW000	1.0	0	0.9	0.80160	0.00132	0.80424
XH2	NA_MURR2_M90FNW010	1.0	0.1	0.9	0.80747	0.00120	0.80987
XH3	NA_MURR2_M90FNW020	1.0	0.2	0.9	0.81288	0.00127	0.81542
XH4	**NA_MURR2_M90FNW030**	**1.0**	**0.3**	**0.9**	**0.81512**	**0.00127**	**0.81766**
XH5	NA_MURR2_M90FNW040	1.0	0.4	0.9	0.81504	0.00120	0.81744
XH6	NA_MURR2_M90FNW050	1.0	0.5	0.9	0.81382	0.00112	0.81606
XH7	NA_MURR2_M90FNW060	1.0	0.6	0.9	0.81369	0.00121	0.81611
XH8	NA_MURR2_M90FNW070	1.0	0.7	0.9	0.81165	0.00129	0.81423
XH9	NA_MURR2_M90FNW080	1.0	0.8	0.9	0.80950	0.00122	0.81194
XH10	NA_MURR2_M90FNW090	1.0	0.9	0.9	0.80311	0.00124	0.80559
XH11	NA_MURR2_M90FNW100	1.0	1.0	0.9	0.79735	0.00117	0.79969

Table 6.10-11 – MIT NCT Array Results

Case ID	Filename	Water Density Inside FHE (g/cm^3)	Water Density Outside FHE (g/cm^3)	Water Density Between Plates (g/cm^3)	k_{eff}	σ	k_s (k+2σ)
Series 1: Variable water density and outside FHE, with neoprene							
YD1	NA_MIT_NW000	0	0	1.0	0.48041	0.00096	0.48233
YD2	NA_MIT_NW010	0.1	0.1	1.0	0.52918	0.00105	0.53128
YD3	NA_MIT_NW020	0.2	0.2	1.0	0.56301	0.00103	0.56507
YD4	NA_MIT_NW030	0.3	0.3	1.0	0.59062	0.00105	0.59272
YD5	NA_MIT_NW040	0.4	0.4	1.0	0.60722	0.00122	0.60966
YD6	NA_MIT_NW050	0.5	0.5	1.0	0.61575	0.00118	0.61811
YD7	**NA_MIT_NW060**	**0.6**	**0.6**	**1.0**	**0.61989**	**0.00114**	**0.62217**
YD8	NA_MIT_NW070	0.7	0.7	1.0	0.61723	0.00110	0.61943
YD9	NA_MIT_NW080	0.8	0.8	1.0	0.61618	0.00116	0.61850
YD10	NA_MIT_NW090	0.9	0.9	1.0	0.61352	0.00112	0.61576
YD11	NA_MIT_NW100	1.0	1.0	1.0	0.60885	0.00112	0.61109
YD12	NA_MIT_CNW060	0.6	0.6	1.0	0.60764	0.00103	0.60970
Series 2: Repeat of Series 1 without neoprene							
YE1	NA_MIT_W000	0	0	1.0	0.46154	0.00093	0.46340
YE2	NA_MIT_W010	0.1	0.1	1.0	0.51291	0.00095	0.51481
YE3	NA_MIT_W020	0.2	0.2	1.0	0.55394	0.00103	0.55600
YE4	NA_MIT_W030	0.3	0.3	1.0	0.58160	0.00113	0.58386
YE5	NA_MIT_W040	0.4	0.4	1.0	0.60184	0.00111	0.60406
YE6	NA_MIT_W050	0.5	0.5	1.0	0.61163	0.00119	0.61401
YE7	**NA_MIT_W060**	**0.6**	**0.6**	**1.0**	**0.61746**	**0.00117**	**0.61980**
YE8	NA_MIT_W070	0.7	0.7	1.0	0.61518	0.00116	0.61750
YE9	NA_MIT_W080	0.8	0.8	1.0	0.61215	0.00106	0.61427
YE10	NA_MIT_W090	0.9	0.9	1.0	0.61082	0.00111	0.61304
YE11	NA_MIT_W100	1.0	1.0	1.0	0.60324	0.00110	0.60544
Series 3: Variable water density outside FHE, with neoprene.							
YF1	NA_MIT_FNW000	1.0	0	1.0	0.55417	0.00118	0.55653
YF2	NA_MIT_FNW010	1.0	0.1	1.0	0.57731	0.00104	0.57939
YF3	NA_MIT_FNW020	1.0	0.2	1.0	0.59825	0.00117	0.60059
YF4	NA_MIT_FNW030	1.0	0.3	1.0	0.60830	0.00119	0.61068
YF5	NA_MIT_FNW040	1.0	0.4	1.0	0.61581	0.00116	0.61813
YF6	NA_MIT_FNW050	1.0	0.5	1.0	0.61968	0.00107	0.62182
YF7	**NA_MIT_FNW060**	**1.0**	**0.6**	**1.0**	**0.62059**	**0.00113**	**0.62285**
YF8	NA_MIT_FNW070	1.0	0.7	1.0	0.62035	0.00110	0.62255
YF9	NA_MIT_FNW080	1.0	0.8	1.0	0.61650	0.00110	0.61870
YF10	NA_MIT_FNW090	1.0	0.9	1.0	0.61120	0.00105	0.61330
YD11	NA_MIT_NW100	1.0	1.0	1.0	0.60885	0.00112	0.61109

(continued)

Table 6.10-11 – MIT NCT Array Results (concluded)

Case ID	Filename	Water Density Inside FHE (g/cm^3)	Water Density Outside FHE (g/cm^3)	Water Density Between Plates (g/cm^3)	k_{eff}	σ	k_s ($k+2\sigma$)
Series 4: Same as Series 3 but with maximum thickness FHE.							
YG1	NA_MIT_TFNW000	1.0	0	1.0	0.55951	0.00106	0.56163
YG2	NA_MIT_TFNW010	1.0	0.1	1.0	0.58058	0.00105	0.58268
YG3	NA_MIT_TFNW020	1.0	0.2	1.0	0.59653	0.00105	0.59863
YG4	NA_MIT_TFNW030	1.0	0.3	1.0	0.60581	0.00118	0.60817
YG5	NA_MIT_TFNW040	1.0	0.4	1.0	0.61242	0.00110	0.61462
YG6	NA_MIT_TFNW050	1.0	0.5	1.0	0.61318	0.00104	0.61526
YG7	NA_MIT_TFNW060	1.0	0.6	1.0	0.61463	0.00120	0.61703
YG8	**NA_MIT_TFNW070**	**1.0**	**0.7**	**1.0**	**0.61501**	**0.00111**	**0.61723**
YG9	NA_MIT_TFNW080	1.0	0.8	1.0	0.61394	0.00114	0.61622
YG10	NA_MIT_TFNW090	1.0	0.9	1.0	0.60894	0.00113	0.61120
YG11	NA_MIT_TFNW100	1.0	1.0	1.0	0.60456	0.00120	0.60696
Series 5: Same as Series 3 with 0.9 g/cm^3 water between fuel plates.							
YH1	NA_MIT_M90FNW000	1.0	0	0.9	0.53177	0.00107	0.53391
YH2	NA_MIT_M90FNW010	1.0	0.1	0.9	0.55655	0.00108	0.55871
YH3	NA_MIT_M90FNW020	1.0	0.2	0.9	0.57776	0.00122	0.58020
YH4	NA_MIT_M90FNW030	1.0	0.3	0.9	0.59349	0.00102	0.59553
YH5	NA_MIT_M90FNW040	1.0	0.4	0.9	0.60205	0.00103	0.60411
YH6	NA_MIT_M90FNW050	1.0	0.5	0.9	0.60659	0.00102	0.60863
YH7	NA_MIT_M90FNW060	1.0	0.6	0.9	0.60651	0.00119	0.60889
YH8	**NA_MIT_M90FNW070**	**1.0**	**0.7**	**0.9**	**0.60753**	**0.00121**	**0.60995**
YH9	NA_MIT_M90FNW080	1.0	0.8	0.9	0.60615	0.00112	0.60839
YH10	NA_MIT_M90FNW090	1.0	0.9	0.9	0.60192	0.00100	0.60392
YH11	NA_MIT_M90FNW100	1.0	1.0	0.9	0.59396	0.00111	0.59618

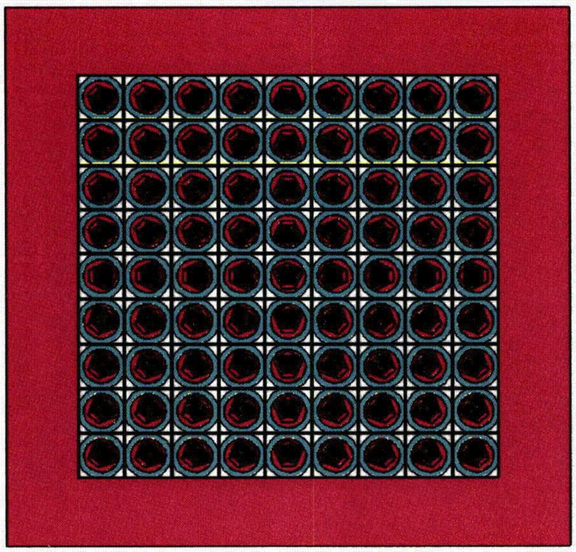

MURR Full view

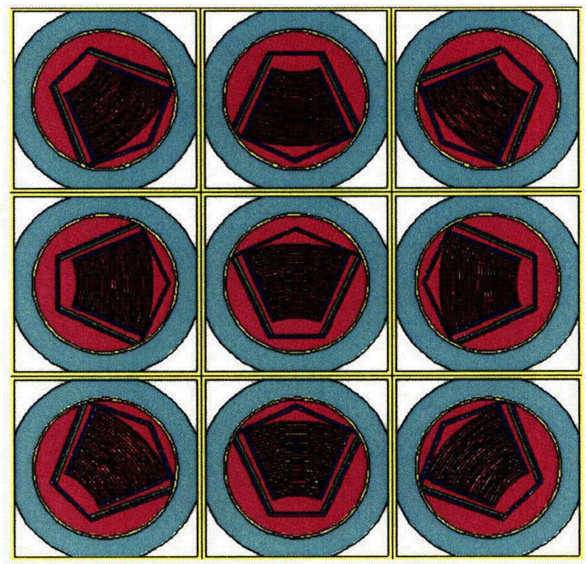

MURR Close-up

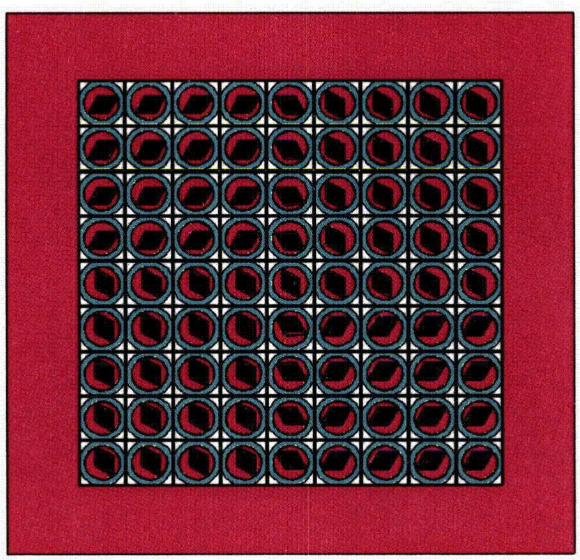

MIT Full view

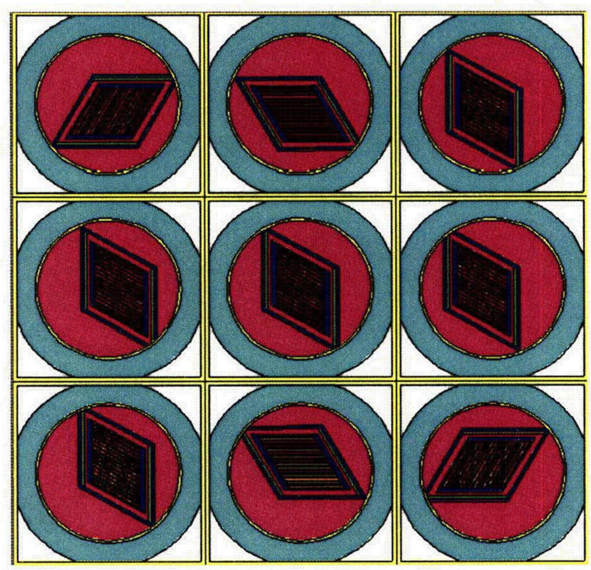

MIT Close-up

Figure 6.10-10 – MURR/MIT NCT Array Geometry

6.10.6 Package Arrays under Hypothetical Accident Conditions

6.10.6.1 HAC Array Condition

The HAC array model is a 5x5x1 array of packages. The primary difference comparing NCT to HAC is the modeled fuel damage, and separation of the FHE halves. Consistent with the HAC single package models, the two FHE halves are allowed to separate to the maximum possible extent, and the fuel element pitch is allowed to increase to the maximum possible value until constrained by the FHE. It is established in the HAC single package analysis that the reactivity is maximized with the maximum pitch, so all HAC array calculations utilize the maximum pitch.

The moderation conditions for the HAC array cases are largely the same as the NCT array moderation conditions, with the exception of the insulation region. In the HAC models, this region may be filled with variable density water. From the NCT array calculations, it was determined that the neoprene has a statistically insignificant effect on the reactivity, although the results showed a negligible increase. Therefore, neoprene is included in all HAC array models. Also, it has also been established in the HAC single package and NCT array cases that reducing the water density between the fuel plates reduces the reactivity. Therefore, the water between the fuel plates is always modeled at full density.

Although it is not feasible in actual practice to push the FHEs to the center of the array if the two FHE halves are already pushed apart, both the MURR and MIT models are shifted by 0.307-in towards the center of the array, as determined in Section 6.10.5.1, *NCT Array Configuration*. Note in Figure 6.10-11 that the FHEs for both MURR and MIT are "sliced off" in the corners because such a translation is not possible without interference, and the aluminum corners of the MIT element are also "sliced off" slightly for the same reason.

6.10.6.1.1 MURR Fuel Element Models

Five calculational series are developed, as described below. Results are summarized in Table 6.10-12.

Series 1 (Cases XJ1 through XJ11): In Series 1, the water density inside and outside the FHE is modeled at the same density, which is allowed to vary between 0 and 1.0 g/cm^3. This moderation condition simulates the partial moderation effect of assuming the plastic bag that surrounds the fuel element retains water. The region between the circular and square tubes is modeled as insulation/void, and the FHE is modeled with the minimum wall thickness.

Series 2 (Cases XK1 through XK11): In Series 2, the water density inside the FHE is fixed at 1.0 g/cm^3, while the water density outside the FHE is allowed to vary between 0 and 1.0 g/cm^3. This moderation condition simulates the partial moderation effect of assuming the FHE retains water. The region between the circular and square tubes is modeled as insulation/void, and the FHE is modeled with a minimum wall thickness. The maximum reactivity increases slightly compared to Series 1, although the effect is well within statistical fluctuation.

An additional case (Case XK11) is developed in which the insulation is replaced with void for the most reactive Series 2 case (Case XK10). Comparing Cases XK10 and XK11, it is slightly more reactive to model the insulation, which is consistent with the trend in the ATR fuel analysis.

Series 3 (Cases XL1 through XL11): In Series 3, the outer insulation/void region is replaced with variable density water. There are now three regions that contain water: (1) between the circular and square tubes, (2) between FHE and circular tube, and (3) between fuel element and FHE. In this series, each of these regions is modeled with the same water density, which is allowed to vary between 0 and 1.0 g/cm^3. Reactivity is significantly lower in Series 3 compared with either Series 1 or 2.

Series 4 (Cases XM1 through XM10): In Series 4, full-density water is modeled inside the FHE, while variable density water between 0 and 1.0 g/cm^3 is modeled outside the FHE and between the inner and outer tubes. This series is less reactive than either Series 1 or 2.

Series 5 (Cases XN1 through XN11): Series 5 is a repeat of Series 2 except using a thick-walled FHE. The reactivity increases slightly when the thick-walled FHE is used.

Series 1, 2 and 5 result in similar reactivities within the statistical uncertainty of the method. Case XN9 is the most reactive MURR case, with k_s = 0.85881. In this case, the fuel elements are pushed to the center of the array, full-density water is modeled between the plates and inside the FHE, 0.8 g/cm^3 water is modeled outside the FHE, insulation/void is modeled between the inner and outer tubes, chlorine-free neoprene is included, and the FHE is modeled with maximum wall thickness. The maximum result is below the USL of 0.9209.

6.10.6.1.2 MIT Fuel Element Models

Five calculational series are developed, as described below. Results are summarized in Table 6.10-13.

Series 1 (Cases YJ1 through YJ11): In Series 1, the water density inside and outside the FHE is modeled at the same density, which is allowed to vary between 0 and 1.0 g/cm^3. This moderation condition simulates the partial moderation effect of assuming the plastic bag that surrounds the fuel element retains water. The region between the circular and square tubes is modeled as insulation/void, and the FHE is modeled with the minimum wall thickness.

Series 2 (Cases YK1 through YK11): In Series 2, the water density inside the FHE is fixed at 1.0 g/cm^3, while the water density outside the FHE is allowed to vary between 0 and 1.0 g/cm^3. This moderation condition simulates the partial moderation effect of assuming the FHE retains water. The region between the circular and square tubes is modeled as insulation/void, and the FHE is modeled with a minimum wall thickness. The maximum reactivity increases slightly compared to Series 1, although the effect is well within statistical fluctuation.

An additional case (Case YK11) is developed in which the insulation is replaced with void for the most reactive Series 2 case (Case YK9). Comparing Cases YK9 and YK11, it is slightly more reactive to model the insulation, which is consistent with the trend in the ATR fuel analysis.

Series 3 (Cases YL1 through YL11): In Series 3, the outer insulation/void region is replaced with variable density water. There are now three regions that contain water: (1) between the circular and square tubes, (2) between FHE and circular tube, and (3) between fuel element and FHE. In this series, each of these regions is modeled with the same water density, which is allowed to vary between 0 and 1.0 g/cm^3. Reactivity is significantly lower in Series 3 compared with either Series 1 or 2.

Series 4 (Cases YM1 through YM10): In Series 4, full-density water is modeled inside the FHE, while variable density water between 0 and 1.0 g/cm^3 is modeled outside the FHE and between the inner and outer tubes. This series is less reactive than either Series 1 or 2.

Series 5 (Cases YN1 through YN11): Series 5 is a repeat of Series 2 except using a thick-walled FHE. The reactivity decreases slightly when the thick-walled FHE is used, although the decrease is within statistical fluctuation.

Series 1, 2 and 5 result in similar reactivities within the statistical uncertainty of the method. Case YK9 is the most reactive MIT case, with $k_s = 0.67309$. In this case, the fuel elements are pushed to the center of the array, full-density water is modeled between the plates and inside the FHE, 0.8 g/cm^3 water is modeled outside the FHE, insulation/void is modeled between the inner and outer tubes, chlorine-free neoprene is included, and the FHE is modeled with minimum wall thickness. The maximum result is below the USL of 0.9209.

6.10.6.2 HAC Array Results

Following are the tabulated results for the HAC array cases. The most reactive configuration in each series is listed in boldface.

Table 6.10-12 – MURR HAC Array Results

Case ID	Filename	Water Density Between Tubes (g/cm³)	Water Density Inside FHE (g/cm³)	Water Density Outside FHE (g/cm³)	k_{eff}	σ	k_s (k+2σ)
Series 1: Insulation modeled, full-density water between plates, variable density water as indicated.							
XJ1	HA_MURR2_NW000	0	0	0	0.76355	0.00115	0.76585
XJ2	HA_MURR2_NW010	0	0.1	0.1	0.78430	0.00122	0.78674
XJ3	HA_MURR2_NW020	0	0.2	0.2	0.80290	0.00111	0.80512
XJ4	HA_MURR2_NW030	0	0.3	0.3	0.81874	0.00124	0.82122
XJ5	HA_MURR2_NW040	0	0.4	0.4	0.83311	0.00127	0.83565
XJ6	HA_MURR2_NW050	0	0.5	0.5	0.84140	0.00122	0.84384
XJ7	HA_MURR2_NW060	0	0.6	0.6	0.84544	0.00124	0.84792
XJ8	HA_MURR2_NW070	0	0.7	0.7	0.85035	0.00118	0.85271
XJ9	HA_MURR2_NW080	0	0.8	0.8	0.84998	0.00127	0.85252
XJ10	**HA_MURR2_NW090**	**0**	**0.9**	**0.9**	**0.85379**	**0.00128**	**0.85635**
XJ11	HA_MURR2_NW100	0	1.0	1.0	0.84975	0.00120	0.85215
Series 2: Insulation modeled, full-density water between plates and inside FHE, variable density water as indicated.							
XK1	HA_MURR2_FNW000	0	1.0	0	0.83610	0.00115	0.83840
XK2	HA_MURR2_FNW010	0	1.0	0.1	0.84001	0.00125	0.84251
XK3	HA_MURR2_FNW020	0	1.0	0.2	0.84152	0.00115	0.84382
XK4	HA_MURR2_FNW030	0	1.0	0.3	0.84875	0.00130	0.85135
XK5	HA_MURR2_FNW040	0	1.0	0.4	0.84946	0.00127	0.85200
XK6	HA_MURR2_FNW050	0	1.0	0.5	0.84850	0.00119	0.85088
XK7	HA_MURR2_FNW060	0	1.0	0.6	0.85141	0.00118	0.85377
XK8	HA_MURR2_FNW070	0	1.0	0.7	0.85076	0.00117	0.85310
XK9	HA_MURR2_FNW080	0	1.0	0.8	0.85054	0.00127	0.85308
XK10	**HA_MURR2_FNW090**	**0**	**1.0**	**0.9**	**0.85391**	**0.00125**	**0.85641**
XJ11	HA_MURR2_NW100	0	1.0	1.0	0.84975	0.0012	0.85215
XK11	HA_MURR2_FNW090X	0	1.0	0.9	0.84922	0.00132	0.85186
Series 3: Insulation not modeled, variable density water as indicated.							
XL1	HA_MURR2_ANW000	0	0	0	0.75710	0.00115	0.75940
XL2	HA_MURR2_ANW010	0.1	0.1	0.1	0.78773	0.00117	0.79007
XL3	**HA_MURR2_ANW020**	**0.2**	**0.2**	**0.2**	**0.78883**	**0.00124**	**0.79131**
XL4	HA_MURR2_ANW030	0.3	0.3	0.3	0.77894	0.00115	0.78124
XL5	HA_MURR2_ANW040	0.4	0.4	0.4	0.75950	0.00114	0.76178
XL6	HA_MURR2_ANW050	0.5	0.5	0.5	0.74010	0.00119	0.74248
XL7	HA_MURR2_ANW060	0.6	0.6	0.6	0.72381	0.00113	0.72607
XL8	HA_MURR2_ANW070	0.7	0.7	0.7	0.70323	0.00130	0.70583
XL9	HA_MURR2_ANW080	0.8	0.8	0.8	0.69154	0.00108	0.69370
XL10	HA_MURR2_ANW090	0.9	0.9	0.9	0.67881	0.00115	0.68111
XL11	HA_MURR2_ANW100	1.0	1.0	1.0	0.67207	0.00113	0.67433

(continued)

Table 6.10-12 – MURR HAC Array Results (concluded)

Case ID	Filename	Water Density Between Tubes (g/cm^3)	Water Density Inside FHE (g/cm^3)	Water Density Outside FHE (g/cm^3)	k_{eff}	σ	k_s ($k+2\sigma$)
Series 4: Insulation not modeled, variable density water as indicated.							
XM1	**HA_MURR2_IFNW000**	**0**	**1.0**	**0**	**0.83196**	**0.00121**	**0.83438**
XM2	HA_MURR2_IFNW010	0.1	1.0	0.1	0.82347	0.00123	0.82593
XM3	HA_MURR2_IFNW020	0.2	1.0	0.2	0.80575	0.00127	0.80829
XM4	HA_MURR2_IFNW030	0.3	1.0	0.3	0.78652	0.00109	0.78870
XM5	HA_MURR2_IFNW040	0.4	1.0	0.4	0.76597	0.00108	0.76813
XM6	HA_MURR2_IFNW050	0.5	1.0	0.5	0.74360	0.00124	0.74608
XM7	HA_MURR2_IFNW060	0.6	1.0	0.6	0.72740	0.00119	0.72978
XM8	HA_MURR2_IFNW070	0.7	1.0	0.7	0.70952	0.00112	0.71176
XM9	HA_MURR2_IFNW080	0.8	1.0	0.8	0.69669	0.00115	0.69899
XM10	HA_MURR2_IFNW090	0.9	1.0	0.9	0.68144	0.00119	0.68382
XL11	HA_MURR2_ANW100	1.0	1.0	1.0	0.67207	0.00113	0.67433
Series 5: Repeat of Series 2 with thick-walled FHE.							
XN1	HA_MURR2_TFNW000	0	1.0	0	0.83999	0.00136	0.84271
XN2	HA_MURR2_TFNW010	0	1.0	0.1	0.84169	0.00120	0.84409
XN3	HA_MURR2_TFNW020	0	1.0	0.2	0.84521	0.00115	0.84751
XN4	HA_MURR2_TFNW030	0	1.0	0.3	0.84875	0.00131	0.85137
XN5	HA_MURR2_TFNW040	0	1.0	0.4	0.84997	0.00117	0.85231
XN6	HA_MURR2_TFNW050	0	1.0	0.5	0.85368	0.00128	0.85624
XN7	HA_MURR2_TFNW060	0	1.0	0.6	0.85219	0.00115	0.85449
XN8	HA_MURR2_TFNW070	0	1.0	0.7	0.85204	0.00121	0.85446
XN9	**HA_MURR2_TFNW080**	**0**	**1.0**	**0.8**	**0.85621**	**0.00130**	**0.85881**
XN10	HA_MURR2_TFNW090	0	1.0	0.9	0.85319	0.00126	0.85571
XN11	HA_MURR2_TFNW100	0	1.0	1.0	0.85277	0.00121	0.85519

Table 6.10-13 – MIT HAC Array Results

Case ID	Filename	Water Density Between Tubes (g/cm³)	Water Density Inside FHE (g/cm³)	Water Density Outside FHE (g/cm³)	k_{eff}	σ	k_s (k+2σ)
Series 1: Insulation modeled, full-density water between plates, variable density water as indicated.							
YJ1	HA_MIT_NW000	0	0	0	0.53667	0.00092	0.53851
YJ2	HA_MIT_NW010	0	0.1	0.1	0.56904	0.00111	0.57126
YJ3	HA_MIT_NW020	0	0.2	0.2	0.59837	0.00116	0.60069
YJ4	HA_MIT_NW030	0	0.3	0.3	0.62139	0.00122	0.62383
YJ5	HA_MIT_NW040	0	0.4	0.4	0.63737	0.00108	0.63953
YJ6	HA_MIT_NW050	0	0.5	0.5	0.65014	0.00109	0.65232
YJ7	HA_MIT_NW060	0	0.6	0.6	0.65850	0.00122	0.66094
YJ8	HA_MIT_NW070	0	0.7	0.7	0.66668	0.00115	0.66898
YJ9	**HA_MIT_NW080**	**0**	**0.8**	**0.8**	**0.67043**	**0.00121**	**0.67285**
YJ10	HA_MIT_NW090	0	0.9	0.9	0.67026	0.00112	0.67250
YJ11	HA_MIT_NW100	0	1.0	1.0	0.67058	0.00104	0.67266
Series 2: Insulation modeled, full-density water between plates and inside FHE, variable density water as indicated.							
YK1	HA_MIT_FNW000	0	1.0	0	0.60486	0.00110	0.60706
YK2	HA_MIT_FNW010	0	1.0	0.1	0.62101	0.00117	0.62335
YK3	HA_MIT_FNW020	0	1.0	0.2	0.63436	0.00121	0.63678
YK4	HA_MIT_FNW030	0	1.0	0.3	0.64759	0.00106	0.64971
YK5	HA_MIT_FNW040	0	1.0	0.4	0.65646	0.00117	0.65880
YK6	HA_MIT_FNW050	0	1.0	0.5	0.66078	0.00117	0.66312
YK7	HA_MIT_FNW060	0	1.0	0.6	0.66656	0.00107	0.66870
YK8	HA_MIT_FNW070	0	1.0	0.7	0.67022	0.00114	0.67250
YK9	**HA_MIT_FNW080**	**0**	**1.0**	**0.8**	**0.67105**	**0.00102**	**0.67309**
YK10	HA_MIT_FNW090	0	1.0	0.9	0.66898	0.00113	0.67124
YJ11	HA_MIT_NW100	0	1.0	1.0	0.67058	0.00104	0.67266
YK11	HA_MIT_FNW080X	0	1.0	0.9	0.66684	0.00110	0.66904
Series 3: Insulation not modeled, variable density water as indicated.							
YL1	HA_MIT_ANW000	0	0	0	0.53173	0.00103	0.53379
YL2	HA_MIT_ANW010	0.1	0.1	0.1	0.58121	0.00100	0.58321
YL3	HA_MIT_ANW020	0.2	0.2	0.2	0.59902	0.00119	0.60140
YL4	**HA_MIT_ANW030**	**0.3**	**0.3**	**0.3**	**0.60054**	**0.00105**	**0.60264**
YL5	HA_MIT_ANW040	0.4	0.4	0.4	0.59003	0.00116	0.59235
YL6	HA_MIT_ANW050	0.5	0.5	0.5	0.57811	0.00109	0.58029
YL7	HA_MIT_ANW060	0.6	0.6	0.6	0.56624	0.00114	0.56852
YL8	HA_MIT_ANW070	0.7	0.7	0.7	0.55438	0.00107	0.55652
YL9	HA_MIT_ANW080	0.8	0.8	0.8	0.54409	0.00114	0.54637
YL10	HA_MIT_ANW090	0.9	0.9	0.9	0.53935	0.00105	0.54145
YL11	HA_MIT_ANW100	1.0	1.0	1.0	0.53078	0.00104	0.53286

(continued)

Table 6.10-13 – MIT HAC Array Results (concluded)

Case ID	Filename	Water Density Between Tubes (g/cm³)	Water Density Inside FHE (g/cm³)	Water Density Outside FHE (g/cm³)	k_{eff}	σ	k_s (k+2σ)
Series 4: Insulation not modeled, variable density water as indicated.							
YM1	HA_MIT_IFNW000	0	1.0	0	0.59996	0.00108	0.60212
YM2	**HA_MIT_IFNW010**	**0.1**	**1.0**	**0.1**	**0.61992**	**0.00112**	**0.62216**
YM3	HA_MIT_IFNW020	0.2	1.0	0.2	0.61899	0.00117	0.62133
YM4	HA_MIT_IFNW030	0.3	1.0	0.3	0.61130	0.00107	0.61344
YM5	HA_MIT_IFNW040	0.4	1.0	0.4	0.59725	0.00106	0.59937
YM6	HA_MIT_IFNW050	0.5	1.0	0.5	0.58253	0.00113	0.58479
YM7	HA_MIT_IFNW060	0.6	1.0	0.6	0.56935	0.00115	0.57165
YM8	HA_MIT_IFNW070	0.7	1.0	0.7	0.56002	0.00118	0.56238
YM9	HA_MIT_IFNW080	0.8	1.0	0.8	0.54870	0.00112	0.55094
YM10	HA_MIT_IFNW090	0.9	1.0	0.9	0.54119	0.00095	0.54309
YL11	HA_MIT_ANW100	1.0	1.0	1.0	0.53078	0.00104	0.53286
Series 5: Repeat of Series 2 with thick-walled FHE.							
YN1	HA_MIT_TFNW000	0	1.0	0	0.61405	0.00116	0.61637
YN2	HA_MIT_TFNW010	0	1.0	0.1	0.62418	0.00114	0.62646
YN3	HA_MIT_TFNW020	0	1.0	0.2	0.63652	0.00110	0.63872
YN4	HA_MIT_TFNW030	0	1.0	0.3	0.64631	0.00101	0.64833
YN5	HA_MIT_TFNW040	0	1.0	0.4	0.65197	0.00108	0.65413
YN6	HA_MIT_TFNW050	0	1.0	0.5	0.65994	0.00114	0.66222
YN7	HA_MIT_TFNW060	0	1.0	0.6	0.66467	0.00118	0.66703
YN8	HA_MIT_TFNW070	0	1.0	0.7	0.66785	0.00120	0.67025
YN9	HA_MIT_TFNW080	0	1.0	0.8	0.66872	0.00123	0.67118
YN10	**HA_MIT_TFNW090**	**0**	**1.0**	**0.9**	**0.66920**	**0.00111**	**0.67142**
YN11	HA_MIT_TFNW100	0	1.0	1.0	0.66847	0.00122	0.67091

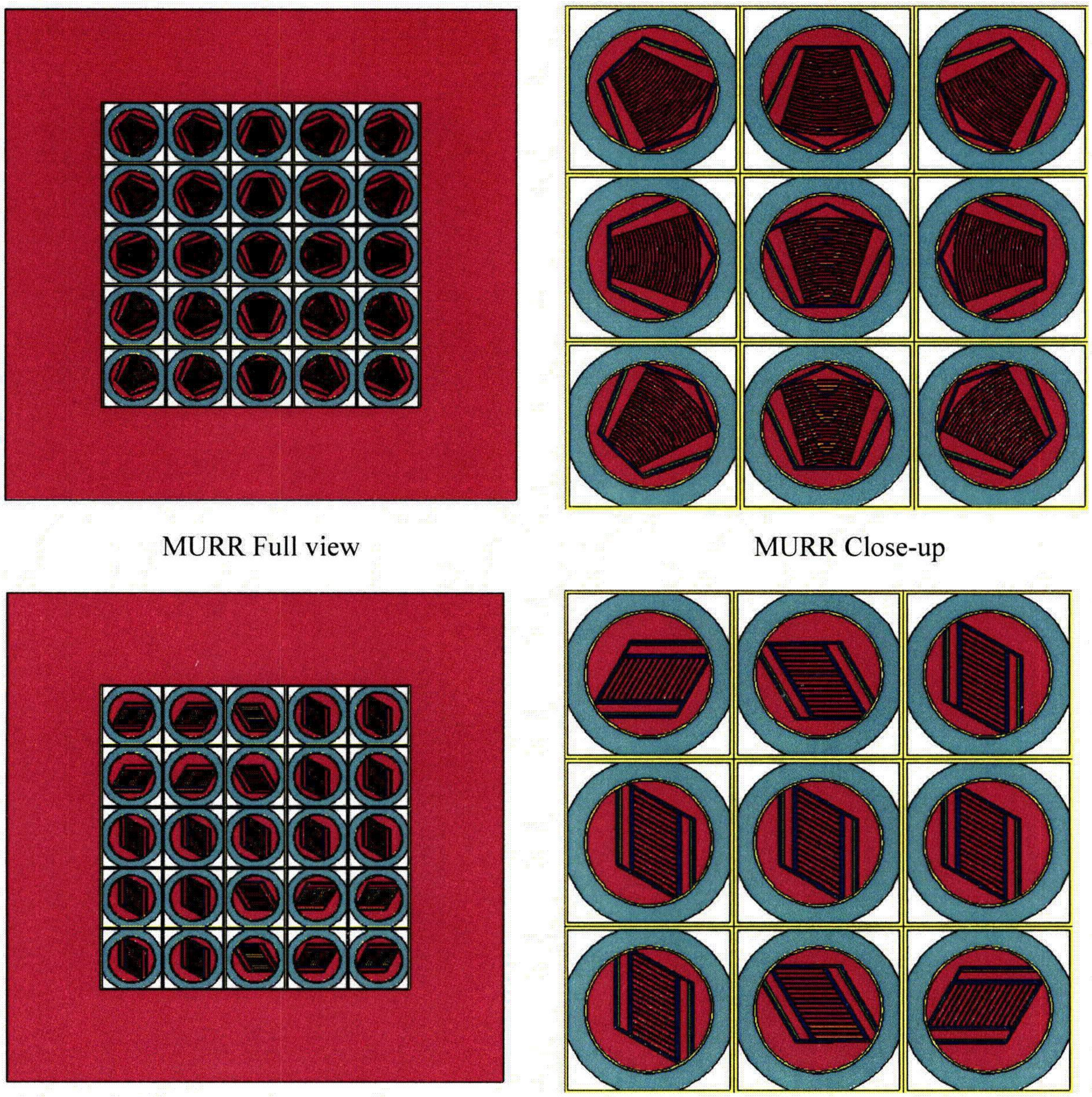

MURR Full view MURR Close-up

MIT Full view MIT Close-up

Figure 6.10-11 – MURR/MIT HAC Array Geometry

6.10.7 Fissile Material Packages for Air Transport

This section is not applicable.

6.10.8 Benchmark Evaluations

MURR and MIT fuel are both high-enriched aluminum plate-type fuel, similar to ATR fuel. Therefore, the benchmarking evaluation performed for the ATR fuel in Section 6.8, *Benchmark Evaluations*, is applicable to the current analysis, and the USL is 0.9209. The Monte Carlo computer program MCNP5 v1.30 was utilized in the benchmark analysis. MCNP has been used extensively in criticality evaluations for several decades and is considered a standard in the industry.

Five parameters were selected for the benchmark evaluation: (1) energy of the average neutron lethargy causing fission (EALF), (2) U-235 number density, (3) channel width, (4) H/U-235 atom ratio, and (5) pitch. The range of applicability of these parameters for the benchmarks utilized is summarized in Table 6.8-2. In the following sections, the range of applicability of the benchmarks is compared with the MURR and MIT criticality analysis.

6.10.8.1 Energy of the Average neutron Lethargy causing Fission (EALF)

Range of Applicability, MURR models: All of the single package models and most of the NCT and HAC array models fall within the range of the applicability. The EALF of the most reactive MURR fuel element model (Case XN9) has an EALF of 9.26E-08 MeV, which is within the range of applicability. Models with significantly more void spaces or low water densities sometimes exceed the range of applicability (maximum EALF = 2.03E-07 MeV for Case XE1), although these cases are not the most reactive. Therefore, the EALF of the most reactive models is acceptably within the range of applicability of the benchmarks.

Range of Applicability, MIT models: All of the single package models and most of the NCT and HAC array models fall within the range of the applicability. The EALF of the most reactive MIT fuel element model (Case YK9) has an EALF of 8.70E-08 MeV, which is within the range of applicability. Models with significantly more void spaces or low water densities sometimes exceed the range of applicability (maximum EALF = 3.30E-07 MeV for Case YE1), although these cases are not the most reactive. Therefore, the EALF of the most reactive models is acceptably within the range of applicability of the benchmarks.

6.10.8.2 U-235 Number Density

The U-235 number density is 3.61E-03 atom/b-cm in the MURR models and 3.68E-03 atom/b-cm in the MIT models. These number densities are within the range of applicability.

6.10.8.3 Channel Width

The NCT channel width is fixed at 0.088-in in the MURR models and 0.094-in in the MIT models. In the HAC models, in which the pitch is allowed to expand, the maximum channel width is 0.125-in in the MURR models and 0.176-in in the MIT models. All of these values exceed the maximum channel width of 0.078-in of the benchmark experiments. However, this parameter was artificially maximized in order to maximize model reactivity. As the channel width is directly related to system moderation, the acceptability of the EALF indicator demonstrates that MCNP is performing acceptably for thermal conditions. Therefore, this parameter is considered to be acceptable.

6.10.8.4 H/U-235 Atom Ratio

The H/U-235 atom ratio is used as the fourth trending parameter for the benchmark cases. The H/U-235 atom ratio is defined here as the ratio of hydrogen atoms to U-235 atoms in a unit cell. This parameter is computed by the following equation:

NH*C/(NU235*M)

where,

NH is the hydrogen number density

C is the channel width

NU235 is the U-235 number density

M is the fuel meat width

Range of Applicability, MURR models: The H/U-235 atom ratio may be computed as:

NCT: 6.687E-02*0.088/(3.6147E-03*0.02) = 81.4

HAC: 6.687E-02*0.125/(3.6147E-03*0.02) = 115.6

Therefore, H/U-235 of the MURR cases is acceptably within the range of applicability of the benchmarks.

Range of Applicability, MIT models: The H/U-235 atom ratio may be computed as:

NCT: 6.687E-02*0.094/(3.6835E-03*0.03) = 56.9

HAC: 6.687E-02*0.176/(3.6835E-03*0.03) = 106.5

The minimum H/U-235 atom ratio of the benchmark models is 65.1. Therefore, this parameter is slightly outside the range of the benchmark experiments for the NCT cases, although the difference is so small that this parameter is considered to be acceptable. For the HAC cases, which bound the NCT cases, this parameter is acceptably within the range of applicability of the benchmarks.

6.10.8.5 Pitch

The NCT pitch is fixed at 0.13-in in the MURR models and 0.16-in in the MIT models. In the HAC models, in which the pitch is allowed to expand, the maximum pitch is 0.167-in in the MURR models and 0.24-in in the MIT models. The maximum pitch of the benchmark models is 0.128-in, so the pitch in the models exceeds the range of the benchmarks, particularly for the HAC cases. However, this parameter was artificially maximized in order to maximize model reactivity. As the pitch is directly related to system moderation, the acceptability of the EALF indicator demonstrates that MCNP is performing acceptably for thermal conditions. Therefore, this parameter is considered to be acceptable.

6.10.9 Sample Input Files

A sample input file is provided for the most reactive MURR and MIT cases.

MURR Case XN9 (HA_MURR2_TFNW080)

```
MURR
999     0      -320:321:-322:323:-324:325                      imp:n=0
900     0      310 -311 312 -313 24 -25     fill=3      imp:n=1
901     2 -1.0 (311:-310:313:-312:-24:25) 320 -321 322 -323 324 -325  imp:n=1
c
c       Universe 1: MURR Fuel Element (infinitely long)
c
10       10 5.4439E-02 52 -53 -16 -15                          u=1 imp:n=1 $
plate 1
11       3 -2.7        (-52:53:16:15) 51 -54 -7 -8             u=1 imp:n=1
12       10 5.4439E-02 401 -402 -406 -407                      u=1 imp:n=1 $
plate 2
13       3 -2.7        (-401:402:406:407) 400 -403 -404 -405 u=1 imp:n=1
14       10 5.4439E-02 411 -412 -416 -417                      u=1 imp:n=1 $
plate 3
15       3 -2.7        (-411:412:416:417) 410 -413 -414 -415 u=1 imp:n=1
16       10 5.4439E-02 421 -422 -426 -427                      u=1 imp:n=1 $
plate 4
17       3 -2.7        (-421:422:426:427) 420 -423 -424 -425 u=1 imp:n=1
18       10 5.4439E-02 431 -432 -436 -437                      u=1 imp:n=1 $
plate 5
19       3 -2.7        (-431:432:436:437) 430 -433 -434 -435 u=1 imp:n=1
20       10 5.4439E-02 441 -442 -446 -447                      u=1 imp:n=1 $
plate 6
21       3 -2.7        (-441:442:446:447) 440 -443 -444 -445 u=1 imp:n=1
22       10 5.4439E-02 451 -452 -456 -457                      u=1 imp:n=1 $
plate 7
23       3 -2.7        (-451:452:456:457) 450 -453 -454 -455 u=1 imp:n=1
24       10 5.4439E-02 461 -462 -466 -467                      u=1 imp:n=1 $
plate 8
25       3 -2.7        (-461:462:466:467) 460 -463 -464 -465 u=1 imp:n=1
26       10 5.4439E-02 471 -472 -476 -477                      u=1 imp:n=1 $
plate 9
27       3 -2.7        (-471:472:476:477) 470 -473 -474 -475 u=1 imp:n=1
28       10 5.4439E-02 481 -482 -486 -487                      u=1 imp:n=1 $
plate 10
29       3 -2.7        (-481:482:486:487) 480 -483 -484 -485 u=1 imp:n=1
30       10 5.4439E-02 491 -492 -496 -497                      u=1 imp:n=1 $
plate 11
31       3 -2.7        (-491:492:496:497) 490 -493 -494 -495 u=1 imp:n=1
32       10 5.4439E-02 501 -502 -506 -507                      u=1 imp:n=1 $
plate 12
33       3 -2.7        (-501:502:506:507) 500 -503 -504 -505 u=1 imp:n=1
34       10 5.4439E-02 511 -512 -516 -517                      u=1 imp:n=1 $
plate 13
35       3 -2.7        (-511:512:516:517) 510 -513 -514 -515 u=1 imp:n=1
36       10 5.4439E-02 521 -522 -526 -527                      u=1 imp:n=1 $
plate 14
37       3 -2.7        (-521:522:526:527) 520 -523 -524 -525 u=1 imp:n=1
```

```
38       10 5.4439E-02 531 -532 -536 -537                         u=1 imp:n=1 $
plate 15
39       3 -2.7        (-531:532:536:537) 530 -533 -534 -535 u=1 imp:n=1
40       10 5.4439E-02 541 -542 -546 -547                         u=1 imp:n=1 $
plate 16
41       3 -2.7        (-541:542:546:547) 540 -543 -544 -545 u=1 imp:n=1
42       10 5.4439E-02 551 -552 -556 -557                         u=1 imp:n=1 $
plate 17
43       3 -2.7        (-551:552:556:557) 550 -553 -554 -555 u=1 imp:n=1
44       10 5.4439E-02 561 -562 -566 -567                         u=1 imp:n=1 $
plate 18
45       3 -2.7        (-561:562:566:567) 560 -563 -564 -565 u=1 imp:n=1
46       10 5.4439E-02 571 -572 -576 -577                         u=1 imp:n=1 $
plate 19
47       3 -2.7        (-571:572:576:577) 570 -573 -574 -575 u=1 imp:n=1
48       10 5.4439E-02 581 -582 -586 -587                         u=1 imp:n=1 $
plate 20
49       3 -2.7        (-581:582:586:587) 580 -583 -584 -585 u=1 imp:n=1
50       10 5.4439E-02 591 -592 -596 -597                         u=1 imp:n=1 $
plate 21
51       3 -2.7        (-591:592:596:597) 590 -593 -594 -595 u=1 imp:n=1
52       10 5.4439E-02 601 -602 -606 -607                         u=1 imp:n=1 $
plate 22
53       3 -2.7        (-601:602:606:607) 600 -603 -604 -605 u=1 imp:n=1
54       10 5.4439E-02 611 -612 -616 -617                         u=1 imp:n=1 $
plate 23
55       3 -2.7        (-611:612:616:617) 610 -613 -614 -615 u=1 imp:n=1
56       10 5.4439E-02 621 -622 -626 -627                         u=1 imp:n=1 $
plate 24
57       3 -2.7        (-621:622:626:627) 620 -623 -624 -625 u=1 imp:n=1
150      2 -1.0  (-51:54:7:8)        (-400:403:404:405) (-410:413:414:415)
                 (-420:423:424:425) (-430:433:434:435) (-440:443:444:445)
                 (-450:453:454:455) (-460:463:464:465) (-470:473:474:475)
                 (-480:483:484:485) (-490:493:494:495) (-500:503:504:505)
                 (-510:513:514:515) (-520:523:524:525) (-530:533:534:535)
                 (-540:543:544:545) (-550:553:554:555) (-560:563:564:565)
                 (-570:573:574:575) (-580:583:584:585) (-590:593:594:595)
                 (-600:603:604:605) (-610:613:614:615) (-620:623:624:625)
                 u=1 imp:n=1
c
c        Universe 19: MURR with FHE
c
200      0         -232 -233 212 213 214 -234 fill=1(1) u=19 imp:n=1
201      5 -0.737  230 -210 212 214               u=19 imp:n=1 $ right
neoprene
202      5 -0.737  231 -211 213 214               u=19 imp:n=1 $ left neoprene
203      2 -1.0    213 212 234                    u=19 imp:n=1 $ top water
outside bag
204      2 -1.0    -230 232 214 212               u=19 imp:n=1 $ side water
outside bag
205      2 -1.0    -231 233 214 213               u=19 imp:n=1 $ side water
outside bag
206      3 -2.7    (210:211:-212:-213:-214) -220 -221 222 223 224 u=19 imp:n=1
$ FHE
207      2 -0.8     220:221:-222:-223:-224       u=19 imp:n=1 $ water
c
c        Universe 20: MURR with pipe (center)
c
210      0           -200 fill=19               u=20 imp:n=1
211      4 -7.94     200 -201                   u=20 imp:n=1 $ pipe
```

```
212     6 -0.096    201 -203 250 -251 252 -253  u=20 imp:n=1 $ insulation
213     0           203 250 -251 252 -253       u=20 imp:n=1 $ insulation to
tube
214     4 -7.94     -250:251:-252:253           u=20 imp:n=1 $ tube to inf
c
c       Universe 21: MURR with pipe (down)
c
220     0           -200 fill=19(2)             u=21 imp:n=1
221     4 -7.94     200 -201                    u=21 imp:n=1 $ pipe
222     6 -0.096    201 -203 250 -251 252 -253  u=21 imp:n=1 $ insulation
223     0           203 250 -251 252 -253       u=21 imp:n=1 $ insulation to
tube
224     4 -7.94     -250:251:-252:253           u=21 imp:n=1 $ tube to inf
c
c       Universe 22: MURR with pipe (up)
c
230     0           -200 fill=19(3)             u=22 imp:n=1
231     4 -7.94     200 -201                    u=22 imp:n=1 $ pipe
232     6 -0.096    201 -203 250 -251 252 -253  u=22 imp:n=1 $ insulation
233     0           203 250 -251 252 -253       u=22 imp:n=1 $ insulation to
tube
234     4 -7.94     -250:251:-252:253           u=22 imp:n=1 $ tube to inf
c
c       Universe 23: MURR with pipe (right)
c
240     0           -200 fill=19(4)             u=23 imp:n=1
241     4 -7.94     200 -201                    u=23 imp:n=1 $ pipe
242     6 -0.096    201 -203 250 -251 252 -253  u=23 imp:n=1 $ insulation
243     0           203 250 -251 252 -253       u=23 imp:n=1 $ insulation to
tube
244     4 -7.94     -250:251:-252:253           u=23 imp:n=1 $ tube to inf
c
c       Universe 24: MURR with pipe (left)
c
250     0           -200 fill=19(5)             u=24 imp:n=1
251     4 -7.94     200 -201                    u=24 imp:n=1 $ pipe
252     6 -0.096    201 -203 250 -251 252 -253  u=24 imp:n=1 $ insulation
253     0           203 250 -251 252 -253       u=24 imp:n=1 $ insulation to
tube
254     4 -7.94     -250:251:-252:253           u=24 imp:n=1 $ tube to inf
c
c       Universe 25: MURR with pipe (up right)
c
260     0           -200 fill=19(6)             u=25 imp:n=1
261     4 -7.94     200 -201                    u=25 imp:n=1 $ pipe
262     6 -0.096    201 -203 250 -251 252 -253  u=25 imp:n=1 $ insulation
263     0           203 250 -251 252 -253       u=25 imp:n=1 $ insulation to
tube
264     4 -7.94     -250:251:-252:253           u=25 imp:n=1 $ tube to inf
c
c       Universe 26: MURR with pipe (up left)
c
270     0           -200 fill=19(7)             u=26 imp:n=1
271     4 -7.94     200 -201                    u=26 imp:n=1 $ pipe
272     6 -0.096    201 -203 250 -251 252 -253  u=26 imp:n=1 $ insulation
273     0           203 250 -251 252 -253       u=26 imp:n=1 $ insulation to
tube
274     4 -7.94     -250:251:-252:253           u=26 imp:n=1 $ tube to inf
c
c       Universe 27: MURR with pipe (down right)
```

```
c
280     0           -200 fill=19(8)             u=27 imp:n=1
281     4 -7.94     200 -201                    u=27 imp:n=1 $ pipe
282     6 -0.096    201 -203 250 -251 252 -253  u=27 imp:n=1 $ insulation
283     0           203 250 -251 252 -253       u=27 imp:n=1 $ insulation to
tube
284     4 -7.94     -250:251:-252:253           u=27 imp:n=1 $ tube to inf
c
c       Universe 28: MURR with pipe (down left)
c
290     0           -200 fill=19(9)             u=28 imp:n=1
291     4 -7.94     200 -201                    u=28 imp:n=1 $ pipe
292     6 -0.096    201 -203 250 -251 252 -253  u=28 imp:n=1 $ insulation
293     0           203 250 -251 252 -253       u=28 imp:n=1 $ insulation to
tube
294     4 -7.94     -250:251:-252:253           u=28 imp:n=1 $ tube to inf
c
c       Universe 3: Array of Packages
c
300   0     -300 301 -302 303 imp:n=1 u=3 lat=1 fill=-2:2 -2:2 0:0
              25 25 22 26 26
              25 25 22 26 26
              23 23 20 24 24
              27 27 21 28 28
              27 27 21 28 28

c 5       p  2.4142136 -1 0 -0.13275   $ right Al outer
c 6       p -2.4142136 -1 0 -0.13275   $ left Al outer
7       p  2.4142136 -1 0 -1.09516   $ right Al inner
8       p -2.4142136 -1 0 -1.09516   $ left Al inner
c 9       cz 6.858                     $ Al boundary
c 10      cz 14.884                    $ Al boundary
c
15      p  2.4142136 -1 0 -1.39997   $ plate meat boundary
16      p -2.4142136 -1 0 -1.39997   $ plate meat boundary
c
24      pz -30.48                    $ bottom of fuel
25      pz  30.48                    $ top of fuel (24")
c
51      cz 7.0460 $ fuel plate 1
52      cz 7.0739
53      cz 7.1247
54      cz 7.1526
c
400 22    cz 7.3762 $ fuel plate 2
401 22    cz 7.4041
402 22    cz 7.4549
403 22    cz 7.4828
404 22    p  2.4142136 -1 0 -1.09516   $ right Al inner
405 22    p -2.4142136 -1 0 -1.09516   $ left Al inner
406 22    p  2.4142136 -1 0 -1.39997   $ plate meat boundary
407 22    p -2.4142136 -1 0 -1.39997   $ plate meat boundary
c
410 23  cz 7.7064 $ fuel plate 3
411 23  cz 7.7343
412 23  cz 7.7851
413 23  cz 7.8130
414 23    p  2.4142136 -1 0 -1.09516   $ right Al inner
415 23    p -2.4142136 -1 0 -1.09516   $ left Al inner
416 23    p  2.4142136 -1 0 -1.39997   $ plate meat boundary
```

```
417 23    p -2.4142136 -1 0 -1.39997   $ plate meat boundary
c
420 24   cz 8.0366 $ fuel plate 4
421 24   cz 8.0645
422 24   cz 8.1153
423 24   cz 8.1432
424 24    p  2.4142136 -1 0 -1.09516   $ right Al inner
425 24    p -2.4142136 -1 0 -1.09516   $ left Al inner
426 24    p  2.4142136 -1 0 -1.39997   $ plate meat boundary
427 24    p -2.4142136 -1 0 -1.39997   $ plate meat boundary
c
430 25   cz 8.3668 $ fuel plate 5
431 25   cz 8.3947
432 25   cz 8.4455
433 25   cz 8.4734
434 25    p  2.4142136 -1 0 -1.09516   $ right Al inner
435 25    p -2.4142136 -1 0 -1.09516   $ left Al inner
436 25    p  2.4142136 -1 0 -1.39997   $ plate meat boundary
437 25    p -2.4142136 -1 0 -1.39997   $ plate meat boundary
c
440 26   cz 8.6970 $ fuel plate 6
441 26   cz 8.7249
442 26   cz 8.7757
443 26   cz 8.8036
444 26    p  2.4142136 -1 0 -1.09516   $ right Al inner
445 26    p -2.4142136 -1 0 -1.09516   $ left Al inner
446 26    p  2.4142136 -1 0 -1.39997   $ plate meat boundary
447 26    p -2.4142136 -1 0 -1.39997   $ plate meat boundary
c
450 27   cz 9.0272 $ fuel plate 7
451 27   cz 9.0551
452 27   cz 9.1059
453 27   cz 9.1338
454 27    p  2.4142136 -1 0 -1.09516   $ right Al inner
455 27    p -2.4142136 -1 0 -1.09516   $ left Al inner
456 27    p  2.4142136 -1 0 -1.39997   $ plate meat boundary
457 27    p -2.4142136 -1 0 -1.39997   $ plate meat boundary
c
460 28   cz 9.3574 $ fuel plate 8
461 28   cz 9.3853
462 28   cz 9.4361
463 28   cz 9.4640
464 28    p  2.4142136 -1 0 -1.09516   $ right Al inner
465 28    p -2.4142136 -1 0 -1.09516   $ left Al inner
466 28    p  2.4142136 -1 0 -1.39997   $ plate meat boundary
467 28    p -2.4142136 -1 0 -1.39997   $ plate meat boundary
c
470 29   cz 9.6876 $ fuel plate 9
471 29   cz 9.7155
472 29   cz 9.7663
473 29   cz 9.7942
474 29    p  2.4142136 -1 0 -1.09516   $ right Al inner
475 29    p -2.4142136 -1 0 -1.09516   $ left Al inner
476 29    p  2.4142136 -1 0 -1.39997   $ plate meat boundary
477 29    p -2.4142136 -1 0 -1.39997   $ plate meat boundary
c
480 30   cz 10.0178 $ fuel plate 10
481 30   cz 10.0457
482 30   cz 10.0965
483 30   cz 10.1244
```

```
484 30    p  2.4142136 -1 0 -1.09516   $ right Al inner
485 30    p -2.4142136 -1 0 -1.09516   $ left Al inner
486 30    p  2.4142136 -1 0 -1.39997   $ plate meat boundary
487 30    p -2.4142136 -1 0 -1.39997   $ plate meat boundary
c
490 31  cz 10.3480 $ fuel plate 11
491 31  cz 10.3759
492 31  cz 10.4267
493 31  cz 10.4546
494 31    p  2.4142136 -1 0 -1.09516   $ right Al inner
495 31    p -2.4142136 -1 0 -1.09516   $ left Al inner
496 31    p  2.4142136 -1 0 -1.39997   $ plate meat boundary
497 31    p -2.4142136 -1 0 -1.39997   $ plate meat boundary
c
500 32  cz 10.6782 $ fuel plate 12
501 32  cz 10.7061
502 32  cz 10.7569
503 32  cz 10.7848
504 32    p  2.4142136 -1 0 -1.09516   $ right Al inner
505 32    p -2.4142136 -1 0 -1.09516   $ left Al inner
506 32    p  2.4142136 -1 0 -1.39997   $ plate meat boundary
507 32    p -2.4142136 -1 0 -1.39997   $ plate meat boundary
c
510 33  cz 11.0084 $ fuel plate 13
511 33  cz 11.0363
512 33  cz 11.0871
513 33  cz 11.1150
514 33    p  2.4142136 -1 0 -1.09516   $ right Al inner
515 33    p -2.4142136 -1 0 -1.09516   $ left Al inner
516 33    p  2.4142136 -1 0 -1.39997   $ plate meat boundary
517 33    p -2.4142136 -1 0 -1.39997   $ plate meat boundary
c
520 34  cz 11.3386 $ fuel plate 14
521 34  cz 11.3665
522 34  cz 11.4173
523 34  cz 11.4452
524 34    p  2.4142136 -1 0 -1.09516   $ right Al inner
525 34    p -2.4142136 -1 0 -1.09516   $ left Al inner
526 34    p  2.4142136 -1 0 -1.39997   $ plate meat boundary
527 34    p -2.4142136 -1 0 -1.39997   $ plate meat boundary
c
530 35  cz 11.6688 $ fuel plate 15
531 35  cz 11.6967
532 35  cz 11.7475
533 35  cz 11.7754
534 35    p  2.4142136 -1 0 -1.09516   $ right Al inner
535 35    p -2.4142136 -1 0 -1.09516   $ left Al inner
536 35    p  2.4142136 -1 0 -1.39997   $ plate meat boundary
537 35    p -2.4142136 -1 0 -1.39997   $ plate meat boundary
c
540 36  cz 11.9990 $ fuel plate 16
541 36  cz 12.0269
542 36  cz 12.0777
543 36  cz 12.1056
544 36    p  2.4142136 -1 0 -1.09516   $ right Al inner
545 36    p -2.4142136 -1 0 -1.09516   $ left Al inner
546 36    p  2.4142136 -1 0 -1.39997   $ plate meat boundary
547 36    p -2.4142136 -1 0 -1.39997   $ plate meat boundary
c
550 37  cz 12.3292 $ fuel plate 17
```

```
551 37  cz 12.3571
552 37  cz 12.4079
553 37  cz 12.4358
554 37    p  2.4142136 -1 0 -1.09516   $ right Al inner
555 37    p -2.4142136 -1 0 -1.09516   $ left Al inner
556 37    p  2.4142136 -1 0 -1.39997   $ plate meat boundary
557 37    p -2.4142136 -1 0 -1.39997   $ plate meat boundary
c
560 38  cz 12.6594 $ fuel plate 18
561 38  cz 12.6873
562 38  cz 12.7381
563 38  cz 12.7660
564 38    p  2.4142136 -1 0 -1.09516   $ right Al inner
565 38    p -2.4142136 -1 0 -1.09516   $ left Al inner
566 38    p  2.4142136 -1 0 -1.39997   $ plate meat boundary
567 38    p -2.4142136 -1 0 -1.39997   $ plate meat boundary
c
570 39  cz 12.9896 $ fuel plate 19
571 39  cz 13.0175
572 39  cz 13.0683
573 39  cz 13.0962
574 39    p  2.4142136 -1 0 -1.09516   $ right Al inner
575 39    p -2.4142136 -1 0 -1.09516   $ left Al inner
576 39    p  2.4142136 -1 0 -1.39997   $ plate meat boundary
577 39    p -2.4142136 -1 0 -1.39997   $ plate meat boundary
c
580 40  cz 13.3198 $ fuel plate 20
581 40  cz 13.3477
582 40  cz 13.3985
583 40  cz 13.4264
584 40    p  2.4142136 -1 0 -1.09516   $ right Al inner
585 40    p -2.4142136 -1 0 -1.09516   $ left Al inner
586 40    p  2.4142136 -1 0 -1.39997   $ plate meat boundary
587 40    p -2.4142136 -1 0 -1.39997   $ plate meat boundary
c
590 41  cz 13.6500 $ fuel plate 21
591 41  cz 13.6779
592 41  cz 13.7287
593 41  cz 13.7566
594 41    p  2.4142136 -1 0 -1.09516   $ right Al inner
595 41    p -2.4142136 -1 0 -1.09516   $ left Al inner
596 41    p  2.4142136 -1 0 -1.39997   $ plate meat boundary
597 41    p -2.4142136 -1 0 -1.39997   $ plate meat boundary
c
600 42  cz 13.9802 $ fuel plate 22
601 42  cz 14.0081
602 42  cz 14.0589
603 42  cz 14.0868
604 42    p  2.4142136 -1 0 -1.09516   $ right Al inner
605 42    p -2.4142136 -1 0 -1.09516   $ left Al inner
606 42    p  2.4142136 -1 0 -1.39997   $ plate meat boundary
607 42    p -2.4142136 -1 0 -1.39997   $ plate meat boundary
c
610 43  cz 14.3104 $ fuel plate 23
611 43  cz 14.3383
612 43  cz 14.3891
613 43  cz 14.4170
614 43    p  2.4142136 -1 0 -1.09516   $ right Al inner
615 43    p -2.4142136 -1 0 -1.09516   $ left Al inner
616 43    p  2.4142136 -1 0 -1.39997   $ plate meat boundary
```

```
617 43    p -2.4142136 -1 0 -1.39997   $ plate meat boundary
c
620 44  cz 14.6406 $ fuel plate 24
621 44  cz 14.6685
622 44  cz 14.7193
623 44  cz 14.7472
624 44    p  2.4142136 -1 0 -1.09516   $ right Al inner
625 44    p -2.4142136 -1 0 -1.09516   $ left Al inner
626 44    p  2.4142136 -1 0 -1.39997   $ plate meat boundary
627 44    p -2.4142136 -1 0 -1.39997   $ plate meat boundary
c
200       cz 7.3838 $ IR pipe
201       cz 7.6581 $ OR pipe
c 202       cz 38.1   $ 12" water
203       cz 10.1981 $ 1" insulation
c
210 50      p  2.194300 -1 0 11.6987 $ right lower inner
211 51      p -2.194300 -1 0 11.6987 $ left lower inner
212 50      p -0.455726 -1 0 -5.7501 $ right upper inner
213 51      p  0.455726 -1 0 -5.7501 $ left upper inner
214         py -5.6175               $ bottom inner
220 50      p  2.194300 -1 0 13.2300 $ right lower outer
221 51      p -2.194300 -1 0 13.2300 $ left lower outer
222 50      p -0.455726 -1 0 -6.4479 $ right upper outer
223 51      p  0.455726 -1 0 -6.4479 $ left upper outer
224         py -6.2525               $ bottom outer
230 50      p  2.194300 -1 0 10.9331 $ right neoprene
231 51      p -2.194300 -1 0 10.9331 $ left neoprene
232         p  3.1993   -1 0 13.2244 $ right plastic bag
233         p -3.1993   -1 0 13.2244 $ left plastic bag
234         c/z 0 -10.065 14.8       $ top of plastic bag
c
250       px  -9.6032 $ square tube
251       px   9.6032
252       py  -9.6032
253       py   9.6032
c
300       px  10.033 $ lattice surfaces/sq. tube
301       px -10.033
302       py  10.033
303       py -10.033
310       px -50.165 $ 5x5 bounds
311       px  50.165
312       py -50.165
313       py  50.165
320       px -80.645 $ outer bounds
321       px  80.645
322       py -80.645
323       py  80.645
324       pz -60.96
325       pz  60.96

m2      1001.62c  2          $ water
        8016.62c  1
mt2     lwtr.60t
m3      13027.62c 1          $ Al
m4      6000.66c   -0.08     $ SS-304
        14000.60c  -1.0
        15031.66c  -0.045
        24000.50c  -19.0
```

```
         25055.62c  -2.0
         26000.55c  -68.375
         28000.50c  -9.5
m5       1001.62c  -0.056920  $ neoprene (no Cl)
         6000.66c  -0.542646
c         17000.66c -0.400434
m6       13027.62c  -26.5     $ insulation material
         14000.60c  -23.4
         8016.62c   -50.2
m10      92234.69c 2.3171E-05
         92235.69c 3.6147E-03
         92236.69c 1.3402E-05
         92238.69c 1.9174E-04
         13027.62c 5.0596E-02
c            total 5.4439E-02
c
*tr1      0 -12.25 0                          $ base to center
*tr2      0 -0.7798 0  180 90 90 90 180 90    $ down
*tr3      0  0.7798 0                         $ up
*tr4      0.7798 0 0   90 180 90 0 90 90      $ right
*tr5     -0.7798 0 0   90 0 90 180 90 90      $ left
*tr6      0.5514   0.5514  0  45 135 90 45 45 90    $ up/right
*tr7     -0.5514   0.5514  0  45 45 90 135 45 90    $ up/left
*tr8      0.5514  -0.5514  0  135 135 90 45 135 90  $ down/right
*tr9     -0.5514  -0.5514  0  135 45 90 135 135 90  $ down/left
tr22 0 0.095 0 $ plate 2
tr23 0 0.190 0 $ plate 3
tr24 0 0.285 0 $ plate 4
tr25 0 0.380 0 $ plate 5
tr26 0 0.475 0 $ plate 6
tr27 0 0.570 0 $ plate 7
tr28 0 0.665 0 $ plate 8
tr29 0 0.760 0 $ plate 9
tr30 0 0.855 0 $ plate 10
tr31 0 0.950 0 $ plate 11
tr32 0 1.045 0 $ plate 12
tr33 0 1.140 0 $ plate 13
tr34 0 1.235 0 $ plate 14
tr35 0 1.330 0 $ plate 15
tr36 0 1.425 0 $ plate 16
tr37 0 1.520 0 $ plate 17
tr38 0 1.615 0 $ plate 18
tr39 0 1.710 0 $ plate 19
tr40 0 1.805 0 $ plate 20
tr41 0 1.900 0 $ plate 21
tr42 0 1.995 0 $ plate 22
tr43 0 2.090 0 $ plate 23
tr44 0 2.185 0 $ plate 24
tr50   0.7798 0 0  $ shift FHE right
tr51  -0.7798 0 0  $ shift FHE left
c
mode   n
kcode  2500 1.0 50 250
sdef    x=d1 y=d2 z=d3
si1     -50 50
sp1     0 1
si2     -50 50
sp2     0 1
si3     -31 31
sp3     0 1
```

MIT Case YK9 (HA_MIT_FNW080)

```
MIT
999     0       -320:321:-322:323:-324:325              imp:n=0
900     0       310 -311 312 -313 24 -25     fill=3      imp:n=1
901     2 -1.0  (311:-310:313:-312:-24:25) 320 -321 322 -323 324 -325  imp:n=1
c
c       Universe 1: MIT Fuel Element (infinitely long)
c
10      3 -2.7          10 -11 50 -124          u=1 imp:n=1 $ right Al piece
11      3 -2.7          13 -12 50 -124          u=1 imp:n=1 $ left Al piece
c 12      2 -1.0          12 -10 18 -50           u=1 imp:n=1
20      10 5.4398E-02 40 -41 70 -90             u=1 imp:n=1 $ plate 1
21      3 -2.7          12 -10 50 -110 #20      u=1 imp:n=1
22      2 -1.0          12 -10 110 -51          u=1 imp:n=1
30      10 5.4398E-02 40 -41 71 -91             u=1 imp:n=1 $ plate 2
31      3 -2.7          12 -10 51 -111 #30      u=1 imp:n=1
32      2 -1.0          12 -10 111 -52          u=1 imp:n=1
40      10 5.4398E-02 40 -41 72 -92             u=1 imp:n=1 $ plate 3
41      3 -2.7          12 -10 52 -112 #40      u=1 imp:n=1
42      2 -1.0          12 -10 112 -53          u=1 imp:n=1
50      10 5.4398E-02 40 -41 73 -93             u=1 imp:n=1 $ plate 4
51      3 -2.7          12 -10 53 -113 #50      u=1 imp:n=1
52      2 -1.0          12 -10 113 -54          u=1 imp:n=1
60      10 5.4398E-02 40 -41 74 -94             u=1 imp:n=1 $ plate 5
61      3 -2.7          12 -10 54 -114 #60      u=1 imp:n=1
62      2 -1.0          12 -10 114 -55          u=1 imp:n=1
70      10 5.4398E-02 40 -41 75 -95             u=1 imp:n=1 $ plate 6
71      3 -2.7          12 -10 55 -115 #70      u=1 imp:n=1
72      2 -1.0          12 -10 115 -56          u=1 imp:n=1
80      10 5.4398E-02 40 -41 76 -96             u=1 imp:n=1 $ plate 7
81      3 -2.7          12 -10 56 -116 #80      u=1 imp:n=1
82      2 -1.0          12 -10 116 -57          u=1 imp:n=1
90      10 5.4398E-02 40 -41 77 -97             u=1 imp:n=1 $ plate 8
91      3 -2.7          12 -10 57 -117 #90      u=1 imp:n=1
92      2 -1.0          12 -10 117 -58          u=1 imp:n=1
100      10 5.4398E-02 40 -41 78 -98             u=1 imp:n=1 $ plate 9
101      3 -2.7          12 -10 58 -118 #100     u=1 imp:n=1
102      2 -1.0          12 -10 118 -59          u=1 imp:n=1
110      10 5.4398E-02 40 -41 79 -99             u=1 imp:n=1 $ plate 10
111      3 -2.7          12 -10 59 -119 #110     u=1 imp:n=1
112      2 -1.0          12 -10 119 -60          u=1 imp:n=1
120      10 5.4398E-02 40 -41 80 -100            u=1 imp:n=1 $ plate 11
121      3 -2.7          12 -10 60 -120 #120     u=1 imp:n=1
122      2 -1.0          12 -10 120 -61          u=1 imp:n=1
130      10 5.4398E-02 40 -41 81 -101            u=1 imp:n=1 $ plate 12
131      3 -2.7          12 -10 61 -121 #130     u=1 imp:n=1
132      2 -1.0          12 -10 121 -62          u=1 imp:n=1
140      10 5.4398E-02 40 -41 82 -102            u=1 imp:n=1 $ plate 13
141      3 -2.7          12 -10 62 -122 #140     u=1 imp:n=1
142      2 -1.0          12 -10 122 -63          u=1 imp:n=1
150      10 5.4398E-02 40 -41 83 -103            u=1 imp:n=1 $ plate 14
151      3 -2.7          12 -10 63 -123 #150     u=1 imp:n=1
152      2 -1.0          12 -10 123 -64          u=1 imp:n=1
160      10 5.4398E-02 40 -41 84 -104            u=1 imp:n=1 $ plate 15
161      3 -2.7          12 -10 64 -124 #160     u=1 imp:n=1
c 162      2 -1.0          12 -10 124 -19           u=1 imp:n=1
```

```
170       2 -1.0        -13:11:-50:124          u=1 imp:n=1 $ water between
fuel and enclosure
c
c       Universe 19: MIT with FHE
c
201      0             30 38 -32 -39 fill=1              u=19 imp:n=1
202      5 -0.737      -33 39 -32 30                     u=19 imp:n=1 $ right
neo
203      5 -0.737      31 -38 -32 30                     u=19 imp:n=1 $ left neo
204      3 -2.7        (-30:-31:32:33) 34 35 -36 -37     u=19 imp:n=1 $
enclosure
205      2 -0.8        -34:-35:36:37                     u=19 imp:n=1 $ water
outside FHE
c
c       Universe 20: FHE in tube (center)
c
210      2 -0.9     -200           fill=19               u=20 imp:n=1 $ inside
pipe
211      4 -7.94     200 -201                            u=20 imp:n=1 $ pipe
212      6 -0.096    201 -203 250 -251 252 -253          u=20 imp:n=1 $
insulation
213      0           203 250 -251 252 -253               u=20 imp:n=1 $ pipe to
tube
214      4 -7.94     -250:251:-252:253                   u=20 imp:n=1 $ tube to
inf
c
c       Universe 21: FHE in tube (down)
c
220      2 -0.9     -200           fill=19(2)            u=21 imp:n=1 $ inside
pipe
221      4 -7.94     200 -201                            u=21 imp:n=1 $ pipe
222      6 -0.096    201 -203 250 -251 252 -253          u=21 imp:n=1 $
insulation
223      0           203 250 -251 252 -253               u=21 imp:n=1 $ pipe to
tube
224      4 -7.94     -250:251:-252:253                   u=21 imp:n=1 $ tube to
inf
c
c       Universe 22: FHE in tube (up)
c
230      2 -0.9     -200           fill=19(3)            u=22 imp:n=1 $ inside
pipe
231      4 -7.94     200 -201                            u=22 imp:n=1 $ pipe
232      6 -0.096    201 -203 250 -251 252 -253          u=22 imp:n=1 $
insulation
233      0           203 250 -251 252 -253               u=22 imp:n=1 $ pipe to
tube
234      4 -7.94     -250:251:-252:253                   u=22 imp:n=1 $ tube to
inf
c
c       Universe 23: FHE in tube (right)
c
240      2 -0.9     -200           fill=19(4)            u=23 imp:n=1 $ inside
pipe
241      4 -7.94     200 -201                            u=23 imp:n=1 $ pipe
242      6 -0.096    201 -203 250 -251 252 -253          u=23 imp:n=1 $
insulation
243      0           203 250 -251 252 -253               u=23 imp:n=1 $ pipe to
tube
```

```
244     4 -7.94     -250:251:-252:253                  u=23 imp:n=1 $ tube to
inf
c
c       Universe 24: FHE in tube (left)
c
250     2 -0.9     -200            fill=19(5)          u=24 imp:n=1 $ inside
pipe
251     4 -7.94     200 -201                           u=24 imp:n=1 $ pipe
252     6 -0.096    201 -203 250 -251 252 -253         u=24 imp:n=1 $
insulation
253     0           203 250 -251 252 -253              u=24 imp:n=1 $ pipe to
tube
254     4 -7.94     -250:251:-252:253                  u=24 imp:n=1 $ tube to
inf
c
c       Universe 25: FHE in tube (up/right)
c
260     2 -0.9     -200            fill=19(6)          u=25 imp:n=1 $ inside
pipe
261     4 -7.94     200 -201                           u=25 imp:n=1 $ pipe
262     6 -0.096    201 -203 250 -251 252 -253         u=25 imp:n=1 $
insulation
263     0           203 250 -251 252 -253              u=25 imp:n=1 $ pipe to
tube
264     4 -7.94     -250:251:-252:253                  u=25 imp:n=1 $ tube to
inf
c
c       Universe 26: FHE in tube (up/left)
c
270     2 -0.9     -200            fill=19(7)          u=26 imp:n=1 $ inside
pipe
271     4 -7.94     200 -201                           u=26 imp:n=1 $ pipe
272     6 -0.096    201 -203 250 -251 252 -253         u=26 imp:n=1 $
insulation
273     0           203 250 -251 252 -253              u=26 imp:n=1 $ pipe to
tube
274     4 -7.94     -250:251:-252:253                  u=26 imp:n=1 $ tube to
inf
c
c       Universe 27: FHE in tube (down/right)
c
280     2 -0.9     -200            fill=19(8)          u=27 imp:n=1 $ inside
pipe
281     4 -7.94     200 -201                           u=27 imp:n=1 $ pipe
282     6 -0.096    201 -203 250 -251 252 -253         u=27 imp:n=1 $
insulation
283     0           203 250 -251 252 -253              u=27 imp:n=1 $ pipe to
tube
284     4 -7.94     -250:251:-252:253                  u=27 imp:n=1 $ tube to
inf
c
c       Universe 28: FHE in tube (down/left)
c
290     2 -0.9     -200            fill=19(9)          u=28 imp:n=1 $ inside
pipe
291     4 -7.94     200 -201                           u=28 imp:n=1 $ pipe
292     6 -0.096    201 -203 250 -251 252 -253         u=28 imp:n=1 $
insulation
293     0           203 250 -251 252 -253              u=28 imp:n=1 $ pipe to
tube
```

```
294     4 -7.94     -250:251:-252:253                 u=28 imp:n=1 $ tube to
inf
c
c       Universe 3: Array of Packages
c
300    0     -300 301 -302 303 imp:n=1 u=3 lat=1 fill=-2:2 -2:2 0:0
               25 25 22 26 26
               25 25 22 26 26
               23 23 20 24 24
               27 27 21 28 28
               27 27 21 28 28

10          px  2.5451    $ Al side
11          px  3.0226    $ Al side
12          px -2.5451    $ Al side
13          px -3.0226    $ Al side
18   10     py -3.02768   $ Al bottom
19   10     py 3.02768    $ Al top
20   10     py -3.34518   $ neoprene
21   10     py  3.34518   $ neoprene
c
24          pz -28.41625  $ bottom of fuel
25          pz  28.41625  $ top of fuel (22.375")
30 20       p -1.71429 -1 0 -7.3152 $ inner FHE
31 21       p  1.71429 -1 0 -7.3152 $ inner FHE
32 21       p -1.71429 -1 0  7.3152 $ inner FHE
33 20       p  1.71429 -1 0  7.3152 $ inner FHE
34 20       p -1.71429 -1 0 -7.9697 $ outer FHE
35 21       p  1.71429 -1 0 -7.9697 $ outer FHE
36 21       p -1.71429 -1 0  7.9697 $ outer FHE
37 20       p  1.71429 -1 0  7.9697 $ outer FHE
38 21       p  1.71429 -1 0 -6.6859 $ left neo
39 20       p  1.71429 -1 0  6.6859 $ right neo
c
40          px -2.3878 $ meat width (w/2*cos(30))
41          px  2.3878 $ meat width
c
50 10       py -4.34848
51 10       py -3.73888
52 10       py -3.12928
53 10       py -2.51968
54 10       py -1.91008
55 10       py -1.30048
56 10       py -0.69088
57 10       py -0.08128
58 10       py 0.52832
59 10       py 1.13792
60 10       py 1.74752
61 10       py 2.35712
62 10       py 2.96672
63 10       py 3.57632
64 10       py 4.18592
c
70 10       py -4.30530
71 10       py -3.69570
72 10       py -3.08610
73 10       py -2.47650
74 10       py -1.86690
75 10       py -1.25730
76 10       py -0.64770
```

```
77 10   py -0.03810
78 10   py 0.57150
79 10   py 1.18110
80 10   py 1.79070
81 10   py 2.40030
82 10   py 3.00990
83 10   py 3.61950
84 10   py 4.22910
c
90 10   py -4.22910
91 10   py -3.61950
92 10   py -3.00990
93 10   py -2.40030
94 10   py -1.79070
95 10   py -1.18110
96 10   py -0.57150
97 10   py 0.03810
98 10   py 0.64770
99 10   py 1.25730
100 10   py 1.86690
101 10   py 2.47650
102 10   py 3.08610
103 10   py 3.69570
104 10   py 4.30530
c
110 10   py -4.18592
111 10   py -3.57632
112 10   py -2.96672
113 10   py -2.35712
114 10   py -1.74752
115 10   py -1.13792
116 10   py -0.52832
117 10   py 0.08128
118 10   py 0.69088
119 10   py 1.30048
120 10   py 1.91008
121 10   py 2.51968
122 10   py 3.12928
123 10   py 3.73888
124 10   py 4.34848
c
199      cz 6.9012 $ Al
200      cz 7.3838 $ IR pipe
201      cz 7.6581 $ OR pipe
203      cz 10.1981 $ 1" insulation
c
250      px  -9.6032 $ square tube
251      px   9.6032
252      py  -9.6032
253      py   9.6032
c
300      px  10.033 $ lattice surfaces/sq. tube
301      px -10.033
302      py  10.033
303      py -10.033
310      px -50.165 $ 5x5 bounds
311      px  50.165
312      py -50.165
313      py  50.165
320      px -80.645 $ outer bounds
```

```
321      px  80.645
322      py -80.645
323      py  80.645
324      pz -58.8963
325      pz  58.8963

m2      1001.62c  2          $ water
        8016.62c  1
mt2     lwtr.60t
m3      13027.62c 1          $ Al
m4      6000.66c   -0.08     $ SS-304
        14000.60c  -1.0
        15031.66c  -0.045
        24000.50c  -19.0
        25055.62c  -2.0
        26000.55c  -68.375
        28000.50c  -9.5
m5      1001.62c  -0.056920  $ neoprene (no Cl)
        6000.66c  -0.542646
c        17000.66c -0.400434
m6      13027.62c  -26.5     $ insulation material
        14000.60c  -23.4
        8016.62c   -50.2
m10     92234.69c 2.3613E-05 $ fuel
        92235.69c 3.6835E-03
        92236.69c 1.3657E-05
        92238.69c 1.9539E-04
        13027.62c 5.0481E-02
c           total 5.4398E-02
c
*tr2     0 -0.7798 0  30 60 90 120 30 90   $ down
*tr3     0  0.7798 0  30 60 90 120 30 90   $ up
*tr4     0.7798 0 0                        $ right
*tr5    -0.7798 0 0                        $ left
*tr6     0.5514    0.5514  0                      $ up/right
*tr7    -0.5514    0.5514  0  90 0 90 180 90 90   $ up/left
*tr8     0.5514   -0.5514  0  90 0 90 180 90 90   $ down/right
*tr9    -0.5514   -0.5514  0                      $ down/left
*tr10    0 0 0  30 120 90 60 30 90 $ rotate fuel surfaces 30 deg CCW
*tr20    -0.7798 0 0  30.2 59.8 90 120.2 30.2 90 j j j -1 $ rotate right FHE
30.2 deg CCW
*tr21     0.7798 0 0  30.2 59.8 90 120.2 30.2 90 j j j -1 $ rotate left FHE
30.2 deg CCW
c
mode   n
kcode  2500 1.0 50 250
sdef    x=d1 y=d2 z=d3
si1     -50 50
sp1     0 1
si2     -50 50
sp2     0 1
si3     -31 31
sp3     0 1
```

7.0 PACKAGE OPERATIONS

This section provides general instructions for loading and unloading operations of the ATR FFSC. Due to the low specific activity of neutron and gamma emitting radionuclides, dose rates from the contents of the package are minimal. As a result of the low dose rates, there are no special handling requirements for radiation protection.

Package loading and unloading operations shall be performed using detailed written procedures. The operating procedures developed by the user for the loading and unloading activities shall be performed in accordance with the procedural requirements identified in the following sections.

The closure handle must be rendered inoperable for lifting and tiedown during transport per 10 CFR §71.45. To satisfy this requirement either the closure handle may be removed or the cover installed. If the closure handle cover is utilized it may be stored with the closure assembly in the installed position. When stored with the closure assembly the cover must be removed prior to the package loading and unloading operations and may be reinstalled following installation of the closure. The installation of the closure handle cover is presented in Section 7.1.4, *Preparation for Transport.*

7.1 Package Loading

7.1.1 Preparation for Loading

Prior to loading the ATR FFSC, the packaging is inspected to ensure that it is in unimpaired physical condition. The packaging is inspected for:

- Damage to the closure locking mechanism including the spring. Inspect for missing hardware and verify the locking pins freely engage/disengage with the package body mating features.
- Damage to the closure lugs and interfacing body lugs. Inspect lugs for damage that precludes free engagement of the closure with the body.
- Deformation of the inner shell (payload cavity) that precludes free entry/removal of the payload.
- Deformed threads or other damage to the fasteners or body of the loose fuel plate basket.
- Damage to the spring plunger, or ball lock pins and end spacers, as applicable, or body of the fuel handling enclosure.

Acceptance criteria and detailed loading procedures derived from this section are specified in user written procedures. These user procedures are specific to the authorized content of the package and inspections ensure the packaging complies with Appendix 1.3.2, *Packaging General Arrangement Drawings.*

Defects that require repair shall be corrected prior to shipping in accordance with approved procedures consistent with the quality program in effect.

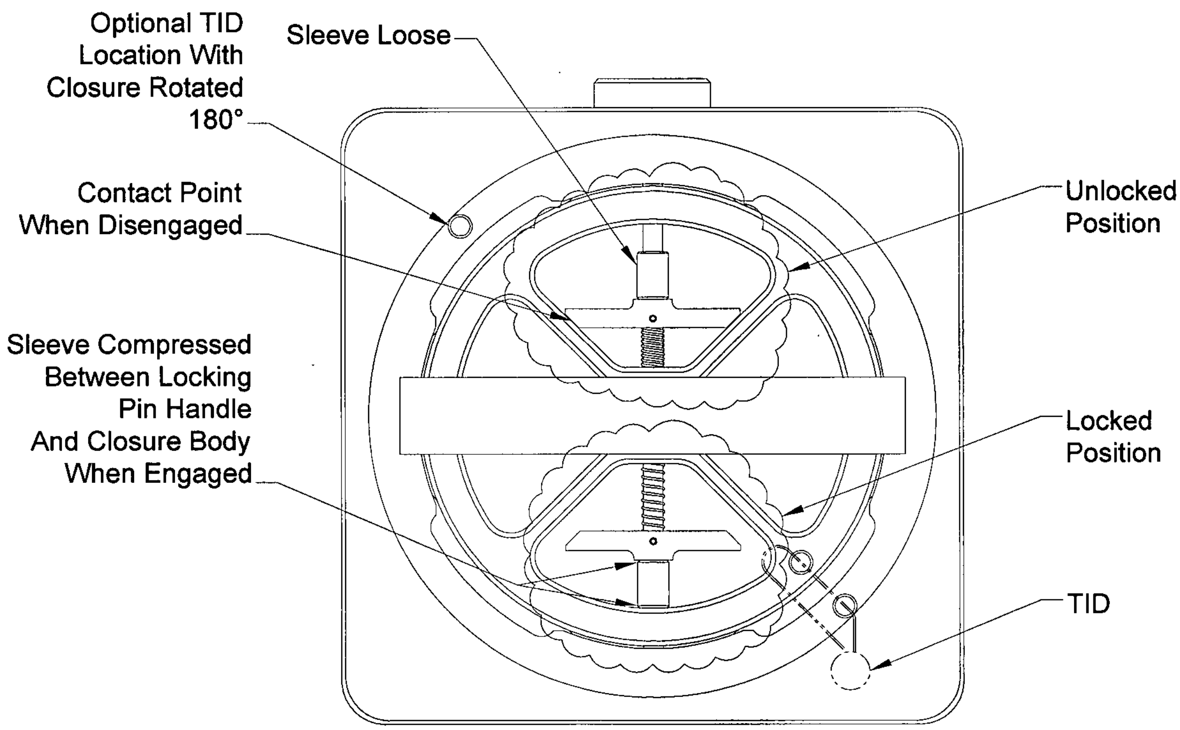

Figure 7.1-1 - Closure Locking Positions

7.1.3 Loading of Contents - Loose Fuel Plates

1. Remove the closure by depressing the spring-loaded pins and rotating the closure 45° to align the closure locking tabs with the mating cut-outs in the body. Remove the closure from the body.
2. Remove the fuel plate basket if present in the payload cavity.
3. Prior to loading, visually inspect the loose fuel plate basket for damage, corrosion, and missing hardware/fastening devices to ensure compliance with Appendix 1.3.2, *Packaging General Arrangement Drawings.*
4. Open the loose fuel plate basket by removing the 8 wing nut fasteners securing each half of the basket.
5. Place the fuel plates into one half of the loose fuel plate basket
    a. Ensure the combined weight of the loose fuel plates and optional dunnage is 20 lbs or less. The loose fuel plates may only be ATR fuel plates.
    b. Ensure the combined fissile mass of the loose fuel plates does not exceed 600 g uranium-235.
    c. Flat and curved fuel plates may not be mixed in the same basket.
    d. As a property protection precaution, the fuel plates may optionally be inserted into a plastic bag prior to placement in the fuel plate basket.

Itemized RAI Responses

RAI 2-1: Demonstrate that the MIT and MURR fuel elements' structural performance is bounded by the structural performance of the previously tested and approved ATR simulated fuel element.

The principal justification provided by the applicant for bounding structural behavior is that all fuel elements are constructed with similar materials and the previously tested ATR simulated fuel element has the most associated mass (11.35 kg, 25 lbs) when compared to the MIT and MURR fuel [4.54 kg (10 lbs) and 6.81 kg (15 lbs) respectively]. The staff does not agree that this justification is sufficient given that the geometry near the ends of the respective fuel elements is significantly different and would result in potentially more damage to the fuel plates due to the lack of incidental impact energy absorption.

Furthermore, the applicant states in Sections 1.2.1.1.3, 1.2.1.1.4, and 1.2.1.1.5, that the Fuel Handling Enclosures (FHE) "[do] not add strength to the package, or satisfy any safety requirement." Given that the spacers for the MIT and MURR FHEs are necessary to maintain their position within the external packaging, there is a structural function being performed by the spacers and the spacers must be evaluated. If the spacers are not evaluated, then an evaluation must be performed to determine the damage associated with the gap that would exist between the fuel assemblies centered within the outer package and the inner surface of the package end fitting.

This information is required by staff to assess compliance with the requirements of 10 CFR 71.71 and 10 CFR 71.73.

Response: The HAC criticality analysis has been revised to consider damage to the MURR and MIT fuel elements by fuel plate pitch expansion to address potential worst case increase in reactivity. The MIT and MURR FHEs restrict postulated fuel element pitch expansion under the HAC conditions. For conservatism in evaluating the HAC conditions, the MIT and MURR FHE postulated damage exceeds the results obtained during testing of the ATR payloads. The spacers securing the MIT and MURR FHE sections are assumed to fail which allows the two sections to spread apart for a worst case reactivity configuration of the fuel elements.

Energy attenuation afforded by the end spacers is not considered in the structural analysis. Under end drop conditions, the external package absorbs and dissipates virtually no energy. This can be seen by the lack of structural damage inflicted to the package during the structural tests. As such, the FHE experiences the same impact velocity of the FHE against the end fitting and is exposed to the same loading conditions with or without the spacers.

RAI 3-1: Revise the application to clarify or justify the apparent discrepancy between the thermal conductivity and specific heat values for Aluminum 6061-T6511 in Table 3.6-3 "Thermal Properties of Package Metallic Materials," in Section 3.6.6.2 of the SAR and the values used for "A96061 Aluminum" in the MIT and MURR Thermal Desktop models.

The thermal conductivity and specific heat values provided in Table 3.6-3 of the SAR are different from those used for "A96061 Aluminum" in the MIT and MURR Thermal Desktop models.

This information is necessary to determine compliance with 10 CFR 71.35.

Response: The properties in Table 3.6-3 inadvertently listed those for Type 5052-H32 aluminum (see Table 3.2-1) instead of the properties for 6061 aluminum. The table has been corrected. These thermal properties match those used in the Thermal Desktop modeling. No changes to the presented temperatures, discussion, or conclusions are required as a result of this revision.

RAI 6-1: Justify not performing analyses for the MIT and MURR loose plate contents.

The applicant states (in Section 6.10, 2nd paragraph) that due to the similarity with ATR fuel and the same mass limit for the loose plate basket the reactivity of the MURR and MIT loose plates contents would be similar to the reactivity of the ATR loose plate contents.

The application does not include any quantitative support for this statement nor does it include any discussion of the similarities relied upon to arrive at the given conclusion. Additionally, it is not clear, based upon the comparison of the maximum reactivities of the MURR and ATR fuel elements, for example, that the reactivities of the loose plate contents of the different fuel types will be similar. The MURR fuel element has less fissile mass but in noticeably more reactive that the ATR fuel element.

The application should include quantitative support for the statement referred to above, or it should describe the similarities upon which the statement relies, properly justifying how those similarities result in the reactivities of the proposed loose plate contents and the approved ATR loose plate contents being similar.

The justification should include consideration of features important to reactivity, such as the hydrogen-to-fissile material ratio and whether a fissile mass less than the maximum would result in a noticeably higher maximum reactivity.

This information is needed to confirm compliance with 10 CFR 71.55(b) and 71.59(a).

Response: The MIT and MURR loose plate contents have been removed from the SAR. This analysis may be added in a future license amendment.

RAI 6-2: Justify the applicability of the tolerance used on the MURR fuel meat arc length.

The application states that a tolerance of 0.1 inch was used to be consistent with the ATR analysis. However, it is not clear from the application that this tolerance is applicable to the MURR fuel. The 0.1-inch tolerance on the ATR fuel can be derived from the dimensions provided on Figure 6.2-1 (based upon the technical drawing for the ATR fuel). The figure for the MURR fuel (Figure 6.10-1) does not provide sufficient information to derive the tolerance value that is appropriate for the fuel meat arc length. The tolerance that is applicable to (or conservative for) the MURR fuel meat arc length should be used in the analysis for the MURR fuel. The application should also describe the basis for the MURR and the MIT fuel element figures (Figures 6.10-1 and 2); the figures should be based upon the applicable technical drawing for the respective fuel type.

This information is necessary to determine compliance with 10 CFR 71.33(b), 71.55(b), and 71.59(a).

Response: The tolerance on the MURR fuel meat arc length may be computed to be ±0.065-in based on information on the MURR fuel drawing. However, while investigating this RAI, it was discovered that the fuel meat arc lengths listed in the MURR fuel drawing are minimum dimensions, and were misinterpreted as nominal dimensions. Therefore, the maximum meat arc lengths as presented in the original license amendment are slightly too smalll. Although the effect on the reactivity is within the statistical uncertainty of the Monte Carlo method, the fuel meat maximum arc lengths have been corrected in all MURR criticality models. In addition, the information necessary to compute the fuel meat arc length tolerance has been added to the MURR fuel element sketch (Figure 6.10-1).

The fuel element sketches provided in the SAR for the ATR, MURR, and MIT fuel elements are based on the respective fuel element drawings:

ATR: Drawing DWG-405400, Rev. 19, *ATR Mark VII Fuel Element Assembly*

MURR: Drawing 409406, Rev. E, *MURR Fuel Plate*
Drawing 409407, Rev. N, *MURR UAl_x Fuel Element Assembly*

MIT: Drawing 410368, Rev. A, *Test Research Reactor 3 Fuel Plate*
Drawing 419486, Rev. A, *Test Research Reactor 3 Welded Fuel Assembly*

These drawings were intentionally not referenced in the SAR or included as attachments to the SAR because it was desired to decouple the license from a particular revision of these drawings. These drawings could be revised in the future, although it is unlikely that any drawing changes would affect the criticality analysis. The dimensions provided on the figures represent the basic fuel dimensions that are not expected to change in any future revisions.

The fuel drawings cited above are included with these RAIs responses for information only.

RAI 6-3: Clarify if and how motion of the loose MURR and MIT plates along the length of the LFPB cavity is prevented, while providing the necessary information in the Package Operations and/or modifying the criticality evaluation as appropriate.

The application indicates that the same LFPB used for loose MURR and MIT fuel plates is also used for loose ATR Fuel plates. Based upon the licensing drawing for the LFPB and the application descriptions of the MURR and MIT fuel plates (see text and figures of Section 6.10.2), there is significant room for the MURR and MIT fuel plates to move around in the LFPB. For example, the LFPB cavity length is 50.5 inches and the length of the MIT plates is 23 inches. Thus, the MIT fuel plates may sustain damage and/or rearrange (under hypothetical accident conditions) in a manner that does not appear to have been considered in the criticality evaluation. The application should describe any means relied upon to protect the loose plates contents and consider those means (or lack thereof) in the technical evaluations.

This information is needed to confirm compliance with 10 CFR 71.33(b), 71.35(c), 71.55(b), 71.59(a), and 71.87(f).

Response: The MIT and MURR loose plate contents has been removed from the SAR. This analysis may be added in a future license amendment.

RAI 6-4: Modify the criticality evaluations for the MURR and MIT fuel elements to address damage to the fuel elements resulting from hypothetical accident conditions (HAC).

The applicant's HAC criticality analysis for the MURR and MIT fuel elements is similar to that done for the ATR fuel element; no damaged fuel element models were developed. The justification for this analysis assumption for the ATR is given on page 6-12 of the application and is based upon actual HAC tests performed with a simulated ATR fuel element, which showed only minor damage that will have a negligible effect on reactivity.

Due to package configuration differences versus the ATR fuel element, it is not clear that this analysis assumption is valid for the MURR and MIT fuel elements (see question 2-1). The condition of the MURR and MIT fuel elements used in the HAC analysis should be well justified and be consistent with or conservative versus the fuel element condition resulting from HAC conditions (as determined in the structural evaluation).

This information is needed to confirm compliance with 10 CFR 71.55(e) and 71.59(a).

Response: The HAC analysis has been revised to consider damage to the MURR and MIT fuel elements. It is assumed that the fuel element pitch may expand beyond maximum possible extent allowed by the fuel handling enclosures. It is further assumed that the two halves that comprise each fuel handling enclosure have separated, so that a rather large and conservative pitch expansion is utilized.

Because the FHE is credited in the HAC analyses (it was not credited in the original amendment application), for consistency, the NCT analyses for MURR and MIT have been modified to include the FHE

RAI 7-1: Modify the last bullet in Section 7.1.1, "Preparation for Loading," on page 7-1 of the application to read similar to: "Damage to the spring plunger*, or ball lock pins and end spacers, as applicable,* or body of the fuel handling enclosure."

The italics indicate the text that should be added. Not all fuel handling enclosures use a spring plunger to lock closed. The enclosures for the MURR and MIT fuel use ball lock pins and end spacers that should e inspected for damage in preparation for loading MURR and MIT contents, as is done for the ATR enclosure spring plunger. The text of the referenced bullet should be modified so as to be clear regarding the required inspections.

This information is needed to confirm compliance with 10 CFR 71.87(b).

Response: The text has been revised as recommended.

Figure Withheld Under 10 CFR 2.390

INEEL

ATR
MARK VII FUEL ELEMENT
ASSEMBLY

SIZE	CAGE CODE	INDEX CODE NUMBER AREA	TYPE	QL	ORIG		REV
E	01MF3	533	0670	43	400	DWG-405400	19

SCALE: NOTED

SHEET 1 OF 3

Figure Withheld Under 10 CFR 2.390

SIZE	CAGE CODE	INDEX CODE NUMBER				DWG-	REV
		AREA	TYPE	QL	ORG		
E	01MF3	533	0670	43	400	405400	19
SCALE: NOTED						SHEET 2	

SD7587

8	7	6	5	4	3	2	1

H

G

F

E

Figure Withheld Under 10 CFR 2.390

D

C

B

A

SIZE	CAGE CODE	INDEX CODE NUMBER					REV
		AREA	TYPE	CL	ORIG		
E	01MF3	533	0670	43	400	DWG-405400	19
SCALE: NOTED						SHEET 3	

Figure Withheld Under 10 CFR 2.390

EG&G Idaho, Inc.

TITLE

UNIVERSITY OF MISSOURI AT COLUMBIA
TEST RESEARCH TRAINING REACTOR 4
MURR FUEL PLATE

DWG. SIZE	AREA	DWG. TYPE	CL	DISC.	DRAWING NUMBER
E	540	9999	43	220	409406

BDWY 653 SHEET 1 PROJECT NO.

409406

Figure Withheld Under 10 CFR 2.390

EG&G Idaho, Inc.

TITLE

UNIVERSITY OF MISSOURI AT COLUMBIA
TEST RESEARCH TRAINING REACTOR 4
MURR UAl_x FUEL
ELEMENT ASSEMBLY

DWG. SIZE	INDEX CODE NUMBER: AREA	DWG. TYPE	CL.	ORIG.	DRAWING NUMBER
E	540	9999	43	220	409407

SHEET 1 OF 2

PROJECT NO.

409407

Figure Withheld Under 10 CFR 2.390

DWG SIZE	INDEX CODE NUMBER AREA	DWG TYPE	CL	ORIG	DRAWING NUMBER
E	540	9999	43	220	409407

SCALE	RELEASE DATE	SHEET
1/1	[illegible]	2

2 | 409407

EDWY 653

Figure Withheld Under 10 CFR 2.390

410368 A

EG&G Idaho, Inc.

TITLE

MASSACHUSETTS INSTITUTE OF TECHNOLOGY
TEST RESEARCH TRAINING REACTOR 3
FUEL PLATE

DWG. SIZE	INDEX CODE NUMBER				DRAWING NUMBER
	AREA	DWG. TYPE	CL	ORIG.	
D	540	9999	43	220	410368
					SHEET

BDWY 1035

PROJECT NO.

Figure Withheld Under 10 CFR 2.390

EG&G

TITLE

MASSACHUSETTS INSTITUTE OF TECHNOLOGY
TEST RESEARCH TRANING REACTOR 3
WELDED FUEL ELEMENT ASSEMBLY

DWG SIZE	INDEX CODE NUMBER				DRAWING NUMBER
	UEA	DWG TYPE	CL	NO.	
E	540	9939	43	220	419486

SHEET

PROJECT NO. 6580

419486

AREVA

INL
Idaho National Laboratory

ATR FFSC

Safety Analysis Report

Docket 71-9330

Revision 4
February 2009